SOLVENT-FREE OXIDATION OF PRIMARY CARBON-HYDROGEN BONDS IN TOLUENE USING SUPPORTED GOLD PALLADIUM ALLOY NANOPARTICLES

Lokesh Kesavan

CARDIFF
UNIVERSITY

PRIFYSGOL
CaRDYð

Thesis submitted in accordance with the regulation of Cardiff
University for the partial fulfillment of degree of doctor of philosophy

December 2011

UMI Number: U585513

DECLARATION

This work has not previously been accepted in substance for any degree and is not concurrently submitted in candidature for any degree.

Signed .... (candidate)   Date ...13/2/12...

STATEMENT 1

This thesis is being submitted in partial fulfillment of the requirements for the degree of PhD

Signed .... (candidate)   Date ...13/2/2012...

STATEMENT 2

This thesis is the result of my own independent work/investigation, except where otherwise stated. Other sources are acknowledged by explicit references.

Signed .... (candidate)   Date ...13/2/2012...

STATEMENT 3

I hereby give consent for my thesis, if accepted, to be available for photocopying and for inter-library loan, and for the title and summary to be made available to outside organisations.

Signed .... (candidate)   Date ...13/2/2012...

Acknowledgement

Abstract

Selective oxidation of primary carbon-hydrogen bonds with oxygen is of crucial importance for the sustainable exploitation of available feedstocks. To date, heterogeneous catalysts have either shown low activity and/or selectivity or have required activated oxygen donors. It is reported here that supported gold-palladium (Au-Pd) nanoparticles on carbon or TiO_2 are active for the oxidation of the primary carbon-hydrogen bonds in toluene and related molecules, giving high selectivities to benzyl benzoate under mild solvent-free conditions. Differences between the catalytic activity of the Au-Pd nanoparticles on carbon and TiO_2 supports are rationalized in terms of the particle/support wetting behaviour and the availability of exposed corner/edge sites. Further these catalysts have been tested for substituted toluene molecules and benzyl alcohol, as these substrates have similarity in their structural configuration. The results are discussed with regard to structure activity relationship.

TABLE OF CONTENTS

CHAPTER - 3

Liquid phase oxidation of toluene using Au Pd alloy
nanoparticles supported catalysts under solvent free
conditions

Chapter 1

Introduction & Literature

1.1. Brief introduction to catalysis

Catalysis is a process which alters the rate of a chemical reaction due to the involvement of a foreign substance called 'catalyst'. Unlike other reagents that participate in the chemical reaction, a catalyst is not consumed by the reaction itself. A catalyst may participate in multiple chemical transformations simultaneously. Substances that speed up the rate of the reaction are called positive catalysts. Materials that slow down the rate of the reaction are called inhibitors (or negative catalysts). There are some other chemical substances which can either increase or decrease the activity of catalysts. They are called promoters and catalytic poisons respectively. Further, catalysts can be divided into two main types known as heterogeneous and homogeneous catalyst. If the catalyst is in a different phase from the reactants, then it is called a heterogeneous catalyst. If the catalyst is in the same phase as the reactants, then it is known as a homogeneous catalyst. As we classified 'catalysts' into subgroups, catalytic processes also can also be classified into two major groups called homogeneous catalysis and heterogeneous catalysis based on the phase of the catalyst employed with respect to reactants (1).

Heterogeneous catalysis involves the use of a catalyst in a different phase from the reactants. Typical examples involve a solid catalyst with the reactants as either liquids or gases. Whereas homogeneous catalysis involves in the use of a catalyst in a same phase as that of reactants.

A typical heterogeneous process happens as follows; initially one or more of the reactant molecules are adsorbed on to the surface of the catalyst at 'active sites' during the reaction. Active sites are the specific sites which are responsible for the activation of the reactant molecules. In other words, active site is a part of the surface which is particularly good at adsorbing things and helping them to react. There is some sort of interaction between the

surface of the catalyst and the reactant molecules which make them more reactive. This might involve an actual reaction with the surface, or some weakening of the bonds in the attached molecules. At this stage, both of the reactant molecules might be attached to the surface, or one might be attached and hit by the other one moving freely in the gas or liquid. Finally, the product molecules are desorbed from the catalyst surface. Desorption simply means that the product molecules break away. This leaves the active site available for a new set of molecules to attach and react.

A good catalyst needs to adsorb the reactant molecules strongly enough for them to react, but not so strongly that the product molecules stick more or less permanently to the surface. Silver, for example, isn't a good catalyst because it does not form strong enough attachments with reactant molecules. Tungsten, on the other hand, isn't a good catalyst because it adsorbs too strongly. Metals like platinum and nickel make good catalysts because they adsorb strongly enough to hold and activate the reactants, but not so strongly that the products cannot break away.

1.2. Heterogeneous catalysis

Heterogeneous catalysis plays a major role worldwide, not only with respect to an economic viewpoint, but it also provides the necessary infrastructure for the well being of society as a whole. Without effective heterogeneous catalysis the manufacture of many materials, pharmaceuticals and foodstuffs would not be possible. It is not surprising, therefore, that as it is a subject that spans chemistry, chemical engineering and materials science, there is intense and broad interest in the design of new catalysts as well as seeking to understand how these materials function as catalysts. With respect to current industrial processes many of these are based on acid–base catalysts, e.g. catalytic cracking of

hydrocarbons for the production of transportation fuels, and hydrogenations with molecular

hydrogen typically using metal catalysts, e.g. the Fischer–Tropsch synthesis (2)

In addition, selective oxidation remains one of the key synthetic steps for the activation

of a broad range of substrates for the production of either finished products or intermediates

for the preparation of pharmaceuticals, agrochemicals, as well as commodity chemicals.

However, in contrast to hydrogenation reactions which are often carried catalytically with

molecular hydrogen, there are relatively few selective oxidation reactions that are catalysed

by heterogeneous catalysts using molecular oxygen as an oxygen source. Often selectivity in

these processes can only be achieved if stoichiometric oxygen donors, e.g. manganates, or

activated forms of oxygen, e.g. hydrogen peroxide, are utilised; this increases the costs as

well as significantly decreasing the atom efficiency of the overall process.

While many would consider hydrogenation with a heterogeneous metal catalyst and

molecular hydrogen as a commonplace laboratory procedure, most would not consider doing

a similar oxidation process with molecular oxygen as a standard laboratory procedure. Why is

the case? There is one essential difference between catalytic hydrogenation and oxidation.

Under most reaction conditions, the hydrogen molecule has to be activated by chemisorption

on a catalyst surface before it can be reacted with a substrate for hydrogenation to occur. At

the relatively low temperatures at which catalytic hydrogenation reactions are carried out,

activation of hydrogen via a competing radical pathway is not feasible. This is not the case

with selective oxidation (2).

Dioxygen in its ground state is a diradical triplet species. This opens up the possibilities

of competing non-catalysed gas or liquid phase reactions in which triplet dioxygen reacts

directly with the substrate without the intervention of a catalyst. Fortunately, most organic

substrates of interest are in singlet states in their ground states and so this effect can be

minimised. However, it is a competing factor that complicates oxidation reactions, and

necessarily makes them far more complex and demanding to study. However, even with this added complication, given its central importance, it is surprising that there have been few new approaches in the design of selective oxidation catalysts using molecular oxygen in the past forty years (3). Indeed, the major advances in selective oxidation were marked out over 50 years ago; since then there have been the remarkable developments of the titanium silicalite TS-1 for the epoxidation of alkenes and iron-doped ZSM-5 zeolite for the oxidation of benzene to phenol. Both of these oxidations are complex and difficult and had previously eluded many talented researchers; however, both processes use activated forms of oxygen, namely H_2O_2 for TS-1 (4) and N_2O for Fe-ZSM-5 (5) and both catalysts are totally non-selective with molecular oxygen. There is, therefore, a real need for new catalytic processes that use molecular oxygen, especially since environmental factors are of paramount importance and we need to develop atom efficient green processes. It is against this background that recent developments in selective oxidation reactions using supported gold and gold–palladium nanoparticles are beginning to make an impact.

1.3. Gold catalysis

Catalysis using gold nanoparticles is a topic of much current interest. There are several general reasons that explain this interest. One of them is the fact that the catalytic activity of gold is directly related to the particle size in the nanometre length scale. Thus, gold catalysis is a paradigmatic example of those properties that are only observed in nanoparticles and can disappear completely as the particle size grows into the micrometric scale. Considering the current impetus of nanoscience, it is understandable that all the aspects related to the preparation of small nanoparticles of narrow size distribution, their stabilization and their unique properties compared to larger particle size are appealing to a large community of researchers from material science, computational chemistry and catalysis (6).

Since the mid 1990s, there has been a dramatic increase in research attention focussed on the use of supported gold catalysts for redox reactions. Initial interest in gold catalysts involved two observations. First, and foremost, Haruta and co-workers (7) identified that nanocrystals of Au supported on oxides were highly effective as a catalyst for CO oxidation at subambient temperature. Second, Hutchings (8) predicted that cationic gold would be the most effective catalyst for the hydrochlorination of acetylene, and this prediction was subsequently experimentally verified (9). In the last few years, the number of publications appearing on gold catalysis involving both homogeneously and heterogeneously catalysed reactions has risen exponentially, and these publication statistics have recently been published by Hashmi (10). With respect to heterogeneously catalysed reactions, most of the publications concern the oxidation of CO at ambient temperature, and these data have been reviewed by Bond and Thompson (11,12) and by Haruta (13). Much less attention has focussed on selective oxidation, and yet supported gold catalysts have been found to be very effective for a broad range of selective oxidation reactions. Haruta and co-workers (14) and Moulijn and co-workers (15) have shown that Au supported on microporous or mesoporous titanium silicate structures is very effective for the oxidation of propene to propene oxide with O_2/H_2 mixtures, and there is currently significant industrial interest in this reaction. The seminal studies of Rossi and Prati (16-19) have shown that supported Au catalysts are effective for the oxidation of alcohols in the liquid phase with O_2 to form monoacids when a base is present. Biella and Rossi (20) extended this to show that the same catalysts can be used with gas phase reactants and aldehydes could be formed in high selectivity. Subsequently, Hutchings *et al* showed (21, 22) that Au/C catalysts could be very selective for glycerol oxidation to glycerate. More recently, P.Landon *et al* have shown that Au/Al_2O_3 catalysts are selective for the oxidation of H_2 with molecular oxygen to form hydrogen peroxide (23, 24).

These examples demonstrate the immense potential of gold catalysts for selective oxidation reactions (25).

1.4. Oxidation of toluene

Selective oxidation of primary carbon-hydrogen bonds is of crucial importance in activating raw materials to form intermediates and final products for use in the chemical, pharmaceutical and agricultural business sectors (26). One class of raw materials is alkyl aromatics; toluene, for example, the simplest member of this class, can be oxidized to benzyl alcohol, benzaldehyde, benzoic acid, and benzyl benzoate as shown in scheme 1.1. These products are commercially significant as versatile intermediates in the manufacture of pharmaceuticals, dyes, solvents, perfumes, plasticizers, dyestuffs, preservatives, and flame retardants.
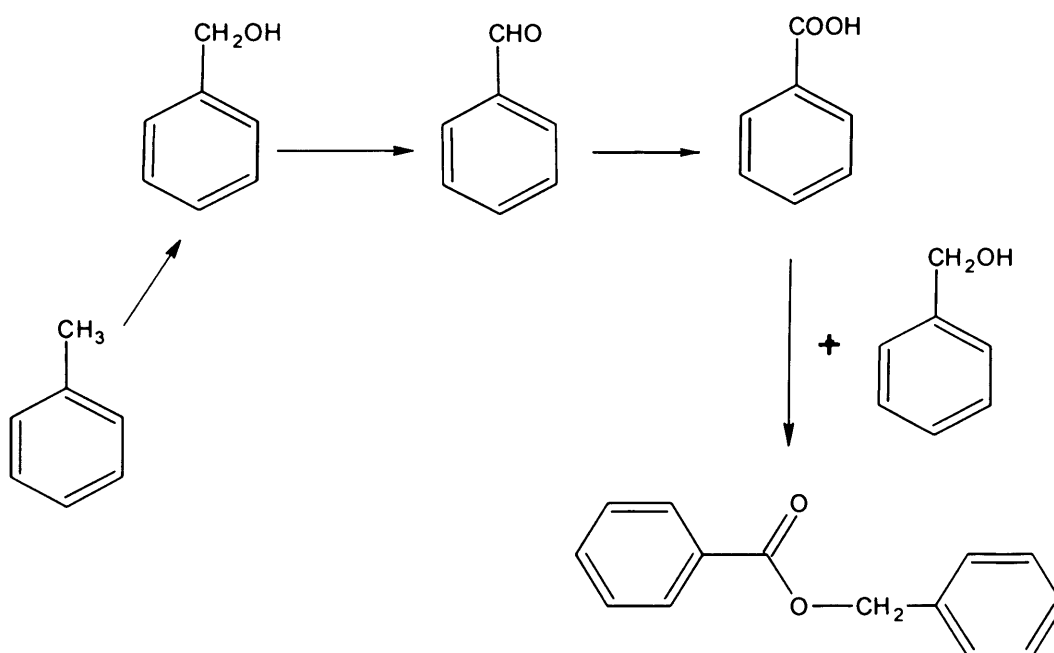
Scheme 1.1. General reaction pathways for toluene oxidation.

W.Partenheimer has reported that benzyl alcohol and benzaldehyde can be produced by the chlorination of toluene followed by hydrolysis/oxidative hydrolysis in some cases (27).

However the chlorination method has its own disadvantage of not conforming to the quality of food chemical codex (F.C.C), relatively high production cost, and large amount of pollutant residues. The major demand for benzaldehdye is being met by the dedicated benzoic acid production plants wherein the benzaldehyde is formed as a by-product in small proportions in air oxidation of toluene at higher conversion. As the process of benzoic acid from phenol is currently uneconomical, the benzoic acid produced through this process is unable to find good markets.

Benzaldeyde and Benzoic acid is produced by the liquid-phase cobalt-catalyzed reaction of toluene using oxygen at 165°C with acetic acid as solvent, but the conversion has to be limited to <15% to retain high selectivities (28–34). The use of halogens and acidic solvents makes these processes environmentally unfriendly.
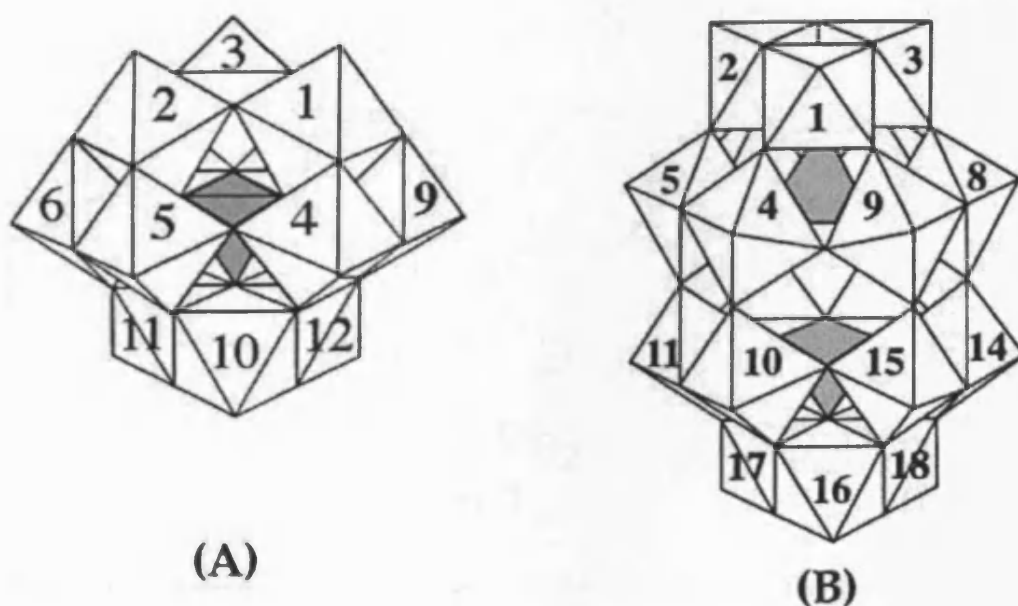
Figure 1.1. (A) Polyhedral representation of the Keggin-type POM, $[\alpha\text{-PW}_{12}\text{O}_{40}]^{3-}$, where one PO_4 group is shown as the internal, black tetrahedron. (B) Polyhedral representation of the Dawson-type POM, $[\alpha\text{-P2W}_{18}\text{O}_{62}]^{6}$, where two PO_4 groups are shown as the internal, gray tetrahedron. (29)

Nomiya *et al* (29) have reported vanadium (V) - substituted polyoxometalates catalyzed toluene oxidation using 30% H_2O_2. This process lacks true synthetic value because

of the relatively low yields (0.2-0.9% conversion). Vanadium (V) - substituted

polyoxometalates used for this process are shown in figure 1.1.

T.G.Carrell *et al* (30) has reported the oxidation of a variety of substrates (thioethers,

hydrocarbons, alkenes, benyzl alcohol and benzaldehyde) by *t*-BuOOH catalyzed by

$Mn_4O_4(O_2PPh_2)_6$ **(1)** and $Mn_4O_4(O_2P(p\text{-MePh})_2)_6$ **(2)** as shown in figure 1.2 .
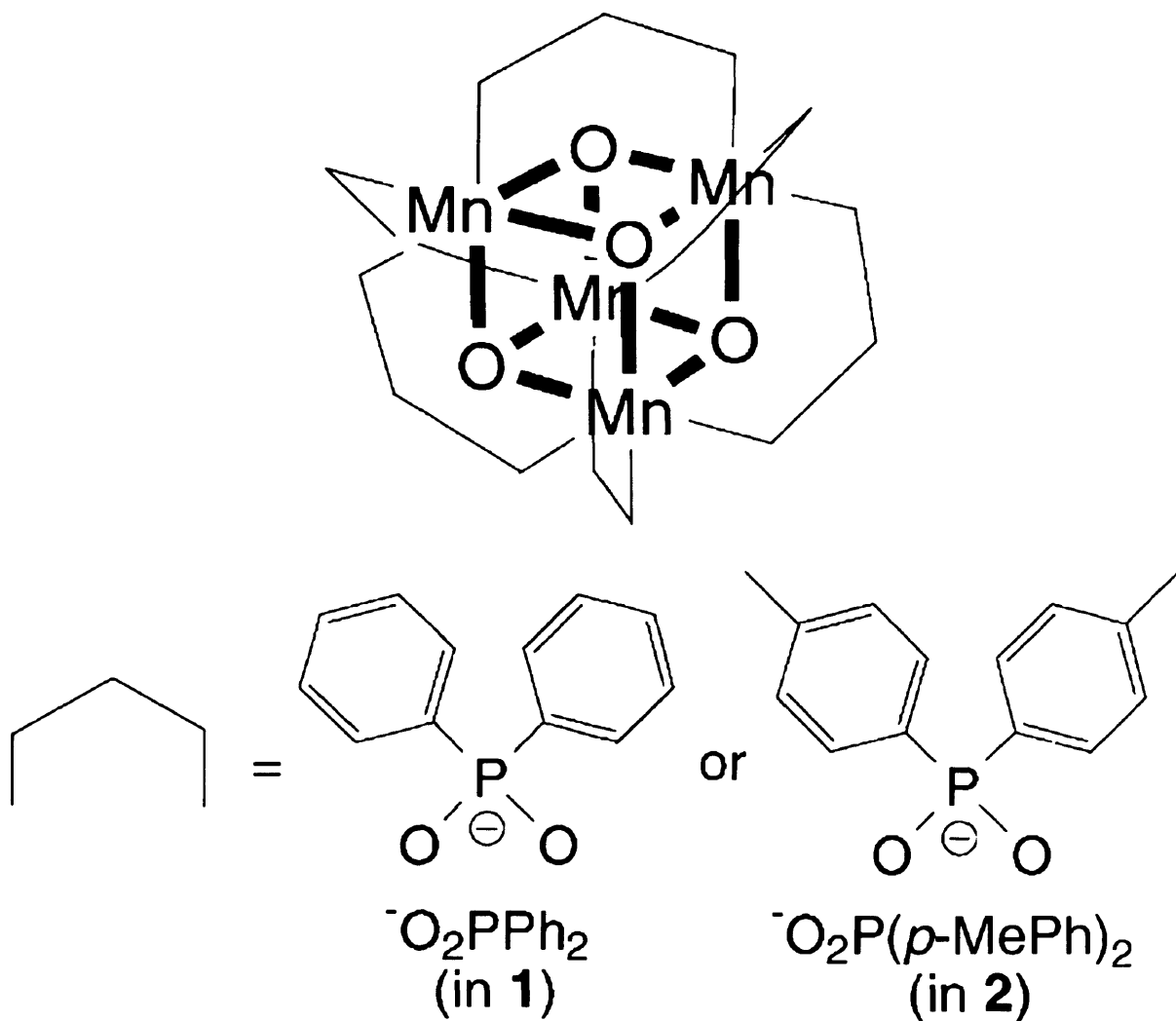
Figure 1.2. Molecular representation of the Manganese oxo cubane catalysts. Catalysts **1** and **2** differ only by a methyl group in the *para*-position of the phenyl moiety in the diphenylphosphinate ligand (30)

Saravanamurugan and co-workers (31) have done oxyfunctionalisation of toluene with

activated *t*-butyl hydroperoxide (TBHP) in the liquid phase over Ti(IV) supported on NaY

zeolite (Ti-NaY), silylated Ti-NaY (Sil-Ti NaY), silica-supported titanium isopropoxide (Si-

Ti(OiPr) and silylated silica-supported Ti(OiPr) {Sil-Si-Ti(OiPr)}at 30 and 80 °C. The major

products obtained with this method were benzaldehyde and benzoic acid. They found that

Silylation of catalysts favours high conversion of TBHP, thus proving that a hydrophobic

environment around the active Ti(IV) sites is important for selective adsorption of TBHP.

Liquid-phase oxidation of toluene by air in acetic acid medium, with cobalt acetate

catalyst and sodium bromide or paraldehyde as promoter, has been investigated by

H.V.Borgaonker and co-workers (32) with a view to developing a process for the production

of benzaldehyde with benzoic acid as a coproduct. Up to 10% conversion, the use of either

sodium bromide or paraldehyde as a promoter gave more than 90% yield of benzaldehyde. At

higher conversions, the yield of benzaldehyde decreased markedly and benzoic acid was

obtained as a co-product. Under suitable conditions it was possible to get 40% yield of

benzaldehyde, provided the overall conversion of toluene was restricted to 20%. Kantam *et al*

(33) have studied the liquid phase oxidation of toluene using Co/Mn/Br⁻ system in order to

produce benzyl alcohol and benzaldehyde from toluene. But the use of bromide as promotor

makes this process undesirable due to environmental and safety issues. Further, in bulk

chemical manufacture, traditional environmentally unacceptable processes are largely being

replaced by cleaner catalytic alternatives.

Attempts have been made to achieve for gas phase oxidation of toluene (35). Many of the

catalysts described are based on molybdenum in combination with tungsten (36), manganese

(37), cerium (38), or iron (39) in the form of mixed oxides or based on carriers such as

molecular sieves (40, 41). One of the most promising gas phase catalysts for benzaldehyde

production, free of molybdenum, is based on V_2O_5-supported on TiO_2, SiO_2, or Al_2O_3 (42–

45). The catalytic activity of these catalysts could be increased in some cases with additives

such as K_2SO_4 (45). But these catalysts are not economically viable as they have got low

surface area.

F.Konietzni *et al* have reported that toluene can be oxidized into benzaldehyde by an amorphous, microporous Mn/Si mixed oxide (46) under vapour phase conditions. After determining reaction conditions that exclude mass transport and pore diffusion limitations, selectivitity of 83% were achieved, but at a total conversion of 4%. The conversion profiles with respect to flow and particle size are shown in figure 1.3 and 1.4.
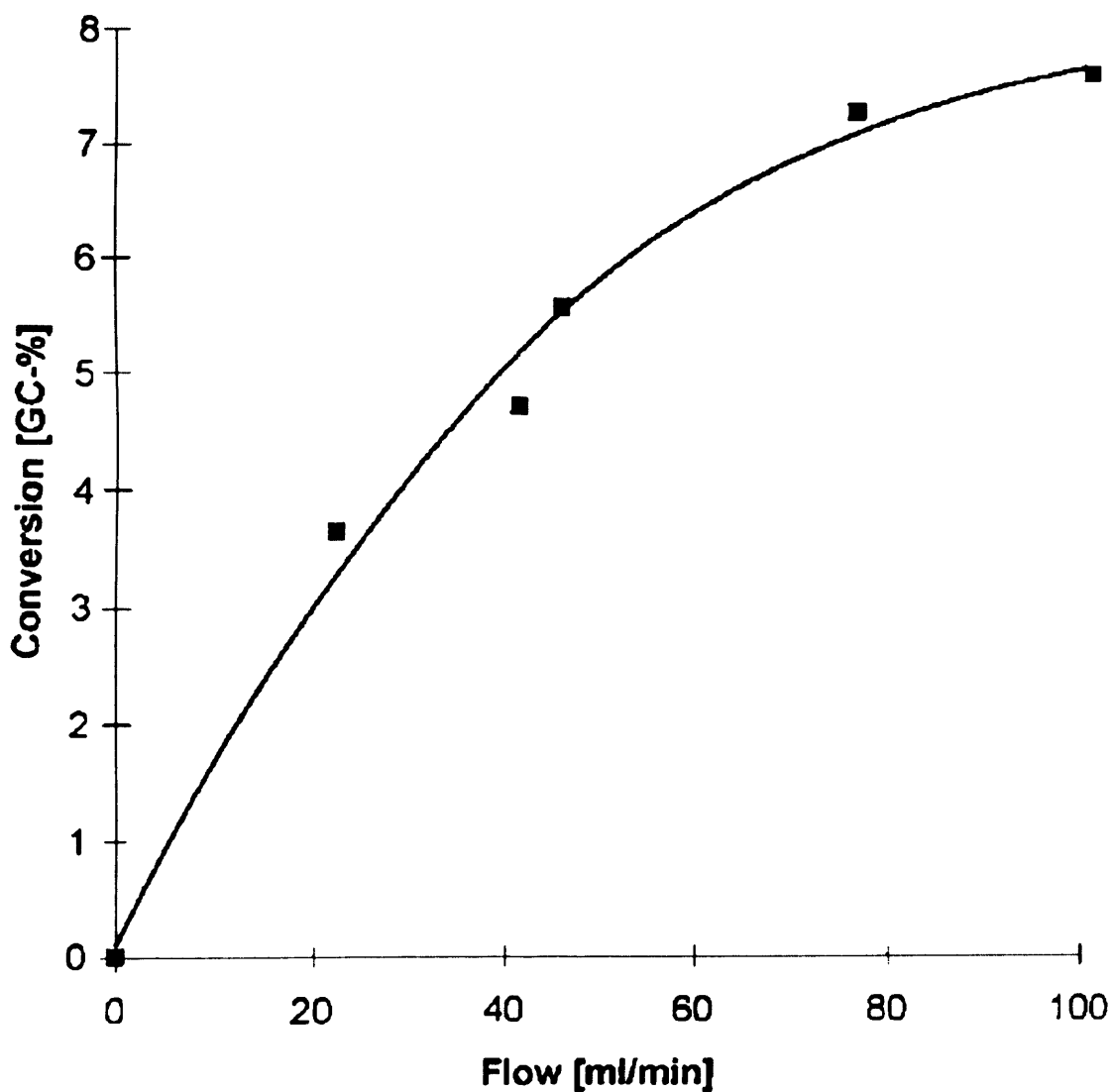
Figure 1.3. Vapour phase oxidation of toluene using Mn/Si mixed oxide (46)
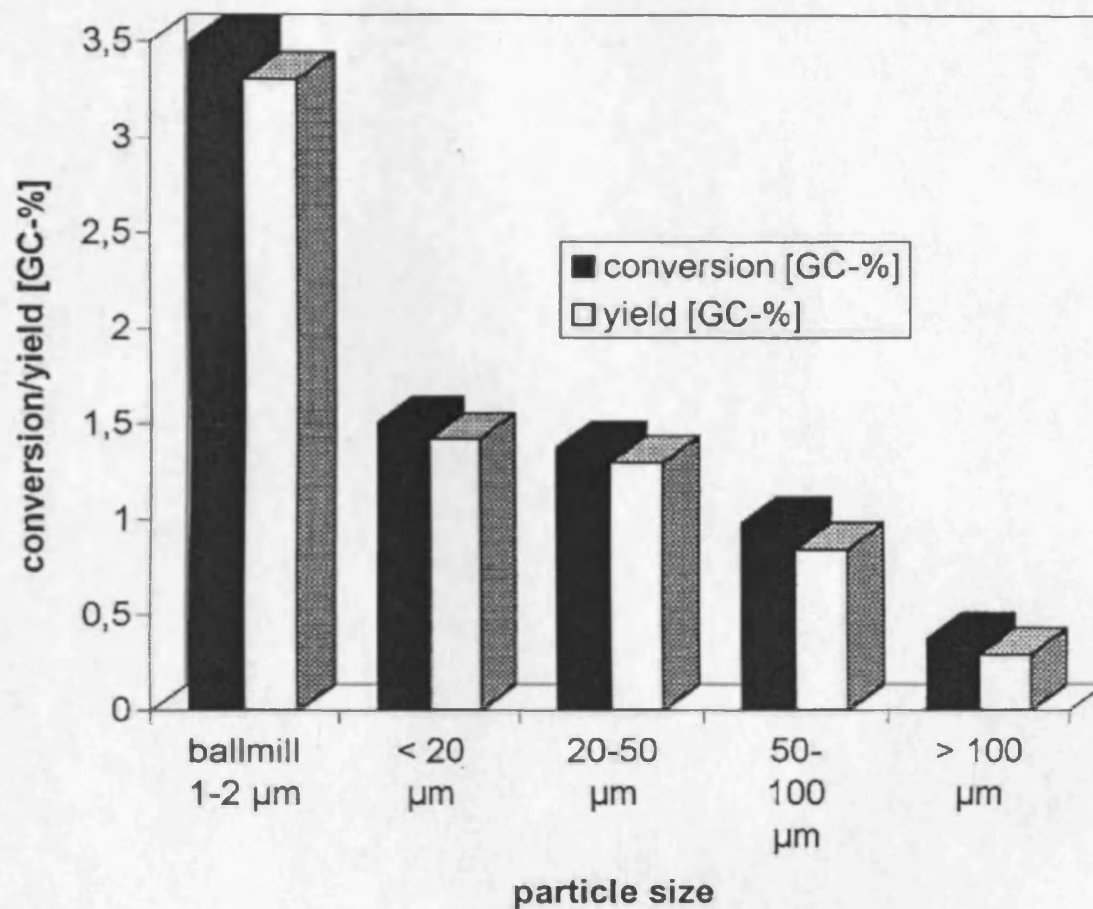
Figure 1.4. Vapour phase oxidation of toluene using Mn/Si mixed oxide. Conversion Vs particle size of Mn/Si mixed oxide (46)

Hence vapor-phase oxidation of toluene has the disadvantage that conversion must be limited to avoid over oxidation to CO_2 and other by-products (46). Attempts to overcome these problems have prompted the investigation of the use of supercritical CO_2 and ionic liquids. J.Zhu and co-workers (47) have studied toluene oxidation using aqueous emulsion containing ionic Co^{2+} and Br_2 species stabilised by fluorous surfactant-like species in supercritical CO_2–air mixture. Unfortunately the conversion was low. Further, Seddon and Stark (48) have reported the use of ionic liquid as a reaction media. Though this methodology works well for benzyl alcohol oxidation, it failed to work for toluene oxidation resulting very low conversion.

Often, heterogeneous catalysts are preferred over homogeneous catalysts, because these materials can be readily separated from the reaction mixture. Heterogeneous catalysts can also be readily used in flow reactors, facilitating the efficient production of materials using continuous processes. Another important aspect is carrying out the reactions under solvent free conditions. The use of a heterogeneous catalyst in the solvent-free condition has the advantages of minimizing separation difficulty and equipment corrosion.

For the oxidation of toluene, there have been many attempts to find a suitable oxidation catalyst, and to date these have used copper and manganese (49–51), cobalt (52), or chromium (53) catalysts. X.Li and co-workers (49) have studied toluene oxidation using molecular oxygen as an oxidant under solvent free conditions in the presence of Cu-Mn mixed oxides. The percentage conversion values of various bimetallic mixed oxides are shown in figure 1.5.
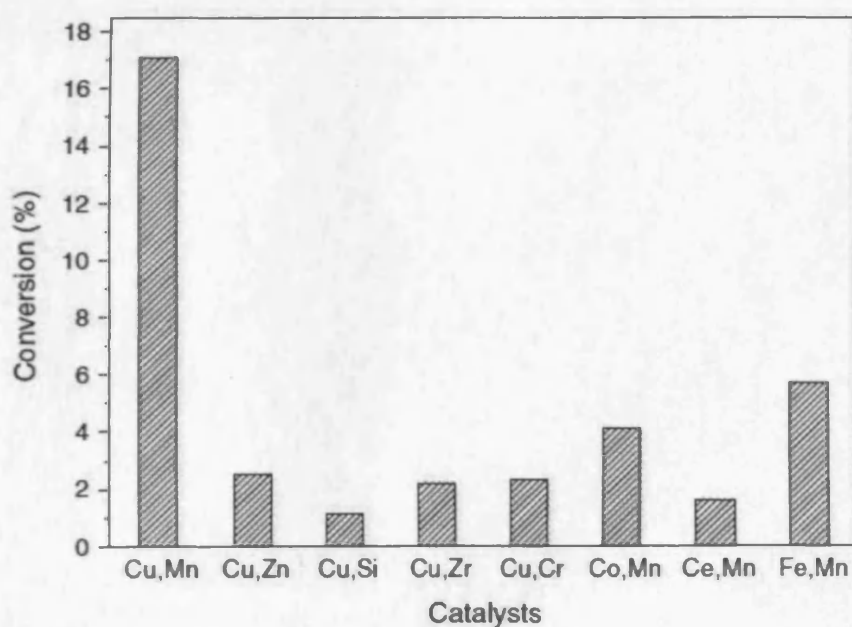
Figure 1.5. Conversion of toluene using copper and manganese based catalysts at 190 °C (49)

F.Wang *et al* (50) has reported that the liquid phase oxidation of toluene with molecular oxygen over heterogeneous catalysts of copper-based binary metal oxides. Among the copper-based binary metal oxides, iron-copper binary oxide (Fe/Cu=0.3 atomic ratio) was found to be the best catalyst in their process yielding 7% toluene conversion.

J.Gao *et al* (51) have reported $MnCO_3$ promoted toluene oxidation at 190 °C, in which $MnCO_3$ can readily form high-valence Mn species in the presence of oxygen and that this high-valence Mn species activates aromatic hydrocarbons to the corresponding radicals. R.L.Brutchy and co-workers (52) have studied the oxidation of alkyl aromatics using a pseudo-tetrahedral Co (II) complex grafted onto the surface of SBA-15 as shown in scheme 1.2, by utilizing tert-butyl hydroperoxide (TBHP) via an H-atom transfer mechanism.
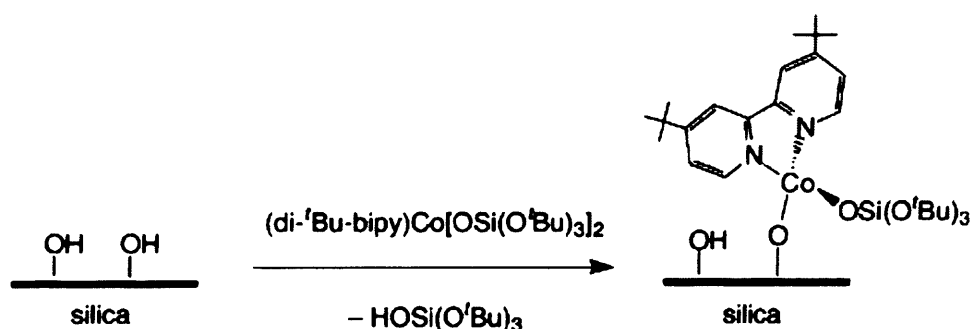
Scheme 1.2. A typical formation of Co (II) complex supported on SBA-15 (52)

A.P.Singh and T.Selvam (53) have reported that oxidation of toluene and alkanes catalyzed by chromium silicalite-1 (CrS-1) using t-butyl hydroperoxide (TBHP) as an oxidant. Mechanistically, it is assumed that catalytic properties of CrS-1 originate from the reversible transformation of Cr^{3+} and Cr^{5+} within the structure of CrS-1. But the use of chromium makes this process unsuitable as the chromium is toxic.

All these catalysts mentioned above perform very poorly with turnover numbers (TONs:

mole of product per mole of metal catalyst) of less than 100, even at temperatures in excess

of 190°C (Table 1.1).

Table 1.1: Reported toluene oxidation system

Catalyst	T/P	Oxidant	Conv (%)	Selectivity (%)				TON
				Benzyl alcohol	Benzal-dehyde	Benzoic acid	Benzyl benzoate	
Cu-Mn (1/1)	190 °C 1MPa	O₂	21.6	1.6	9.2	73.7	13.6	8
Cu-Fe/γ-Al₂O₃	190 °C 1MPa	O₂	25.4	1.0	27.4	71.6	n.d.	74
MnCO₃	190 °C 1MPa	O₂	25.0	5.3	9.7	80.8	n.d.	50
CoSBA-15	80 °C 1 atm	TBHP	8.0	n.d.	64.0	n.d.	n.d.	103
Cr/Silicalite	80 °C 1 atm	TBHP	18.4	5.2	23.3	25.7	n.d.	n.d.

There is clearly a need to develop heterogeneous catalysts for toluene oxidation that have

greatly improved activity while retaining selectivity. Recently, it has been shown that Au-Pd

alloy nanoparticles are very effective for the direct synthesis of hydrogen peroxide (54) and

the oxidation of primary alcohols using oxygen (55). J.K.Edwards *et al* (54) have synthesized

sub 10 nm Au-Pd nanoparticles (prepared by impregnation), which have shown that very

active for the synthesis of hydrogen peroxide, directly from oxygen and hydrogen (Scheme.

1.3).

$$H_2 + O_2 \xrightarrow{} H_2O_2 \nearrow^{H_2} 2\,H_2O$$
$$\searrow H_2O + 0.5\,O_2$$
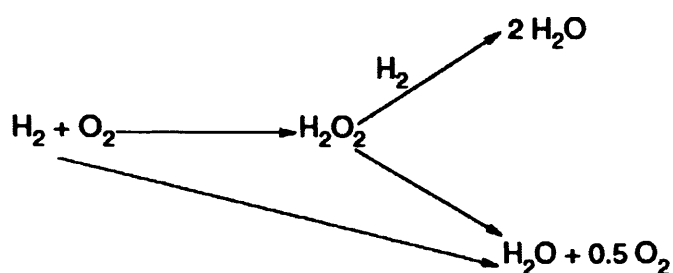
Scheme 1.3. Direct synthesis of hydrogen peroxide (54)

Further, Enache and co-workers (55) studied the oxidation of primary alcohols using oxygen (figure 1.6) in place of stoichiometric oxygen donors under solvent free conditions in the presence of AuPd core shell nanoparticles (Pd-shell, Au-core) prepared by impregnation. These catalysts have shown high turnover frequencies (86 500 – 270 000 turnovers per hour) for benzyl alcohol (relative of toluene) and 1-phenylethanol at 160 °C.
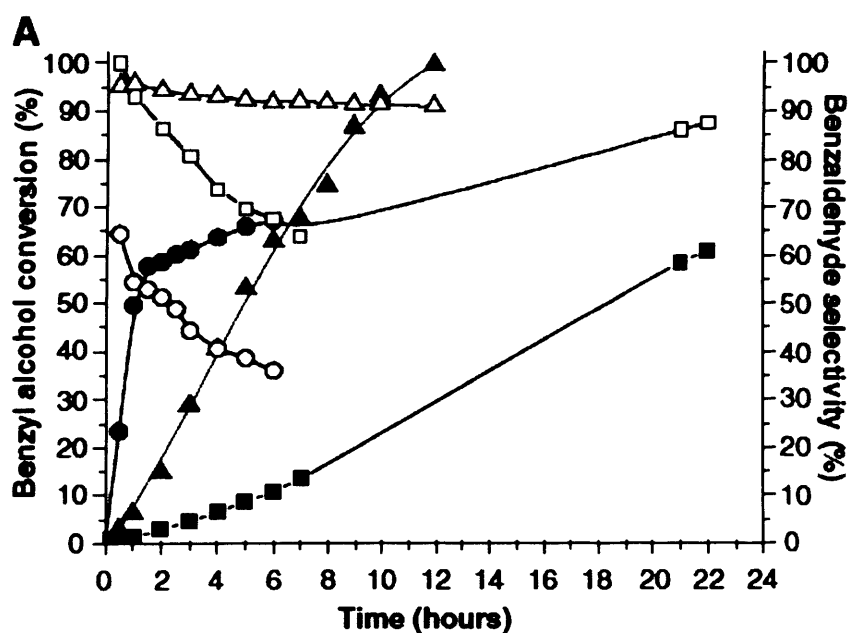
Figure 1.6. Benzyl alcohol conversion and selectivity in benzaldehyde with the reaction time at 373 K and 0.1 MPa pO_2. Squares, Au/TiO_2; circles, Pd/TiO_2; and triangles, $Au\text{-}Pd/TiO_2$. Solid symbols indicate conversion, and open symbols indicate selectivity (55)

The catalytic data show that the introduction of Au to Pd improves selectivity, and they believed that the surface of the bimetallic nanoparticles will still contain some gold. Hence,

they argued that the Au acts as an electronic promoter for Pd and that the active catalyst has a surface that is significantly enriched in Pd. Recent studies have started to provide insights into the nature of such effects. For example, Okazaki et al. (56) have shown, using a combination of experiment and theory that the electronic structure of Au in Au/TiO_2 catalysts is dependent on the particle size and Goodman and co-workers (57), using model studies, have shown that Au can isolate Pd sites within bimetallic systems.

This catalyst operates by establishing a reactive hydroperoxy intermediate as these intermediates are known to be involved in the enzymatic oxidation of primary carbon-hydrogen bonds (58). Colby *et al* (58) have found that Methane mono-oxygenase of Methylococcus capsulatus (Bath) catalyses the hydroxylation of C1-C8 n-alkanes, yielding mixtures of the corresponding 1- and 2-alcohols via reactive hydroperoxy intermediate. This indicates that both primary and secondary alkyl C-H bonds can be hydroxylated. The enzyme is apparently specific for the 1- and 2-alkyl carbon atoms, however, as there was negligible formation of 3- or 4-alcohols from pentane, hexane, heptane or octane.

Colby *et al* also tested toluene as a potential enzyme substrate because it is the phenyl derivative of methane and the methyl derivative of benzene and therefore contains two different groups that could be hydroxylated. A mixture of benzyl alcohol and cresol was produced when the enzyme was incubated with toluene, indicating that both the aromatic ring and the methyl group were hydroxylated (58). Hence, it is reasoned that it should be feasible for Au-Pd nanoparticles to be active for the oxidation of the primary carbon-hydrogen bonds in toluene too. The present works conveys that Au-Pd alloy nanoparticles prepared by a sol immobilization technique can give significantly improved activity for the oxidation of toluene under mild solvent-free conditions.

References:

1. Heterogeneous Catalysis: Principles and Applications, G.C. Bond, Oxford chemistry series.

2. Graham J. Hutchings, Chem. Commun., 1148–1164 (2008)

3. G. J. Hutchings and M. S. Scurrell, CATTECH, 7, 90 (2003)

4. M.C. Capel-Sanchez et al. Applied Catalysis A: General 246, 69–77 (2003)

5. Mehmet Ferdi Fellah, Rutger A. van Santen, and Isik Onal, J. Phys. Chem. C, 113 (34), 15307–15313 (2009)

6. Avelino Corma, Hermenegildo Garcia, Chem. Soc. Rev., 37, 2096–2126 (2008)

7. M. Haruta, T. Kobayashi, H. Sano and N. Yamada, Chem. Lett, 405 (1987)

8. G.J. Hutchings, J. Catal, 96, 292 (1985)

9. B. Nkosi, N.J. Coville, G.J. Hutchings, M.D. Adams, J. Friedl and F. Wagner, J. Catal. 128, 366 (1991)

10. A.S.K. Hashmi, Gold Bull. 37, 51 (2004)

11. G.C. Bond and D.T. Thompson, Catal. Rev.-Sci. Eng. 41, 319 (1999)

12. G.C. Bond and D.T. Thompson, Gold Bull. 33, 41 (2000)

13. M. Haruta, Gold Bull. 37, 27 (2004)

14. T. Hayashi, K. Tanaka and M. Haruta, J. Catal. 178, 566 (1998)

15. T.A. Nijhuis, B.J. Huizinga, M. Makkee and J.A. Moulijn, Ind. Eng. Chem. Res. 38, 884 (1999)

16. L. Prati and M. Rossi, J. Catal. 176, 552 (1998)

17. F. Porta, L. Prati, M. Rossi, S. Colluccia and G. Martra, Catal. Today, 61, 165 (2000)

18. C. Bianchi, F. Porta, L. Prati and M. Rossi, Top. Catal. 13, 231 (2000)

19. L. Prati, Gold Bull. 32, 96 (1999)

20. S. Biella and M. Rossi, Chem. Comm. 378 (2003)

21. S. Carrettin, P. McMorn, P. Johnston, K. Griffin and G.J. Hutchings, Chem. Commun. 696 (2002)

22. S. Carretin, P. McMorn, P. Johnston, K. Griffin, C.J. Kiely and G.J. Hutchings, Phys. Chem. Chem. Phys. 5, 1329 (2003)

23. P. Landon, P.J. Collier, A.J. Papworth, C.J. Kiely and G.J.Hutchings, Chem. Commun. 2058, (2002)

24. P. Landon, P.J. Collier, A.F. Carley, D. Chadwick, A.J.Papworth, A. Burrows, C.J. Kiely and G.J. Hutchings, Phys.Chem. Chem. Phys. 5, 1917 (2003)

25. Graham J. Hutchings, Silvio Carrettin, Philip Landon, Jennifer K. Edwards, Dan Enache,David W. Knight, Yi-Jin Xu, and Albert F. Carley. Topics in Catalysis, 38, 4 (2006)

26. R. A. Sheldon, J. K. Kochi, Metal-Catalyzed Oxidations of Organic Compounds (Academic Press, New York, 1981).

27. W. Partenheimer, Catal. Today 23, 69 (1995).

28. Y. Ishii, S. Sakaguchi, T. Iwahama, Adv. Synth. Catal. 343, 393 (2001).

29. K. Nomiya, K. Hashino, Y. Nemoto, M. Watanabe, J. Mol. Catal. Chem. 176, 79 (2001).

30. T. G. Carrell, S. Cohen, G. C. Dismukes, J. Mol. Catal. Chem. 187, 3 (2002).

31. S. Saravanamurugan, M. Palanichany, V. Murugesan, Appl. Catal. A Gen. 273, 143 (2004).

32. H. V. Borgaonkar, S. R. Raverkar, S. B. Chandalia, Ind. Eng. Chem. Prod. Res. Dev. 23, 455 (1984).

33. M. L. Kantam et al., Catal. Lett. 81, 223 (2002).

34. Snia-Viscosa, Hydrocarbon Proc. 134, 210 (1977).

35. Costantini, M., and Krumenacker, L., Stud. Surf. Sci. Catal. 44, 159 (1989).

36. Reddy,K. A., and Doraiswamy, L. K., Chem. Eng. Sci. 24, 1415 (1969).

37. Barbaux, Y., Dejonghe, S., Gengenbre, L., and Grzybowska, B., React. Kinet. Catal. Lett. 47, 1 (1992).

38. Fan, Y., Kuang,W., and Chen, Y., Chem. Let. 3, 231 (1997).

39. Zhang, H., Shen, J., and Ge, X., Hyperfine Interact. 69, 859 (1991).

40. Yoo, J. S., Lin, P. S., and Elfline, S. D., Appl. Catal. A General 124, 139 (1995).

41. Yoo, J. S., Appl. Catal. A General 143, 29 (1996).

42. Matralis, H. K., Papadopoulou, C., Kordulis, C., Elguezabal, A. A. Corberan, V. C. Appl. Catal. A General 126, 365 (1995).

43. Elguezabal, A. A., and Corberan, V. C., Catal. Today 32, 265 (1996).

44. G'und' uz, G., and Akpolat, O., Ind. Eng. Chem. Res. 29, 45 (1990).

45. Das, A., Chatterji, S. K., and Ray, S. K., Fuel Sci. Technol. 10, 85 (1991).

46. F. Konietzni, U. Kolb, U. Dingerdissen, W. F. Maier, J. Catal. 176, 527 (1998).

47. J. Zhu, A. Robertson, S. C. Tsang, Chem. Commun. (Camb.) 18, 2044 (2002).

48. K. R. Seddon, A. Stark, Green Chem. 4, 119 (2002).

49. X. Li et al., Catal. Lett. 110, 149 (2006).

50. F. Wang et al., Adv. Synth. Catal. 347, 1987 (2005).

51. J. Gao, X. Tong, X. Li, H. Miao, J. Xu, J. Chem. Technol. Biotechnol. 2002, 620 (2007).

52. R. L. Brutchey, I. J. Drake, A. T. Bell, T. Tilley, Chem. Commun. (Camb.) 2005, 3736 (2005).

53. A. P. Singh, T. Selvam, J. Mol. Catal. Chem. 113, 489 (1996).

54. J. K. Edwards et al., Science 323, 1037 (2009).

55. D. I. Enache et al., Science 311, 362 (2006).

56. K. Okazaki, S. Ichikawa, Y. Maeda, M. Haruta, M. Kohyama, Appl. Catal. A 291, 45 (2005).

57. M. Chen, D. Kumar, C.-W. Yi, D. W. Goodman, Science, 310, 291 (2005).

58. J. Colby, D. I. Stirling, H. Dalton, Biochem. J. 165, 395 (1977).

Chapter 2

Experimental

2.1. Outline

This chapter discusses the experimental methodology employed in this research project which is ''Solvent-free oxidation of primary carbon-hydrogen bonds in toluene using supported gold palladium alloy nanoparticles''. In this section, various preparation protocols of catalyst materials including impregnation, sol immobilisation are discussed. Further, instrumental methods for miscellaneous characterizations of catalysts, application of these catalysts for the oxidation of desired substrates, qualitative and quantitative analysis of products are detailed.

2.2. Catalyst Preparation

2.2.1. Impregnation method

2.5wt%Au-2.5wt%/TiO$_2$ catalyst was prepared by impregnation method. An aqueous solution of HAuCl$_4$.3H$_2$O (Johnson Matthey) (4.0816 ml, which is pipetted out from the stock solution containing 12.25 mg/ml Au) and an aqueous solution of PdCl$_2$ (Johnson Matthey) (16.51 ml, which is pipetted out from the stock solution containing 3.0287 mg/ml), 1.9 g of TiO$_2$ were added in a clean, empty 25 ml beaker. The beaker was placed on a heating plate with magnetic stirrer and started to stir and heat (temperature set point 90°C). Initially the solution was milk white. When the temperature increased, the colour of the solution turned to purple slowly. Once the water in the beaker evaporated out, the beaker was taken out from the heating plate and it was covered with aluminium foil and kept in oven for drying at 110°C for 16 hours and the small portion of the dried catalyst (typical 0.5 g) calcined at 400°C for 3 hours under static air condition. Similarly 2.5%Au-only and 2.5%Pd-only were prepared.

2.2.2. Sol immobilisation method (SI)

Au-Pd monometallic and bimetallic sols were prepared using the following procedure: An aqueous PdCl$_2$ and HAuCl$_4$ solution of the desired concentration was prepared individually (for

monometallic) as well as together (for bimetallic). The desired amount of a Polyvinyl alcohol (PVA) (Aldrich, MW=10 000, 80% hydrolyzed) 1 wt % solution was added (PVA/Total metals (wt/wt) = 1.2); a 0.1 M freshly prepared solution of $NaBH_4$ (Aldrich) ($NaBH_4$/Total metals (mol/mol) = 5) was then added to form a dark-brown sol. After 30 minutes of sol generation, the colloid was immobilised by adding activated carbon (or titania) (acidified to pH 1, by sulphuric acid) under vigorous stirring. The amount of support was calculated as having a total final metal loading of 1% wt. After 2 h the slurry was filtered, the catalyst washed thoroughly with distilled water (neutral mother liquors) and dried at 110 °C for 16 hours.

2.3. Characterization of catalysts

2.3.1. UV- Visible spectroscopy

The colloidal sols (before immobilising on a support) were characterised using a UV spectrometer (V-570, JASCO) in H_2O between 200 and 900 nm, in a quartz cuvette to monitor the intensity and position of the plasmon resonance band of metal nanoparticles.

For the pure Au sol, the appearance of the plasmon resonance was observed at 505 nm. This resonance peak is characteristic for gold nanoparticles with particle sizes below 10 nm (1, 2). In the case of the Pd monometallic sol, there is no surface plasmon band (1). The spectra resulting from the mixture of the two metal sols indicate the disappearance of the gold surface plasmon band as previously reported for this system (1) (figure 2.1). This is a phenomenon commonly found in the formation of sols of bimetallic nanoparticles where one of the component metals lacks a surface plasmon band. Deki et al (3) found dispersed nanoparticles of several Au-Pd compositions on a polymer thin film matrix and concluded that the progressive decrease of the gold plasmon band in the UV-vis spectra observed by increasing the palladium content was the result of changes in the band structure of the Au particles due to alloying with Pd.
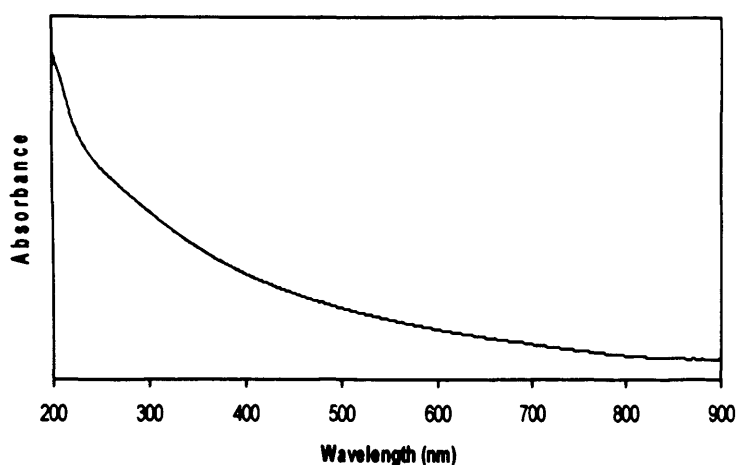
Figure 2.1. A typical UV-vis spectra of Au-Pd (0) sol showing no plasmon resonance band (4)

2.3.2. X-ray photoelectron spectroscopy

X-ray photoelectron spectra were recorded on a Kratos Axis Ultra DLD spectrometer employing a monochromatic Al Kα X-ray source (75-150W) and analyzer pass energy of 160 eV (for survey scans) or 40 eV (for detailed scans). Samples were mounted using double-sided adhesive tape, and binding energies were referenced to the C(1s) binding energy of adventitious carbon contamination which was taken to be 284.7 eV.

2.3.3. Transmission electron microscopy (TEM/STEM)

Samples of sol-immobilized catalysts were prepared for TEM/STEM analysis by dry dispersing the catalyst powder onto a holey carbon TEM grid. In the case of the starting AuPd-PVA sol, a drop of the colloidal sol was deposited, and then allowed to evaporate, onto a 300-mesh copper TEM grid covered with an ultrathin continuous C film. Phase contrast lattice imaging and high-angle annular dark field (HAADF) imaging experiments carried out using a 200kV JEOL 2200FS transmission electron microscope equipped with a CEOS aberration corrector kV in order to study the structural and compositional details of individual metal nanoparticles . This instrument was also fitted with an Oxford Instruments INCA TEM 300

system for energy dispersive X-ray (XEDS) analysis in order to determine particle size distributions and compositions.

2.4. Catalyst testing

2.4.1. Toluene oxidation

The toluene oxidation reactions were carried out in a stirred reactor (100 mL, Parr reactor). The vessel was charged with the desired substrate (10-40 mL) and catalyst (0.2-1.6 g). The autoclave was then purged 5 times with oxygen leaving the vessel at 150 psi pressure. The stirrer was set at 1500 rpm and the reaction mixture was raised to the required temperature. Samples from the reactor were taken periodically, *via* a sampling system.

2.4.2. Catalyst reuse studies

Decantation method

After the completion of the reaction, the mixture was centrifuged and the liquid above the solid catalyst was completely decanted. A fresh solution of the required volume of toluene was added and the reaction was repeated. The decanted liquid was analysed for leached metals using atomic absorption spectroscopy and inductively coupled plasma spectroscopy and metal concentrations were below the detection limits.

2.4.3. Benzyl alcohol oxidation

The benzyl alcohol oxidation reactions were carried out in a stirred reactor (Parr autoclave, 100 ml). The cleaned empty reactor vessel was charged with 40 ml of benzyl alcohol and 50 mg of a catalyst. The autoclave was purged 5 times with oxygen and the pressure inside the vessel was adjusted to 10 bar gauge. The stirrer was set at 1500 r.p.m. and the reaction mixture was heated at

the desired temperature. Samples from the reactor were taken out periodically through the sampling tube.

2.4.4. Analysis of products

For the identification and analysis of the products a GC-MS and GC (a Varian star 3400 cx with a 30 m CP-Wax 52 CB column) were employed. In addition the products were identified by comparison with known commercially pure samples. For the quantification of the amounts of reactants consumed and products generated, the external calibration method was used.

2.4.5. Toluene oxidation using H_2O_2

The toluene oxidation using H_2O_2 experiments were carried out in a stainless steel autoclave containing a Teflon liner vessel with a total volume of 50 ml. The hydrogen peroxide (50 %, 0.34 g, 5000 μmol) was weighed in a 10 ml standard flask and then the flask was made up to the mark with an aqueous solution of toluene (4.34×10^{-3} M, 10 ml, 43.4 mmol). Then the whole homogeneous solution was transferred to a reactor vessel containing a measured amount of catalyst, corresponding to 10^{-5} moles of total metal. The reactor was purged with helium with the pressure of 440 psi for 5 times, to get rid of all the atmospheric air from the system. The autoclave was heated to the desired reaction temperature (50°C), and the reaction mixture was vigorously stirred at 1500 rpm once the target temperature was reached. The reactions were carried out for a total of 0.5 h, after which the reactor was cooled in ice to below 12°C, in order to minimise the volatility of substrate as well as products. The resultant mixture was filtered and analysed with a combination of GC-MS and GC-FID.

References:

1. Bianchi, C. L.; Canton, P.; Dimitratos, N.; Porta, F.; Prati, L. Catal. Today 2005, 102-103, 203–212.

2. Link, S.; El-Sayed, M. A. J. Phys. Chem. B 1999, 103, 4212–4217.

3. S. Deki, K. Akamatsu, Y. Hatakenaka, M. Mizuhata and A. Kajinami, Nanostructured Mat. 11 (1999) 59.

4. James Pritchard, Lokesh Kesavan, Marco Piccinini, Qian He, Ramchandra Tiruvalam, Nikolaos Dimitratos, Jose A. Lopez-Sanchez, Albert F. Carley, Jennifer K. Edwards, Christopher J. Kiely, Graham J. Hutchings, Langmuir 2010, 26 (21), 16568–16577

Chapter 3

Solvent-Free Oxidation of Toluene

3.1. Outline

This chapter deals with the reaction optimisation of toluene oxidation under solvent free conditions. The effect of temperature, choice of supports, selection of catalyst preparation method, studying the effect of Au:Pd mol ratio in bimetallic Au-Pd sol catalysts, and attempts made to increase the conversion of toluene has been studied. These studies helped to screen the active catalyst and optimum reaction conditions to obtain high conversion of toluene. Further, this chapter discusses the results obtained from longer reactions of toluene oxidation with increased mass of catalyst, structure – activity relationship of the Au-Pd bimetallic sol catalysts, and results gained through low temperature oxidation of toluene. The catalysts are prepared by either impregnation or sol immobilisation methods. Most of the catalysts prepared uses activated carbon as the support although a few comparisons were made with TiO_2. Molecular oxygen is used as an oxidant for all the reactions throughout these studies. No solvent has been used throughout the studies.

3.2. Reaction optimization

3.2.1. Blank toluene oxidation

Toluene oxidation has been carried out in an autoclave parr reactor as described in chapter 2. As a first step, toluene oxidation has been performed with oxygen in the absence of a catalyst at elevated temperature *ca.* 160 - 190 °C in order to determine the blank baseline rate. The reason for choosing this temperature range is that many of the workers (1-3) have suggested activity for toluene in this window. A considerable conversion of toluene into its oxygenates was observed at 190 °C, but not at 160 °C as shown in figure 3.1 and table 3.1 respectively. The products which we identified from these reactions are benzyl alcohol, benzldehyde, benzoic acid and benzyl benzoate. There was no CO_2 formed.
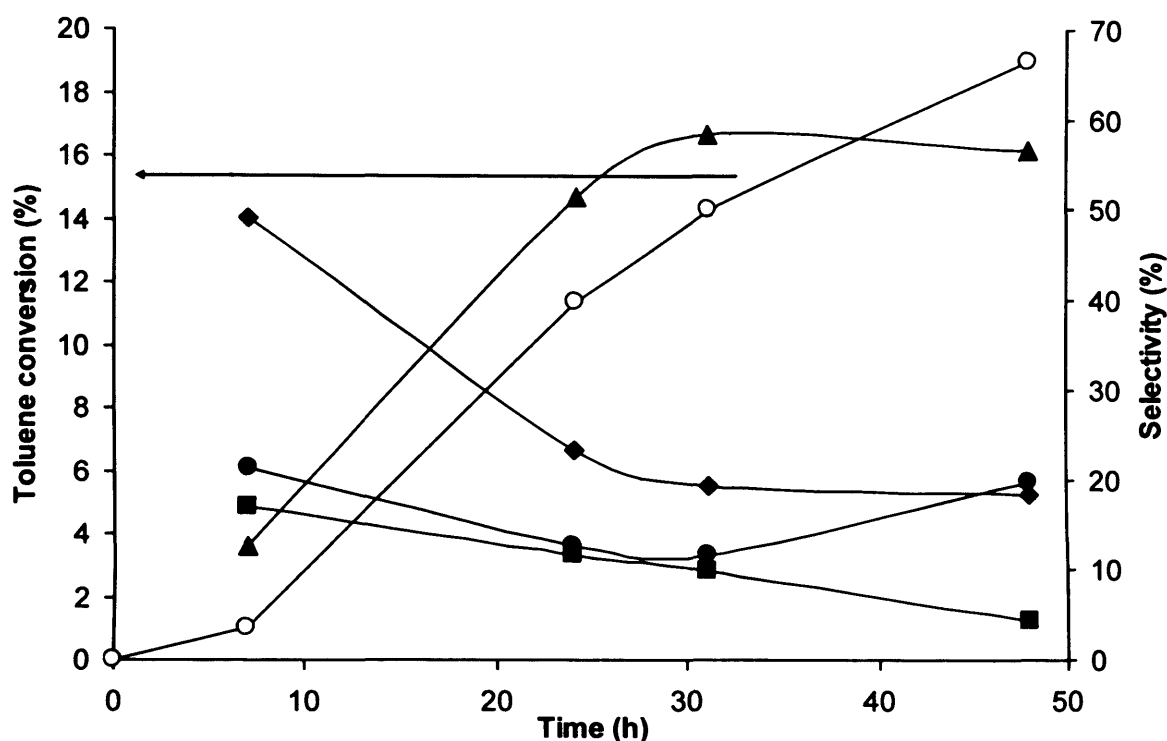
Figure 3.1. Toluene conversion and selectivity to benzyl alcohol, benzaldehyde, benzoic acid and benzyl benzoate in the absence of a catalyst at 190 °C. Reaction conditions: T = 190 °C (463K), pO_2 = 10 bar (0.1 MPa), stirring rate - 1500 rpm, substrate - 40 ml toluene, 48 h. Open symbol indicates conversion and solid symbols indicate selectivity. Key: ■ indicate selectivity to benzyl alcohol, ◆ indicate selectivity to benzaldehyde, ▲ indicate selectivity to benzoic acid, ● indicate selectivity to benzyl benzoate.

The blank toluene oxidation at 160 °C gave conversion of 0.2% after 7 h, whereas the experiment carried out at 190 °C yielded conversion of 0.9%. But at 48 h, the conversion drift was 2.9% and 18% respectively. This can be due to the involvement of O_2 di-radical which can initiate homogeneous oxidation processes at elevated temperatures and pressures. It has been found that such processes become substantial (18%) at 190 °C under our reaction conditions. In view of the potential role of O_2 di-radicals, the maximum reaction temperature in our studies has been restricted to 160 °C as the blank conversion at shorter reaction period was negligible and was very low at longer reaction times at this temperature.

Table 3.1: Liquid phase oxidation of toluene in the absence of catalyst at 160 °C

Catalyst	Time (h)	Conv (%)	Selectivity (%)				TON
			Benzyl alcohol	Benzaldehyde	Benzoic acid	Benzyl benzoate	
None	7	0.2	18.3	69.4	1.9	10.4	-
None	48	2.9	5.8	43.6	38.2	12.4	-

Reaction conditions: T = 160 °C (433K), pO_2 = 10 bar (0.1 MPa), stirring rate - 1500 rpm, substrate - 20 ml toluene

3.2.2. Toluene oxidation in the presence of catalyst supports

Further toluene oxidation experiments have been performed with the chosen catalytic supports which are carbon and TiO_2 at 160 °C for 7 h to check their contribution of activity in this system. The reason for choosing carbon and TiO_2 as catalytic supports is due to their high surface area (~900 m^2g^{-1}) and less acidic nature respectively. Moreover, these two supports have shown the ability to adsorb metal nanoparticles effectively followed by a homogeneous distribution and to reduce the by product formation during the course of the reaction (4, 5). The blank reaction in the absence of catalyst but in the presence of support is negligible for short reaction times (Table 3.2). This has allowed using these materials as catalytic supports.

Table 3.2: Liquid phase oxidation of toluene in the absence of catalyst, but in the presence of support at 160 °C

Support	Time (h)	Conv (%)	Selectivity (%)				TON
			Benzyl alcohol	Benzaldehyde	Benzoic acid	Benzyl benzoate	
Carbon*	7	0.1	11.4	72.6	0.1	16.0	-
TiO_2*	7	0.2	0.1	6.0	85.1	8.9	-

Reaction conditions: T = 160 °C (433K), pO_2 = 10 bar (0.1 MPa), stirring rate - 1500 rpm, substrate - 20 ml toluene, support - 0.4 g.

3.2.3. Toluene oxidation using mono and bimetallic Au Pd supported catalysts prepared by impregnation

To study the influence of catalysts on toluene oxidation, monometallic Au and Pd, bimetallic Au Pd supported on TiO_2 prepared by impregnation were tested initially, because these had previously been shown to be very active for H_2O_2 synthesis (6) and alcohol oxidation (5). The preparation of catalysts by the impregnation method was detailed in chapter 2. The reaction was performed in an autoclave parr reactor as described in chapter 2. The reaction conditions are as follows; T = 160 °C (433K), pO_2 = 10 bar (0.1 MPa), stirring rate - 1500 rpm, substrate - 40 ml toluene, substrate/metal molar ratio - 5200, t = 48 h. The catalyst amount used in this study has been adjusted for every reaction in order to maintain the substrate to metal molar ratio constant. It has been observed that monometallic Au/TiO_2 having 2.5wt% Au was not at all active for this reaction, whereas monometallic $2.5\%Pd/TiO_2$ and bimetallic $2.5\%Au2.5\%Pd/TiO_2$ gave 3.5% and 4.4% conversion after 48 hrs respectively (Table 3.3). The turnover numbers with these catalysts were poor. Thus, the Au, Pd monometallic and bimetallic catalysts prepared by the simple impregnation method were not found to be particularly active for toluene oxidation, although they did not produce any CO_2.

Table 3.3: Liquid phase oxidation of toluene at 160 °C for mono and bimetallic supported catalysts prepared by impregnation method.

Catalyst	Time (h)	Conv (%)	Selectivity (%)				TON
			Benzyl alcohol	Benzaldehyde	Benzoic acid	Benzyl benzoate	
2.5%AuTiO$_2$	0.5	0.2	89.9	10.1	0.0	0.0	
	1	0.2	91.4	8.6	0.0	0.0	
	7	0.2	78.0	13.7	8.3	0.0	
	24	0.3	70.4	20.3	5.4	3.9	
	31	0.3	47.1	35.5	7.4	10.0	
	48	0.5	20.0	53.1	5.8	21.2	23
2.5%Au2.5%Pd/TiO$_2$	0.5	0.1	52.3	32.8	9.5	5.3	
	1	0.1	31.3	56.9	2.5	9.3	
	7	0.4	14.9	63.4	12.7	9.0	
	24	3.0	5.3	43.4	31.3	20.0	
	31	3.5	4.7	41.4	32.1	21.8	
	48	4.4	3.6	31.4	40.4	24.6	174
2.5%Pd/TiO$_2$	0.5	0.1	30.6	44.1	23.8	1.5	
	1	0.1	6.8	47.5	39.0	6.7	
	7	0.6	7.7	66.8	16.5	9.1	
	24	2.7	5.7	50.7	30.4	13.2	
	31	2.9	4.8	47.6	33.8	13.8	
	48	3.5	3.2	37.4	43.3	16.1	185

Reaction conditions: T = 160 °C (433K), pO_2 = 10 bar (0.1 MPa), stirring rate - 1500 rpm, substrate - 40 ml toluene, substrate/metal molar ratio = 5200, TON (moles of products/moles of metal) at 48 h reaction. TON numbers were calculated on the basis of total loading of metals.

This can be understood by the fact that Au-Pd nanoparticles synthesized by the impregnation method can be relatively large (typically >6 nm) and have substantial compositional variations (Au core-Pd shell) (5, 7) (figure 3.2), which limits their reactivity.
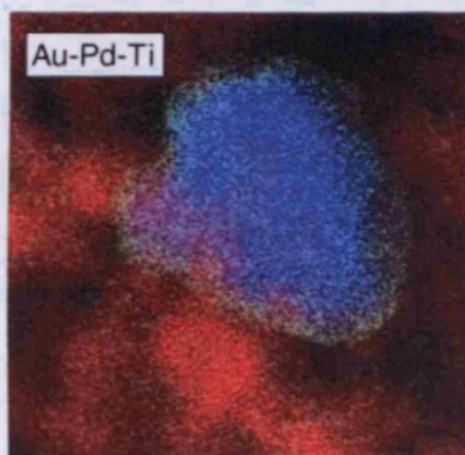
Figure 3.2. A reconstructed MSA-filtered Au-Pd-Ti composition map of a single particle (map - Ti, red; Au, blue; and Pd, green) for the impregnated 2.5wt%Au-2.5wt%Pd/TiO$_2$ (5)

3.2.4. Toluene oxidation using mono and bimetallic Au Pd supported catalysts

prepared by sol immobilisation

In order to design more effective catalysts for toluene oxidation, supported Au-Pd nanoparticles with smaller median particle sizes and a more controlled composition have been prepared and investigated. These were synthesized by sol immobilization of Au-Pd colloids, with carbon and TiO_2 as supports, a method that afforded tightly controlled particle size distributions and composition. Initially, bimetallic AuPd/C and AuPd/TiO_2 having a total metal loading 1wt% (the mol ratio of Au:Pd was 1:1.85 or often called as 1:1 wt ratio of Au:Pd, i.e. 0.5wt%Au, 0.5wt%Pd) catalysts were tested for toluene oxidation at 160 °C. The conversion was 4.8% and 2.1% respectively, after 7 hrs (Table 3.4), which is a promising result when compared with the literature (1-3).

Table 3.4: Liquid phase oxidation of toluene at 160 °C using the catalysts prepared by sol immobilisation method.

Catalyst	Time (h)	Conv (%)	Selectivity (%)				TON
			Benzyl alcohol	Benzaldehyde	Benzoic acid	Benzyl benzoate	
1%AuPd/C (1:1 wt or 1:1.85 mol)	7	4.8	0.9	12.7	10.3	76.1	310
1%AuPd/TiO_2 (1:1wt or 1:1.85 mol)	7	2.1	2.9	6.6	1.0	89.5	135

Reaction conditions: T = 160 °C (433K), pO_2 = 10 bar (0.1 MPa), stirring rate - 1500 rpm, substrate - 20 ml toluene, catalyst - 0.4 g, substrate/metal molar ratio = 6500, TON (moles of products/moles of metal) at 7 h reaction. TON numbers were calculated on the basis of total loading of metals.

This encouraging result lead to the search for the optimal Au:Pd ratio for toluene oxidation by keeping 1wt% total metal on the catalysts. Having shown double the activity of $Au-Pd/TiO_2$, the Au-Pd/C has been chosen for further studies throughout this work.

3.2.4.1. Studying the effect of Au:Pd molar ratio of Au-Pd bimetallic sol catalysts upon toluene oxidation

A systematic set of carbon supported Au-Pd colloidal nanoparticles having a range of Au/Pd ratios (by keeping 1wt% total metal) prepared by sol immobilisation were tested for toluene oxidation at 160 °C for 7 hrs (Table 3.5). The molar ratio of substrate to metal was kept constant as 6500 for all the reactions in this section. For all catalysts, no CO_2 formation was observed; the only products were benzyl alcohol, benzaldehyde, benzoic acid, and benzyl benzoate. By itself, Au was not active for toluene oxidation, but the addition of Pd significantly enhanced the conversion, demonstrating a clear synergistic effect for the Au-Pd catalysts as compared with the monometallic species. The catalysts have been structurally characterized using a combination of UV-visible spectroscopy, transmission electron microscopy, STEM HAADF/XEDS, and X-ray photoelectron spectroscopy (See Thesis section 5.2.1). Characterizations of these catalysts are well detailed in associated with benzyl alcohol oxidation using the same set of catalysts. The Au-Pd nanoparticles are found in the majority of cases to be homogeneous alloys, although some variation is observed in the AuPd composition at high Pd/Au ratios.

Also, a physical mixture of the separate Au/C and Pd/C catalysts showed no enhancement (Table 3.5, last entry), highlighting the molecular-scale nature of the synergy. The observed synergy is due to electronic and morphological features because transmission electron microscopy (TEM) shows that the mean particle size of the nanoparticles decreases slightly on the addition of Au to Pd (Table 3.6).

Table 3.5: Effect of Au:Pd mol ratio studied for liquid phase oxidation of toluene at 160 °C using the catalysts prepared by sol immobilisation method

Catalyst	Metal (%)	Au:Pd mol ratio	Conv (%)	Selectivity (%)				TON
				Benzyl alcohol	Benzal-dehyde	Benzoic acid	Benzyl benzoate	
Au/C	1	1:0	0.2	9.0	81.9	0	8.1	11
Au-Pd/C	1	7:1	0.3	28.4	57.6	6.2	7.8	17
Au-Pd/C	1	3:1	1.5	1.8	63.4	3.1	31.4	95
Au-Pd/C	1	1:1.85	4.8	0.9	12.7	10.3	76.1	310
Au-Pd/C	1	1:2	5.3	1.2	8.3	11.1	79.3	350
Au-Pd/C	1	1:3	5.2	1.9	8.5	10.3	79.3	340
Au-Pd/C	1	1:7	4.3	9.6	13.6	7.3	69.5	280
Pd/C	1	0:1	1.6	3.9	56.4	3.3	36.4	105
Au/C + Pd/C*	1	1:1.85	1.6	0.8	26.2	11.4	61.6	105

Reaction conditions: T = 160 °C (433K), pO_2 = 10 bar (0.1 MPa), stirring rate - 1500 rpm, substrate - 20 ml toluene, catalyst – variable, substrate/metal molar ratio = 6500, *Reaction of a physical mixture composed of 1 wt % Au/C and 1 wt % Pd/C. TON (moles of products/moles of metal) at 7 h reaction. TON numbers were calculated on the basis of total loading of metals.

Table 3.6: Particle sizes of metal clusters in mono and bimetallic supported catalysts prepared by sol immobilisation

Catalysts[a]	Au/C	Pd/C	Au-Pd/C[b]	Au/TiO$_2$	Pd/TiO$_2$	Au-Pd/TiO$_2$[b]
Mean particle size nm	4.7	6.3	3.7	4.6	4.8	3.9
Median particle size nm	4.0	5.0	3.3	3.9	3.8	3.5

[a] metal loading – 1% total in all the catalysts, [b] Au:Pd = 1:1 wt (1:1.85 mol)

When Au-rich catalysts (1:0, 7:1, 3:1) were used, some benzyl alcohol was formed, but this was readily oxidized to the main product benzaldehyde, as this sequential oxidation is rapid at this temperature (5). We consider the initial oxidation of toluene to involve a surface hydroperoxy intermediate formed from the interaction of the metal with oxygen and toluene. However, as the fraction of Pd in the alloy was increased (1:1.85, 1:2, 1:3, 1:7), the selectivity to benzyl benzoate became dominant. The optimum catalyst composition found was a 1:2 Au:Pd molar ratio (approximately 1:1 by weight or 1:1.85 by mol). The turnover frequency (TOF: mole of product formed per mole of metal per hour) of toluene oxidation after 7 hours of reaction using this catalyst was ~50. For the sake of convenience, catalyst having equal weight of each metal (Au:Pd 1:1 wt or 1:1.85 mol) with 1wt% total metal loading has been used for further studies.

3.3. Attempts to increase the conversion of toluene

There were several approaches considered to increase the conversion of toluene under our reaction conditions which are 160 °C temperature, 10 bar O_2 partial pressure. The first approach was to increase the catalyst amount in our reaction conditions as the number of substrate molecules activated in a given time is proportional to the number of active sites. The second approach was to increase the contact time (Reaction duration) between catalyst surface and substrate molecules, So that the conversion of the substrate can be elevated. The experimental results are shown in the following sections.

3.3.1. Effect of catalyst mass on toluene oxidation
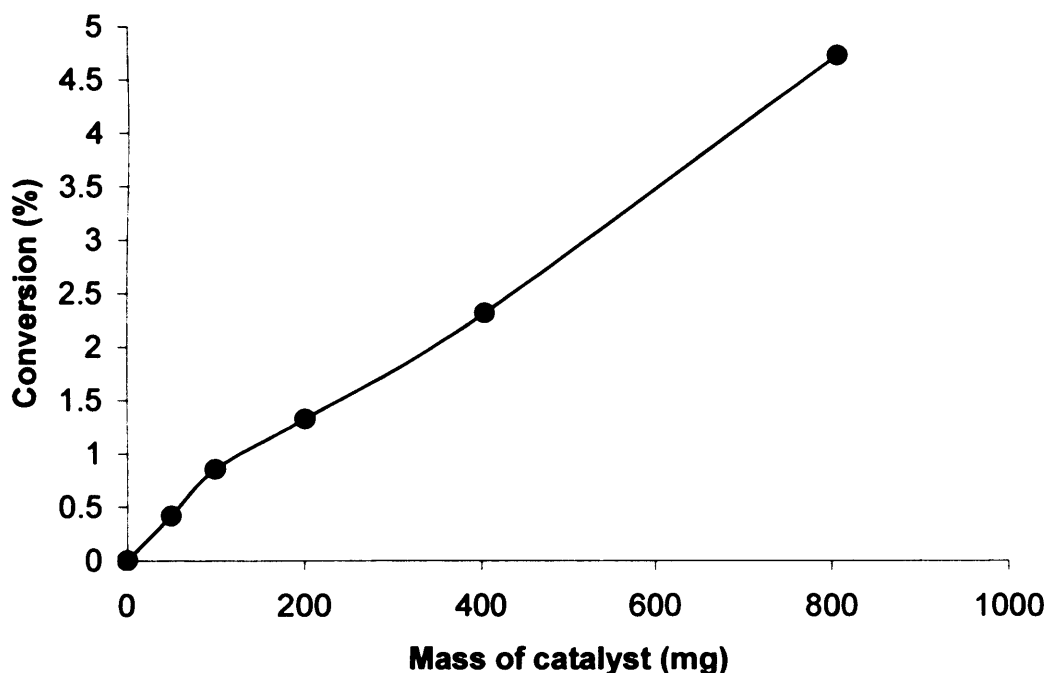
Figure 3.3. Toluene conversion as a function of catalyst mass: T = 160 °C (433K), pO_2 = 10 bar (0.1 MPa), stirring rate - 1500 rpm, substrate - 40 ml toluene, catalyst – 0.05-0.8 g 1wt%AuPd/C_{SIw} SI: sol-immobilisation method, w: weight ratio (1/1), substrate/metal mol ratio - 104000-6500, reaction time - 7 h. (Data table given in appendix, at the end of this chapter)

In this study, toluene oxidation reactions have been carried out using various masses of catalyst. The catalyst employed in all these reactions was the most active 1%AuPd/C (1:1 wt) prepared by sol immobilisation. The other reaction conditions were remained unchanged. The results reveal that increasing the catalyst mass has a linear effect on the conversion of toluene (figure 3.3) and turnover frequency (TOF) remained constant indicating that there were no diffusion limitations apparent.
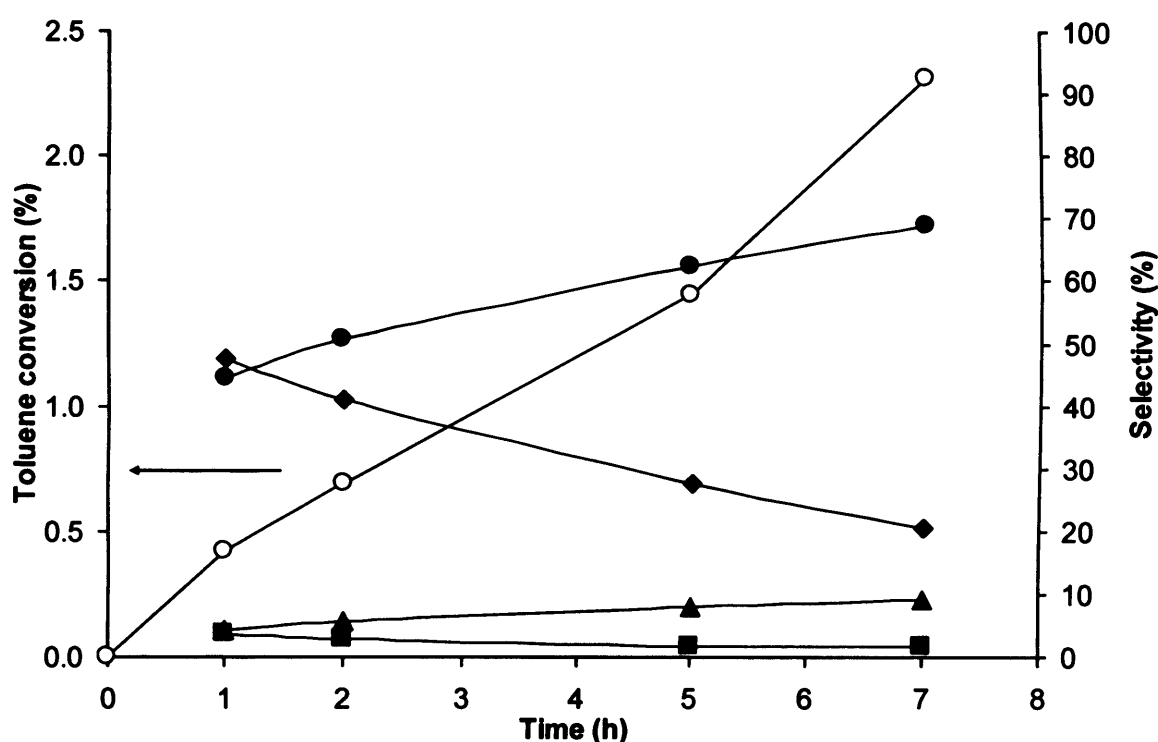
Figure 3.4. Toluene conversion and selectivity to benzyl alcohol, benzaldehyde, benzoic acid and benzyl benzoate: Reaction conditions: T = 160 °C (433K), pO_2 = 10 bar (0.1 MPa), stirring rate - 1500 rpm, substrate - 40 ml toluene, catalyst – 0.4 g 1wt%AuPd/C$_{SIw}$, SI: sol-immobilisation method, w: weight ratio (1/1). substrate/metal molar ratio = 13000, t = 7 h. Open symbol indicates conversion and solid symbols indicate selectivity. Key: ■ indicate selectivity to benzyl alcohol, ◆ indicate selectivity to benzaldehyde, ▲ indicate selectivity to benzoic acid, ● indicate selectivity to benzyl benzoate.

A typical reaction profile over an initial 7-hour reaction period using a higher substrate-to-metal ratio at 160°C has been shown in figure 3.4. This experiment showed that the toluene

conversion increases linearly over this time scale and the selectivity to benzyl benzoate also increases as the selectivity to benzaldehyde decreases.

3.3.2. Effect of reaction time on toluene oxidation

In order to increase the conversion of toluene, the toluene oxidation experiment has been prolonged for 48 h as the contact time (Reaction duration) between catalyst surface and substrate molecules may play a significant role in increasing the conversion.

Table 3.7: Toluene oxidation performed for 48 hrs using the catalysts prepared by sol immobilisation

Catalyst	Time (h)	Conv (%)	Selectivity (%)				TON
			Benzyl alcohol	Benzaldehyde	Benzoic acid	Benzyl benzoate	
1%Au-Pd/C	48	50.8	0.1	1.1	4.5	94.3	3300
1%Au-Pd/TiO$_2$	48	24.1	0.5	1.2	2.8	95.5	1570

Reaction conditions: T = 160 °C (433K), pO_2 = 10 bar (0.1 MPa), stirring rate - 1500 rpm, substrate - 10 ml toluene, catalyst – 0.2 g, substrate/metal molar ratio = 6500, TON (moles of products/moles of metal) at 48 h reaction. TON numbers were calculated on the basis of total loading of metals.

In this regime, much higher toluene conversions were attained and no CO_2 was observed. Once again only four products were observed: benzyl alcohol, benzaldehyde, and benzoic acid in trace amounts and benzyl benzoate as the dominant product (~95%) for both catalysts. The carbon supported catalyst was typically twice as active as TiO$_2$ supported catalysts over this longer time scale, exhibiting a TON of 3300 with ~3150 mol of benzyl benzoate per mole of metal produced over the reaction period (Table 3.7).

From these two approaches, it is obvious that increasing catalyst mass and prolonging the reaction time can facilitate the conversion of toluene under our reaction conditions. Hence, the

further experiments have been designed to have low substrate to metal molar ratio and longer

reaction times.

3.4. Toluene oxidation using a lower substrate/metal ratio at longer reaction times

Toluene oxidation experiments have been carried out using a lower substrate/metal molar

ratio for longer hours to obtain high conversion. Initially, the most active 1%AuPd/C was

tested at 160 °C under 10 bar O_2 pressure. Samples were collected periodically through our

in-built sampling system in the autoclave in order to know the course of the reaction. The

conversion continued to increase steadily, fully depleting the toluene after 110 hrs (figure

3.5.). The selectivity of benzyl benzoate was ~86% at 110 hrs. To claim the contribution of

synergistic effect arose from gold and palladium, catalysts containing individual metal was

tested for toluene oxidation under the same conditions. The monometallic Au and Pd

catalysts showed very low conversion (8%) over 110 hours (Table 3.8), confirming again that

there is a synergistic effect in bimetallic gold palladium sol catalysts for toluene oxidation

system.
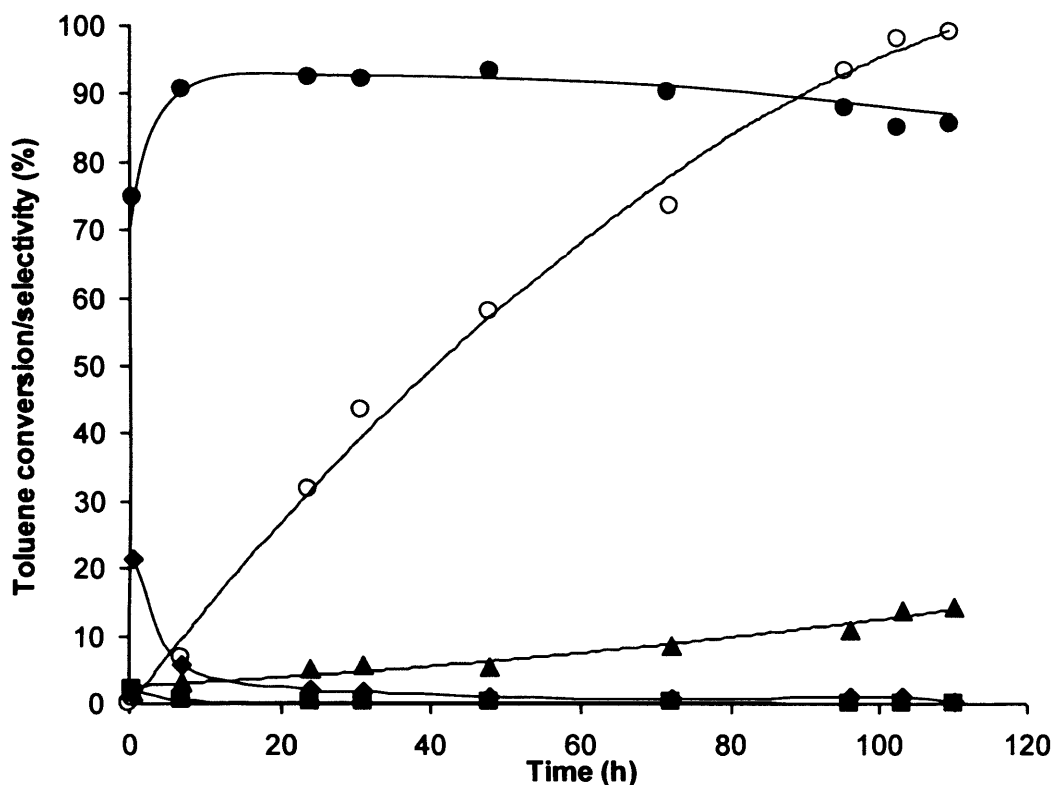
Figure 3.5. Toluene conversion and selectivity to benzyl alcohol, benzaldehyde, benzoic acid and benzyl benzoate:: Reaction temperature at 160 °C (433K) and 0.1 MPa pO_2, 20 ml toluene, 0.8 g of catalyst, toluene/metal molar ratio=3250 and reaction time: 110 h. Circles, 1wt% AuPd/C_{SIm}, SI: sol-immobilisation method, m: molar ratio (Au/Pd=1/1.85). Open symbol indicates conversion and solid symbols indicate selectivity. Key: ■ indicate selectivity to benzyl alcohol, ◆ indicate selectivity to benzaldehyde, ▲ indicate selectivity to benzoic acid, ● indicate selectivity to benzyl benzoate.

Table 3.8: Toluene oxidation performed using a lower substrate/metal molar ratio by employing the catalysts prepared by sol immobilisation

| Catalyst | Time (h) | Conv (%) | Selectivity (%) | | | | TON |
			Benzyl alcohol	Benzaldehyde	Benzoic acid	Benzyl benzoate	
1%Au/C	0.5	0.7	35.6	53.1	6.9	4.4	
	7	0.8	6.9	82.8	3.3	7.0	
	24	2.5	0.8	77.1	13.9	8.2	
	31	3.3	0.7	69.3	21.3	8.7	
	48	3.9	0.5	57.4	32.7	9.4	
	72	5.5	0.3	38.1	51.3	10.3	
	96	7.0	0.2	28.1	61.3	10.4	
	103	7.9	0.2	24.8	64.2	10.8	
	110	8.1	0.2	23.7	64.9	11.2	264
1%AuPd/C^5	0.5	0.9	2.1	21.4	1.8	74.7	
	7	6.9	0.6	5.7	3.0	90.7	
	24	31.8	0.2	2.0	5.3	92.5	
	31	43.4	0.2	1.7	5.8	92.3	
	48	58.1	0.3	1.0	5.4	93.4	
	72	73.8	0.2	0.9	8.6	90.3	
	96	93.4	0.1	1.0	10.9	88.0	
	103	98.1	0.1	1.1	13.8	85.1	

	110	99.3	0.1	0.2	14.2	85.6	3226.9
1%Pd/C	0.5	0.4	2.7	62.2	1.8	33.3	
	7	1.3	2.4	53.5	6.4	37.7	
	24	2.8	1.7	30.8	14.4	53.1	
	31	3.1	1.4	27.4	15.4	55.8	
	48	3.9	1.0	22.5	16.9	59.6	
	72	5.7	1.0	16.9	15.1	67.0	
	96	6.7	0.7	13.7	17.5	68.1	
	103	7.8	0.3	12.0	18.5	69.2	
	110	8.0	0.2	10.7	19.1	70.0	262

Reaction conditions: T = 160 °C (433K), pO_2 = 10 bar (0.1 MPa), stirring rate - 1500 rpm, substrate - 20 ml toluene, catalyst – variable amount, substrate/metal molar ratio = 3250, TON (moles of products/moles of metal) at 110 h reaction. TON numbers were calculated on the basis of total loading of metals. $ - 1:1 wt Au:Pd

The toluene conversion was also found to increase linearly with catalyst mass (figure 3.3)

Hence, with appropriate tuning of catalyst loading and reaction conditions, it is evident that

complete and selective conversion of toluene to the desirable products can be achieved (Table

3.9, show results of an initial optimization).

Table 3.9: Toluene oxidation performed using a very low substrate/metal molar ratio by employing the catalysts prepared by sol immobilisation

| Time (h) | Conversion (%) | Selectivity (%) | | | | TON[b] |
		Benzyl alcohol	Benzaldehyde	Benzoic acid	Benzyl benzoate	
0.5	1.8	2.1	11.6	0.8	85.5	29
7	21.5	0.3	1.8	3.1	94.8	350
24	82.9	0.1	0.8	7.3	91.8	1347
27	94.4	0.2	1.0	13.3	85.5	1534

Reaction conditions: T = 160 °C (433K), pO_2 = 10 bar (0.1 MPa), stirring rate - 1500 rpm, substrate - 20 ml toluene, catalyst - 1.6 g of 1%AuPd/C_{SIw}. SI – Sol immobilisation, w- 1:1 wt Au:Pd, substrate/metal molar ratio = 1625, TON (moles of products/moles of metal) numbers were calculated on the basis of total loading of metals.

Furthermore, toluene oxidation experiment has been done at the temperature little less

than 160 °C, which is 140 °C. The idea behind this experiment was to increase the selectivity

of benzyl benzoate to certain extent as the temperature can play a role of tuning the

selectivity distribution of the products. The experiment had shown 95% yield of benzyl

benzoate with full conversion of toluene (Table 3.10). The formation of benzyl benzoate is

discussed in chapter 4.

Table 3.10: Toluene oxidation performed at 140 °C by employing the catalysts prepared by sol immobilisation

Time (h)	Conversion (%)	Selectivity (%)				TON
		Benzyl alcohol	Benzaldehyde	Benzoic acid	Benzyl benzoate	
0.5	0.02	0	59.3	0	40.7	
7	3.2	0.2	7.6	1.0	91.2	
24	14.3	0.2	2.7	2.2	94.9	
31	17.3	0.1	2.5	2.5	94.9	
96	65.6	0.1	0.6	2.2	97.1	
120	78.7	0.1	0.5	1.2	98.2	
134	82.1	0.1	0.4	1.2	98.2	
162	89.9	0.1	0.4	1.4	98.1	
182	92.8	0.1	0.6	2.7	96.6	
205	95.9	0.1	0.6	4.3	95.0	
231	97.1	0.1	0.9	6.0	93.0	1578

Reaction conditions: T = 140 °C (433K), pO_2 = 10 bar (0.1 MPa), stirring rate - 1500 rpm, substrate - 20 ml toluene, catalyst – 0.8 g of 1%AuPd/C_{SIw}. SI – Sol immobilisation, w- 1:1 wt Au:Pd, substrate/metal molar ratio = 3250, TON (moles of products/moles of metal) numbers were calculated on the basis of total loading of metals.

3.5. Structure-activity relationship of Au-Pd bimetallic sol catalyst system

To determine the origin of the differences in activity (Table 3.7) between the two catalysts (based on carbon and TiO₂), we have characterized the common starting sol and the two sol-immobilized materials using electron microscopy. Figure 3.6 shows a representative scanning TEM (STEM) high-angle annular dark field (HAADF) image of the starting colloidal particles deposited onto a carbon film.
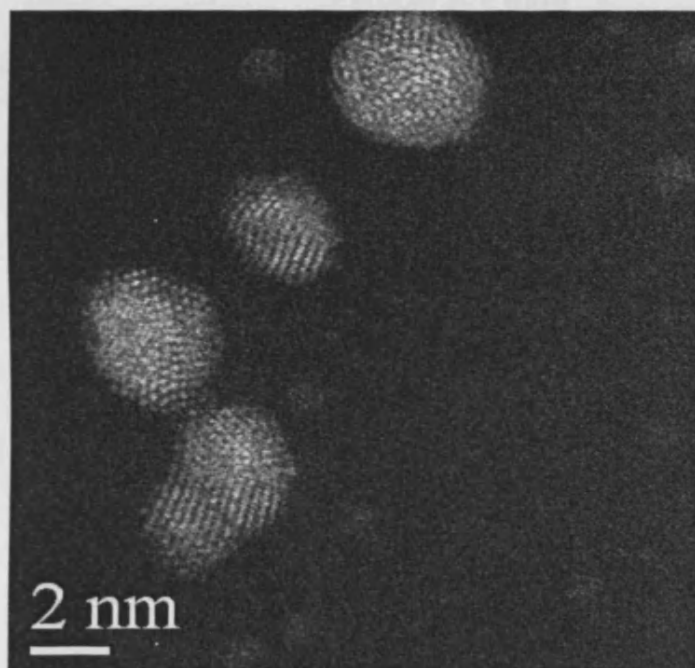
Figure 3.6. A representative STEM HAADF image of the starting Au Pd (1:1 wt) sol deposited onto a continuous carbon TEM grid. (Image taken by Ramachandra et al)

The bimetallic nanoparticles have a mean particle size of 2.9 nm (figure. 3.7A) and were found to be homogeneous Au-Pd alloys. More than 80% of the particles were icosahedral or decahedral (multiply twinned), with the remainder being cub-octahedral or just single/double twinned in character. They were also distinctly rounded in shape because they were still coated with protective polyvinyl alcohol ligands.
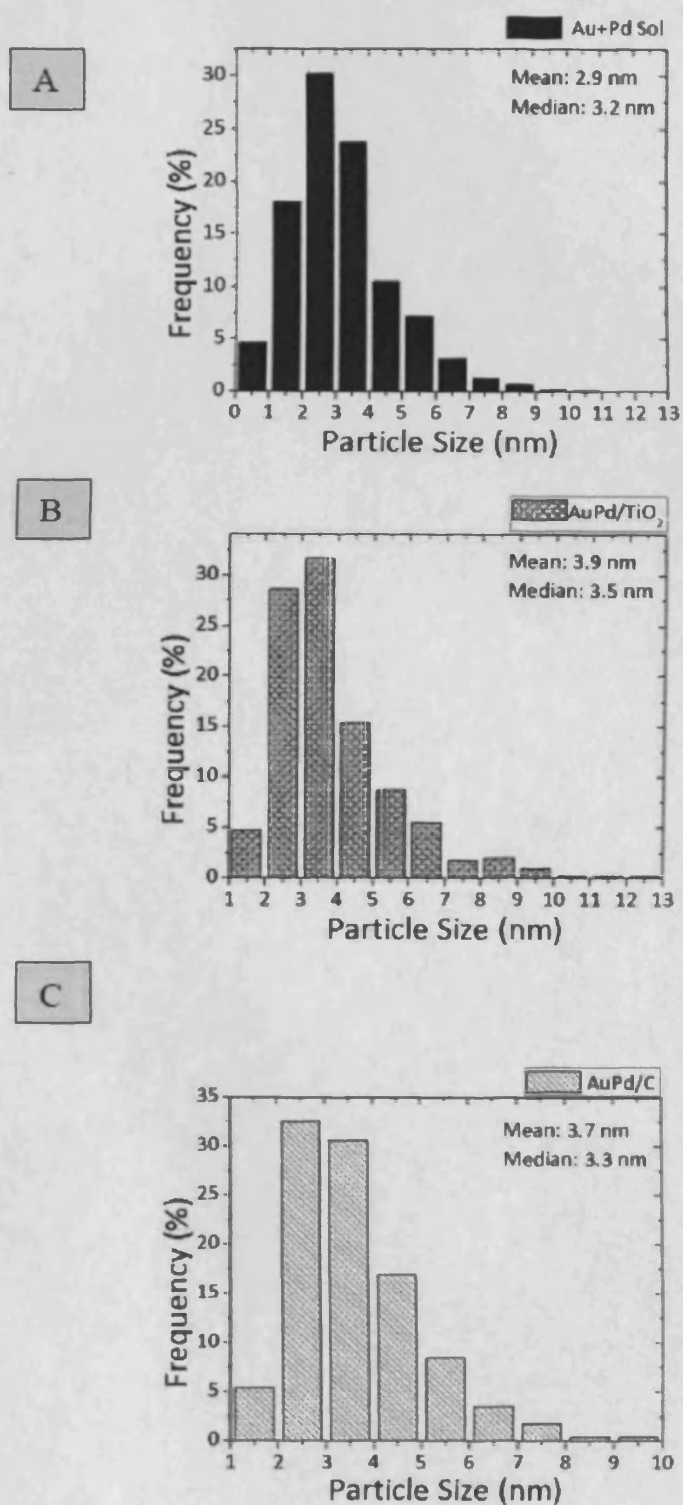
Figure 3.7. Particle size distributions for (A) starting Au-Pd colloidal sol, (B) sol–immobilized Au-Pd/TiO$_2$ dried at 120°C, and (C) sol–immobilized Au-Pd/C dried at 120°C. (Image taken by Ramachandra et al)
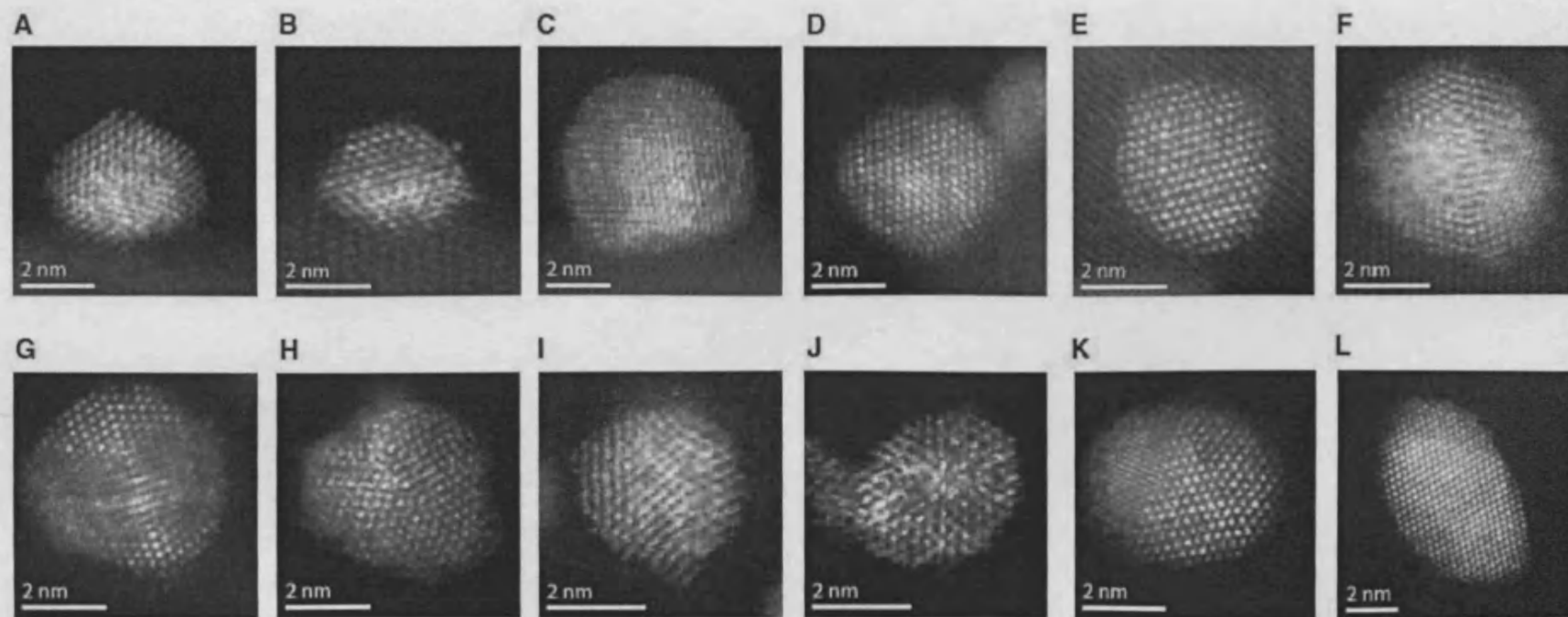
Figure 3.8. (A to F): Representative STEM HAADF micrographs of Au-Pd nanoparticles in the Au-Pd/TiO$_2$ sol-immobilized sample.

(G to L): Representative STEM HAADF micrographs of Au-Pd nanoparticles in the Au-Pd/C sol-immobilized sample. (Image taken by Ramachandra et al)
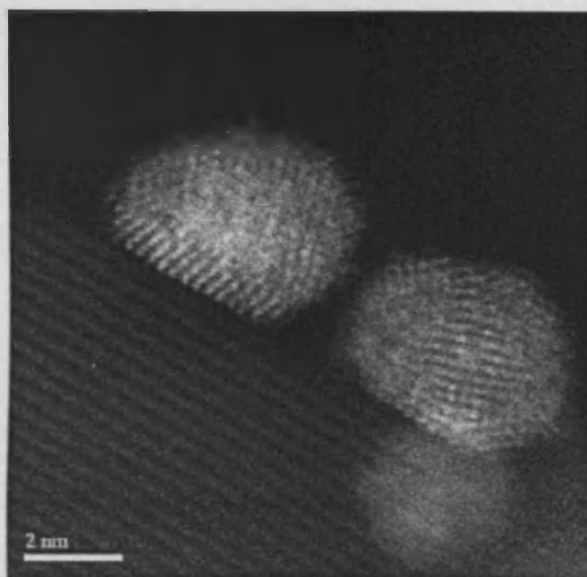
Figure 3.9. A representative HAADF-STEM image of the AuPd/TiO$_2$ sol-immobilized catalyst after drying at 120 °C, in which it is clear that flat interfaces have developed between the metal particle and the support. (Image taken by Ramachandra et al)

After deposition of the colloids onto either activated amorphous carbon or TiO$_2$, the sol-immobilized material was dried at 120 °C for 16 hours. The low-temperature drying process in each case caused a very modest size increase in the Au-Pd particles, leading to HAADF-measured mean sizes for the TiO$_2$- and carbon-supported catalysts of 3.9 and 3.7 nm, respectively (figure. 3.7 B and C).

The most important difference noted between the two samples relates to the morphology of the Au-Pd particles. In contrast to the starting colloid, many of the smaller particles were now found to be highly faceted, and primarily cub-octahedral (figure 3.8A to D) or singly twinned (figure 3.8E) in character. Such particles preferentially exposed distinct {111} - and {200}-type facets. The larger particles (figure 3.8F) still tended to be multiply twinned and exclusively exposed {111}-type facet planes. In addition, the Au-Pd particles tended to form an extended flat interface structure with the crystalline TiO$_2$ substrate (figure 3.9), which could serve to improve particle adhesion and inhibit sintering at higher temperatures. In

contrast, the corresponding HAADF images (figure 3.8 G to I) from the carbon-supported samples show that the Au-Pd particles are more rounded and have a much lower ability to wet the amorphous carbon support. The distribution of Au-Pd particle morphologies on the carbon support was much closer to that of the starting colloid, with icosahedral and decahedral (five fold- twinned) particles predominating (figure 3.8 G to J) and comparatively few single/double twinned (figure 3.8K) and cubo-octahedral (figure 3.8L) particles present. It is plausible that the strong interaction of the Au-Pd metal with the TiO_2 support in the former case templates many of the smaller multiply twinned particles to restructure as cub-octahedral particles or simple single/ double-twinned crystals during the drying step.

X-ray photoelectron spectroscopy (XPS) analysis of the Au-Pd catalysts immobilized on carbon and TiO_2 showed them to have a Pd/Au ratio of 2.1 and 2.2, respectively, and confirmed that in both cases, the Pd was predominantly in the metallic state. The AuPd/C sample had approximately double the catalytic activity of the $AuPd/TiO_2$ sample, despite having a very similar size distribution of Au-Pd particles. This suggests that simple metal surface area considerations are not dominating the catalytic activity in this instance, because the total numbers of exposed surface atoms are almost identical (8), and the TONs per surface-exposed atoms (Calculation of the number of surface exposed atoms is demonstrated separately in 3.5.1) for the most-active catalysts are 1.03×10^4 for Au-Pd/C and 0.56×10^4 for $Au-Pd/TiO_2$ (Table 3.7) (Tables 3.11 & 3.12). In addition, the similarity in surface composition, as evidenced by XPS, does not provide a clue as to the source of the activity difference.

The Au-Pd/ TiO_2 catalyst does clearly have more support/ particle periphery sites relative to the Au-Pd/C catalyst, by virtue of its flatter, better wetting interface. However, such periphery sites are probably not implicated in the catalytic process in this instance, because the $Au-Pd/TiO_2$ catalyst displays the lower activity. It is possible that the disparity in catalytic

activity may be related to subtle differences in the number of low coordination facet-edge and corner sites in the two cases. The flatter, more faceted, Au-Pd particles have fewer of these low coordination number sites, whereas the more irregular, rougher Au-Pd particles have substantially more of them. If these low coordination number corner and/or edge positions are implicated as active sites for toluene oxidation, then their relatively higher occurrence in the Au-Pd/C sample could account for the superior performance displayed by this catalyst.

Another possible explanation could lie in the difference in the distribution of Au-Pd particle morphologies found in the two catalyst samples. The Au-Pd/C catalyst predominantly has multiply twinned (icosahedral and decahedral) particles, which tend to have {111} facet terminations. In comparison, the Au-Pd/TiO$_2$ materials show an increased fraction of cuboctahedral and singly/doubly twinned particles, which exhibit mixed {100}/ {111} facet terminations. Hence, the increasing proportion of {100}-type facets in the Au-Pd/TiO$_2$ sample correlates with a lowering of the catalytic activity, and preparation strategies need to avoid them.

3.5.1. Calculation of the number of surface exposed atoms

Calculations of the number of exposed surface atoms were performed by Ramachandra *et al* assuming that all the nanoparticles had either perfect icosahedral or cub-octahedral morphologies. The number of atoms in the cluster as well as the number of exposed surface atoms for a given cluster size is the same for both morphologies (9, 10). According to the Mackay model an assembly of *n* icosahedral shells about a central atom, contains N total atoms where:-

$$N = (10/3)n^3 + 5n^2 + (11/3)n + 1$$

The number of atoms in the n$^{\text{th}}$ shell is given by $N_n = 10n^2 + 2$

The total number of surface atoms on activated carbon and TiO_2 can then be calculated as follows: Since the catalyst has a total metal loading of 1 wt% on both supports, the number of Au and Pd atoms in 100 grams of the sample is 4.36 x 10^{21} and the number of exposed surface atoms, assuming an equal distribution of gold and palladium on the surface, is then 1.40 x 10^{21} for the activated carbon support and 1.22x10^{21} for the TiO_2 support.

The calculations for Au–Pd nanoparticles immobilized on activated carbon and TiO_2 supports are shown in Tables 3.11 and 3.12 respectively.

Table 3.11. Calculation of the percentage of exposed surface atoms based on the measured particle size distribution for the AuPd/ activated carbon sample.

Cluster Size (nm)[a]	Frequency (%)[b]	Number of atoms in cluster[c]	Fraction of atoms on the surface (%)[d]	Percentage of total atoms[e]	Percentage of surface atoms[f]
1.4	1.34	55	76.3	0.07	0.05
2.0	11.12	147	62.5	1.36	0.85
2.5	21.78	309	52.4	5.6	2.94
3.1	22.67	561	44.9	10.58	4.75
3.7	12.45	923	39.2	9.56	3.75
4.3	13.34	1415	34.7	15.7	5.45
4.8	4.45	2057	31.2	7.61	2.38
5.4	5.34	2869	28.3	12.73	3.61
6.0	2.67	3871	25.8	8.59	2.22
6.6	2.23	5083	23.8	9.4	2.24
7.2	1.34	6525	22.1	7.24	1.6
7.7	0.89	8216	20.5	6.08	1.25
8.3	0	10178	19.2	0	0
8.9	0	12431	18.1	0	0
9.5	0.45	14993	17.1	5.55	0.95

[a] Cluster size for n shell is calculated as to $(2n+1)d_{atom}$ for n>1, where $d_{atom} \sim 0.288$ nm

[b] Frequency using the particle size distribution histogram

[c,d] Calculated from Mackay model

[e,f] Distribution of total atoms per cluster size calculated using the particle size distribution histogram

([a, b, c, d, e, f] are common for Table 11 & 12)

(The above data supplied by Ramachandra et al)

Table 3.12. Calculation of the percentage of exposed surface atoms based on the measured particle size distribution for the AuPd/ TiO$_2$ sample.

Cluster Size (nm)[a]	Frequency (%)[b]	Number of atoms in cluster[c]	Fraction of atoms on the surface (%)[d]	Percentage of total atoms[e]	Percentage of surface atoms[f]
1.4	1.25	55	76.3	0.05	0.04
2.0	10.7	147	62.5	0.95	0.59
2.5	17.17	309	52.4	3.18	1.67
3.1	21.15	561	44.9	7.1	3.19
3.7	17.17	923	39.2	9.49	3.72
4.3	9.46	1415	34.7	8.01	2.78
4.8	5.73	2057	31.2	7.05	2.2
5.4	5.48	2869	28.3	9.4	2.66
6.0	3.74	3871	25.8	8.65	2.24
6.6	3.24	5083	23.8	9.84	2.35
7.2	1	6525	22.1	3.89	0.86
7.7	1.25	8216	20.5	6.12	1.26
8.3	0.75	10178	19.2	4.55	0.88
8.9	0.75	12431	18.1	5.56	1.01
9.5	0.5	14993	17.1	4.47	0.77
10.0	0	17885	16.1	0	0
10.6	0.25	21127	15.3	3.15	0.49
11.2	0.25	24739	14.6	3.69	0.54
11.8	0	28741	13.9	0	0
12.3	0.25	33153	13.3	4.94	0.66

(The above data supplied by Ramachandra et al)

3.6. Effect of temperature and pressure on toluene oxidation

Experiments have been designed with various temperatures and pressures in order to know the influence of these experimental parameters on the rate of the reaction. The results are shown in Table 3.13.

Table 3.13: Effect of temperature and pressure studied on toluene oxidation using sol immobilised catalysts

Catalyst[S]	T °C	pO₂ bar	Time h	Conv %	Selectivity (%)				TON
					Benzyl alcohol	Benzal- dehyde	Benzoic acid	Benzyl benzoate	
AuPd/C	160	10	48	50.8	0.1	1.1	4.5	94.3	3300
AuPd /TiO₂	160	10	48	24.1	0.5	1.2	2.8	95.5	1570
AuPd/C	120	10	48	10.6	0.2	7.1	13.1	79.7	690
AuPd /TiO₂	120	10	48	4.0	1.1	6.0	4.8	88.1	260
AuPd/C	80	10	48	0.9	8.6	34.2	0.1	57.2	60
AuPd/C	120	6	48	4.9	0.1	5.7	2.9	91.4	320

Reaction conditions: substrate - 10 ml toluene, catalyst – 0.2 g, substrate/metal molar ratio = 6500, stirring rate - 1500 rpm, TON (moles of products/moles of metal) at 48 h reaction. TON numbers were calculated on the basis of total loading of metals. [S] - 1wt % total metal loading (1:1 wt Au:Pd) for all the catalysts

The reaction performed at 120 °C, 10 bar O₂ pressure has shown less conversion than the reaction carried out at 160 °C, 10 bar O₂ pressure by a factor of 5 to 6., whereas the reaction performed at 80 °C at 10 bar O₂ pressure resulted in very low conversion. The reaction carried out at 120 °C, 6 bar O₂ pressure has shown 10 times less conversion than the reaction done at 160 °C, 10 bar O₂ pressure.

The rate of any chemical reaction can be influenced by several factors. In general, a factor that increases the number of collisions between particles will increase the reaction rate and a factor that decreases the number of collisions between particles will decrease the chemical reaction rate. Usually, an increase in temperature or pressure is accompanied by an increase in the reaction rate. Temperature is a measure of the kinetic energy of a system, so higher temperature implies higher average kinetic energy of molecules and more collisions per unit time. Hence, the conversion of toluene is directly proportional to the reaction temperature and pressure too.

References:

1. X. Li, J. Xu, L. Zhou, F. Wang, J. Gao, C. Chen, J. Ning, H. Ma, Catal. Lett. 110, 149 (2006)

2. F. Wang, J. Xu, X. Li, J. Gao, L. Zhou, R. Ohnishi, Adv. Synth. Catal. 347, 1987 (2005).

3. J. Gao, X. Tong, X. Li, H. Miao, J. Xu, J. Chem. Technol. Biotechnol. 82, 620 (2007).

4. N. Dimitratos et al., Phys. Chem. Chem. Phys. 11, 5142 (2009).

5. D. I. Enache et al., Science, 311, 362 (2006).

6. J. K. Edwards et al., Science, 323, 1037 (2009).

7. J.K. Edwards, B.E. Solsona, P. Landon, A.F. Carley, A. Herzing, C.J. Kiely and G.J. Hutchings, J. Catal. 236, 69 (2005).

8. A. Borodziński, M. Bonarowska, Langmuir, 13, 5613 (1997).

9. A. Mackay, Acta Crystallographica, 15, 916 (1962).

10. J. M. Montejano-Carrizales, F. Aguilera-Granja, J. L. Morán-López, Nanostructured Materials, 8, 269 (1997).

Appendix

Reproducibility of experiments:

In a final set of experiments, the reproducibility of catalyst preparation method and catalyst testing has been evaluated together (Table 3.14). Three trials have been done to study the reproducibility. Two of them have been performed by one experimenter (Lokesh, trial 2 & 3) and one of them has been performed by another experimenter (Izham, trial 3). This way it was possible to check the variations between the users. The results were in good agreement with each other except the selectivity of benzoic acid and benzyl benzoate. This might be due to the interruption of oxygen flow occurred for a while at the end of reaction, performed by Izham. It has been claimed that oxygen concentration may affect the selectivity of ester as the oxygen is involved in the transformation of hemiacetal (coupling of aldehyde and alcohol) to ester as shown in scheme 1 of chapter 4. At the same time, low concentration of oxygen has facilitated the over oxidation of benzaldehyde to benzoic acid.

Table 3.14: Liquid phase oxidation of toluene using three different batches of the same catalyst

Trial	Conversion %	Selectivity %				TOF
		Benzyl alcohol	Benzaldehyde	Benzoic acid	Benzyl benzoate	
1	33.9	0.8	4.1	33.0	62.2	45.9
2	33.1	0.4	3.3	14.2	82.1	44.8
3	35.3	0.2	2.0	8.5	89.2	47.9

Reaction conditions: T = 160 °C (433K), pO_2 = 10 bar (0.1 MPa), substrate - 10 ml toluene, catalyst − 0.2 g 1%AuPd/C$_{SI}$ (1:1 wt) SI- Sol immobilisation, substrate/metal molar ratio = 6500, stirring rate - 1500 rpm, t = 48 hrs. TON (moles of products/moles of metal) numbers were calculated on the basis of total loading of metals.

Conversion profile with error bars

Figure 3.10a

Selectivity profile with error bars
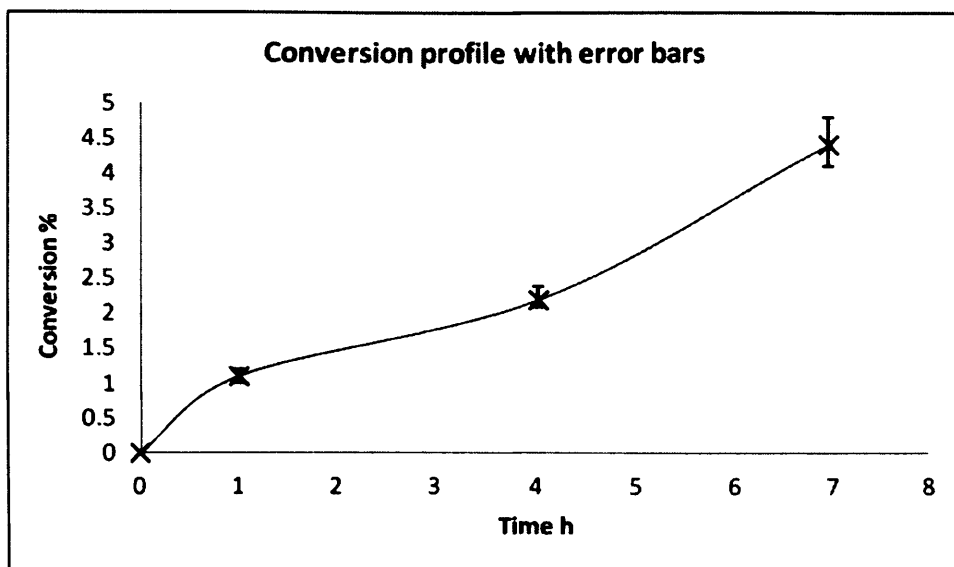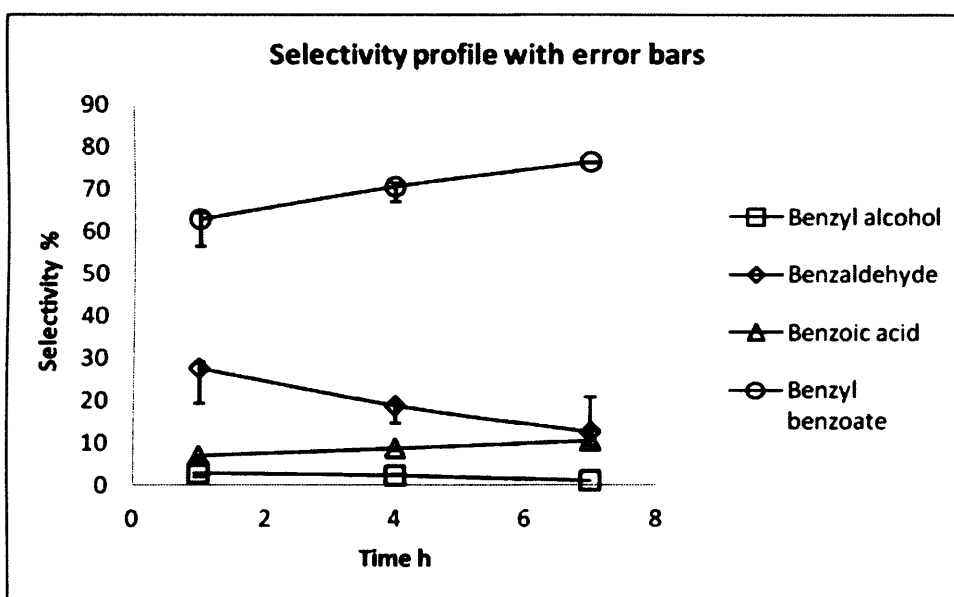
Figure 3.10b

Figure 3.10 a&b: Toluene conversion & selectivity profile with error bars. [a]Reaction conditions: Toluene – 188 mmol (20 ml), T = 160 °C, pO_2 = 10 bar, stirring rate 1500 rpm., Time – 7 h.

The Figure 3.10 a&b shows the variation in the catalytic data through error bars. The error bars have been drawn based on the catalytic data from three different reaction runs by using same batch of the catalyst. The median value of percentage conversion has been considered to draw a reference graph. Further, positive and negative error values were added

to the reference graph by subtracting the numerical values (Conversion % & selectivity %) from high to low on either side of the median. The error bars shows that there is no much difference in conversion as well as selectivity, stating that the selectivity here does not vary as much as seen in Table 3.14. It suggests that the variation between catalyst batches is greater than within the same batch. Also this observation shows much better agreement that is in line with trial 2 & 3 (done by Lokesh), but not with trial 1 (done by Izham) in table 3.14. The reason for the deviation in trial 1 has been already discussed. To conclude that the toluene oxidation experiments are reproducible, this is evident from the Table 3.14 and figure 3.10 a&b.

Table 3.15: Effect of catalyst mass studied on toluene oxidation

| Catalyst | Time h | Conv % | Selectivity % | | | | S/M | TON |
			Benzyl alcohol	Benzaldehyde	Benzoic acid	Benzyl benzoate		
50 mg	1.0	0.093	9.3	55.4	27.5	7.7	104000	97.2
	2.0	0.120	9.6	74.7	3.2	12.5		124.7
	5.0	0.249	6	69.4	8	16.5		259
	7.0	0.415	4.2	66	8.8	21		431
100 mg	1.0	0.185	6.6	69.7	8.6	13.5	52000	95.9
	2.0	0.283	8.2	71.8	4.3	17.3		147.3
	5.0	0.437	0.1	71.5	0.1	28.5		227
	7.0	0.854	0.1	52.8	15.3	31.8		443.7
200 mg	1.0	0.316	5.3	76.2	2.4	16.1	26000	82.2
	2.0	0.462	4	70.6	3.1	22.3		120.1
	5.0	0.932	2.8	54.2	5.7	37.3		242.2
	7.0	1.325	1.8	46.0	6.9	45.2		344.3
400 mg	1.0	0.419	3.6	47.7	4.2	44.4	13000	54.5
	2.0	0.691	2.8	40.9	5.6	50.7		89.7
	5.0	1.444	1.8	27.6	8.1	62.4		187.7
	7.0	2.314	1.6	20.4	9.0	69.0		300.7
800 mg	1.0	0.947	2.0	35.6	6.1	56.3	6500	61.5
	2.0	1.315	2.0	31.3	7.0	59.7		85.4
	5.0	2.745	1.2	19.1	8.8	70.8		178.3
	7.0	4.730	1.0	13.4	9.4	76.1		307.3

Reaction conditions: T = 160 °C (433K), pO_2 = 10 bar (0.1 MPa), stirring rate - 1500 rpm, substrate - 40 ml toluene, catalyst – 1% AuPd/C (various amounts), S/M – substrate to metal molar ratio, TON - (moles of products/moles of metal) at 7 h reaction. TON numbers were calculated on the basis of total loading of metals.
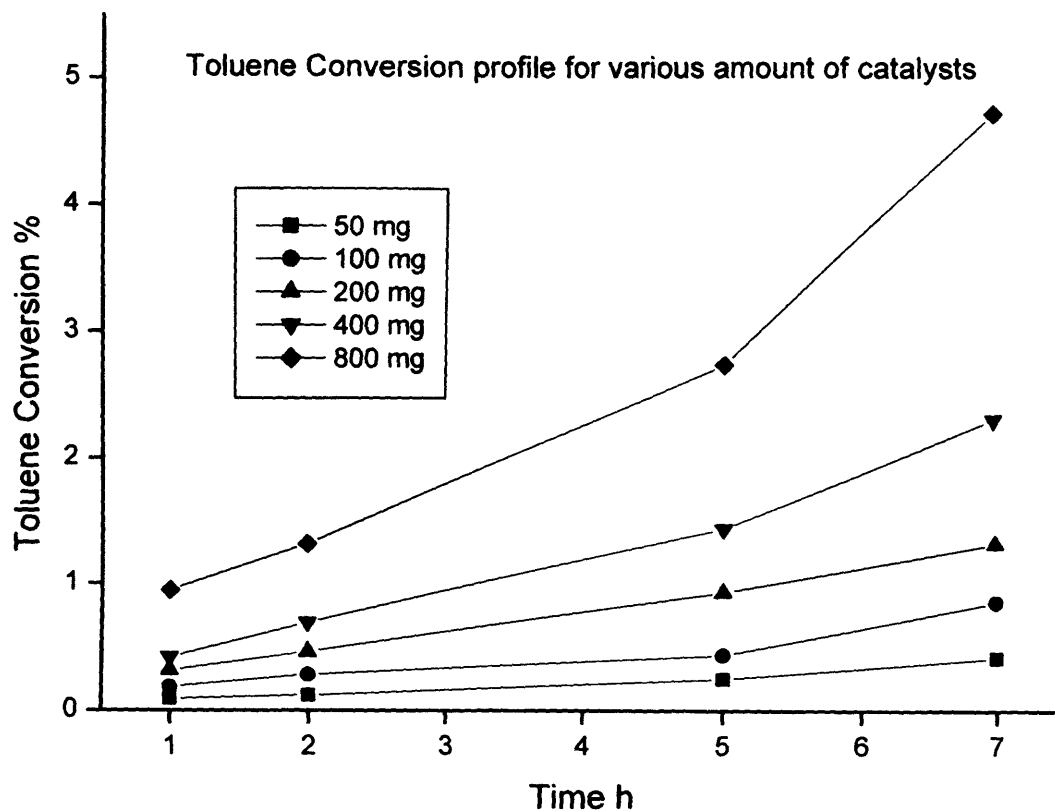
Figure 3.11: Toluene conversion profile for various catalyst masses. [a]Reaction conditions: Toluene – 376 mmol (40 ml), T = 160 °C, pO_2 = 10 bar, stirring rate 1500 rpm., Time – 7 h.

Chapter 4

Toluene Oxidation and Catalyst Reuse Studies

4.1. Outline

On continuing the studies of toluene oxidation which were dealt with chapter 3, this chapter discusses the possible routes for the formation of benzyl benzoate, which is the major product under the current reaction conditions of liquid phase oxidation of toluene using sol immobilised catalysts. Further, experimental results to demonstrate the reusability of the catalysts with the evidence of electron microscopic images have been detailed. Finally, the preliminary results from the solvent free oxidation of substituted toluenes using carbon supported Au-Pd bimetallic nanoparticles prepared by sol immobilisation are shown.

4.2. Discussion about the formation of benzyl benzoate

Toluene is oxidized to benzyl alcohol , benzaldehyde and benzoic acid through the reactive hydroperoxy species as Colby *et al* (1) and W. Partenheimer (2) demonstrated. These transformations are shown in step 1, 2, 3, and 4. It is considered that the high selectivity to benzyl benzoate could result from four possible mechanisms of either coupling of the benzaldehyde with the benzyl alcohol to give the hemiacetal, followed by oxidation to the ester as shown in scheme 1 or direct thermal (catalyzed) dehydrative esterification between benzoic acid with alcohol scheme 2 or Cannizzaro reaction between benzyl alcohol with benzaldehyde via alkoxide as shown in scheme 3 or Tishchenko coupling of two benzaldehyde molecules via "dimer" directly to the ester as shown in scheme 4.

Recently, Bäumer and co-workers (3) have shown that methyl formate is formed on an Au catalyst when methanol is oxidized with O_2 under very dilute conditions; we consider that this precedent favours mechanism of coupling of aldehyde and alcohol in

the present case as shown in scheme 1. We performed several control experiments to rule out the other three possible pathways. Heating the oxidized intermediates with O_2 in the absence of catalyst gave little ester (Table 4.1), establishing the involvement of the catalyst in steps beyond the initial toluene-to-alcohol oxidation.

Step: 1

$$2 \; \text{Toluene} + 2O_2 \longrightarrow 2 \; \text{[benzyl radical, *CH}_2\text{]} + 2 \; \text{*O-OH}$$

$$\downarrow$$

$$O_2 + 2 \; \text{*OH}$$

Step: 2

$$\text{[*CH}_2\text{]} + \text{*OH} \longrightarrow \text{Benzyl alcohol [CH}_2\text{OH]}$$

Step: 3

$$\text{Benzyl alcohol [CH}_2\text{OH]} \longrightarrow \text{[intermediate with O*]} + \text{H*}$$

$$\downarrow$$

$$\text{Benzaldehyde} + \text{H*}$$

Step: 4

$$\text{Benzaldehyde} \longrightarrow \text{[intermediate with *O and *OH]} \longrightarrow \text{Benzoic acid [C(O)OH]} + \text{H*}$$
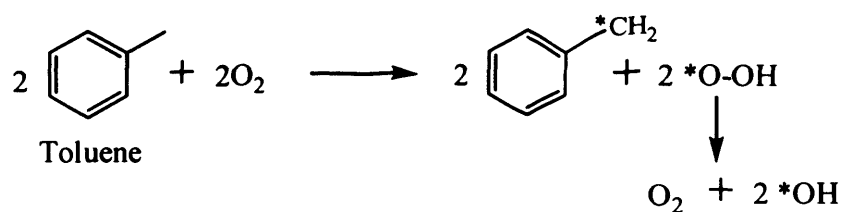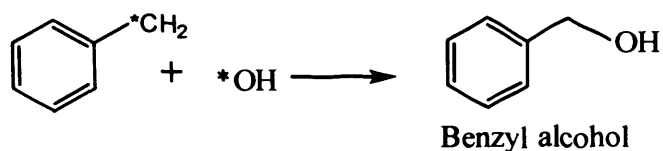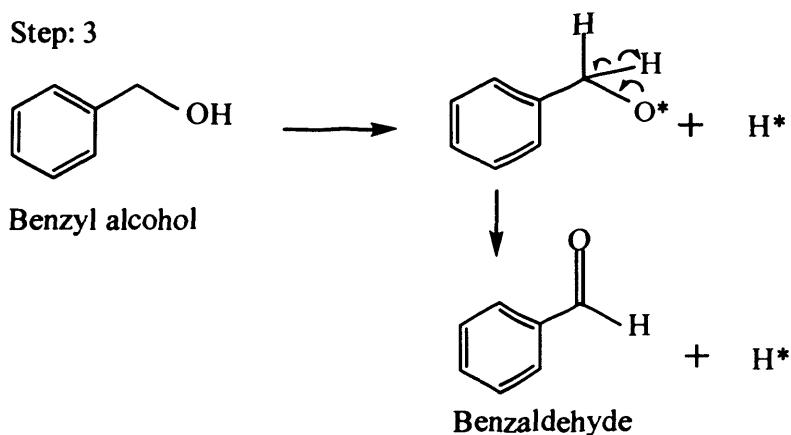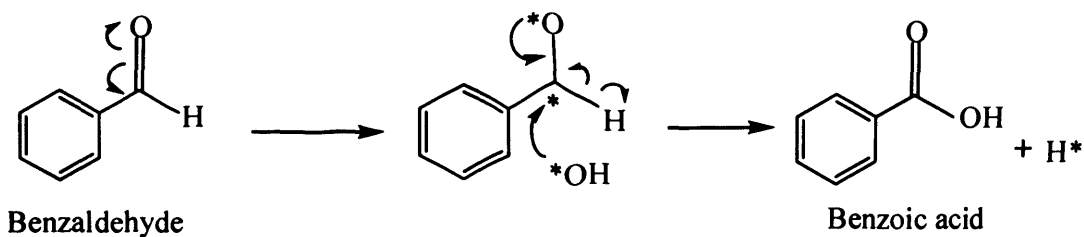
Heating mixtures of benzyl alcohol with benzoic acid in the absence of O_2, with and

without catalyst, did not result in ester (Benzyl benzoate) formation (Tables 4.3 & 4.2),

ruling out direct esterification (Scheme 2). Similarly, treating alcohol with

benzaldehyde also failed to produce ester (Tables 4.2 & 4.3), ruling out the Cannizzaro

mechanism (scheme 3). Finally, we investigated reactions of the benzaldehyde alone in

the absence of O_2, with and without catalyst, and again observed no ester formation

(Tables 4.3 & 4.2), precluding the Tishchenko mechanism (scheme 4). Hence we

conclude that the high selectivities observed are consistent with the involvement of the

hemiacetal (scheme 1).

Scheme 1:

Benzyl benzoate

Scheme 2:

Benzoic acid   Benzyl alcohol   Heat   Benzyl benzoate
                                          -H$_2$O

Scheme 3:

Cannizaro reaction

Benzyl alcohol   Alkoxide
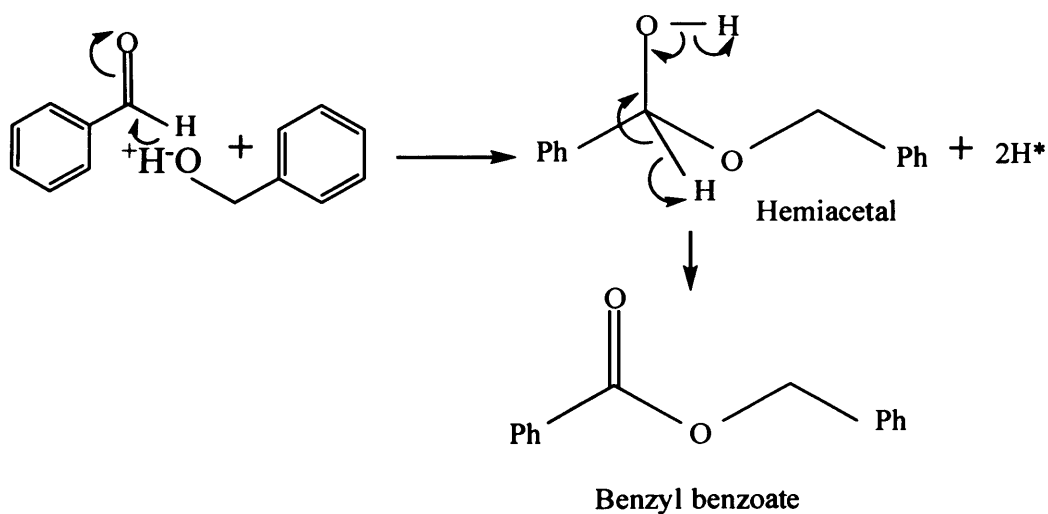
Benzyl benzoate $\xleftarrow{\text{Heat}}$ Benzoic acid + Benzyl alcohol
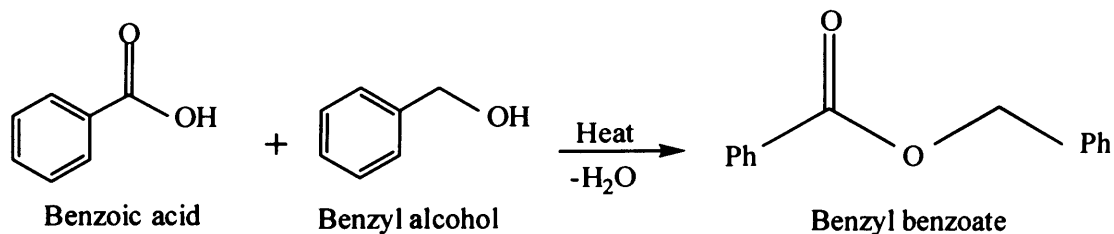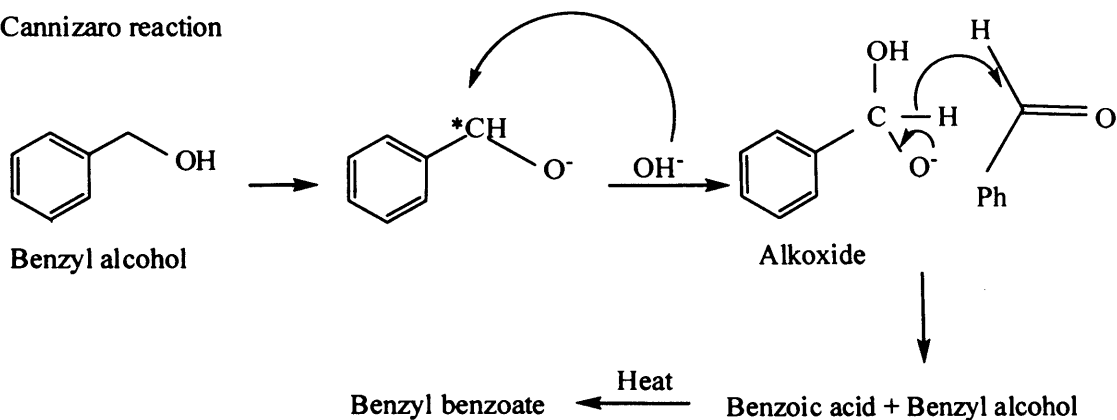
Scheme 4:

Tischenko reaction
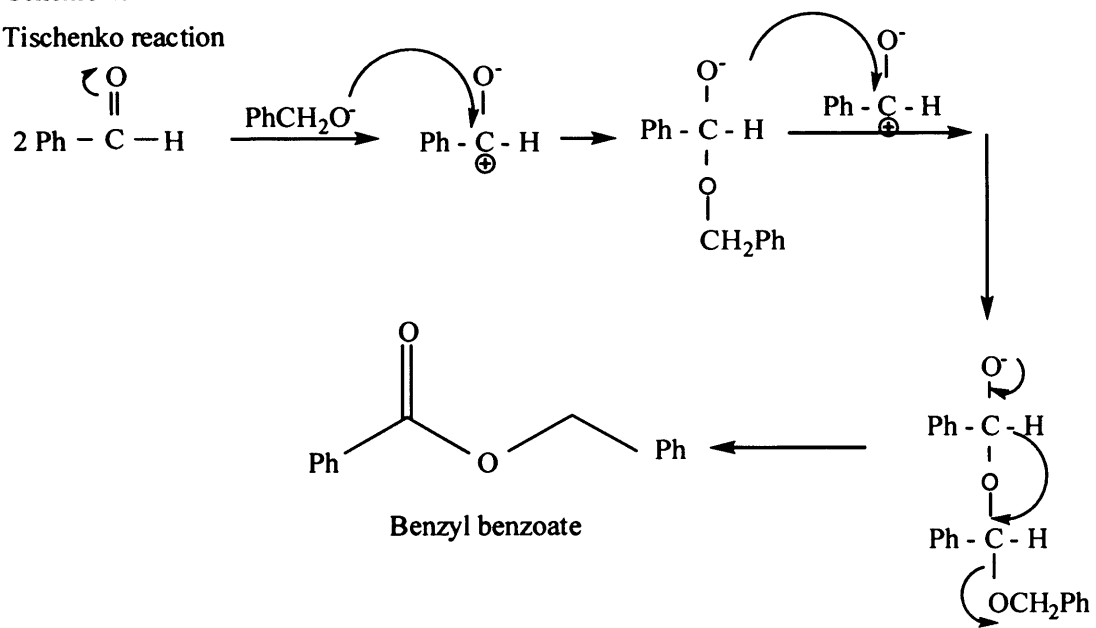
Benzyl benzoate

Table 4.1. Liquid phase reaction of benzyl alcohol, benzaldehyde and benzoic acid in toluene at 160 °C without catalysts in the presence of O_2.

Reaction	Time (h)	Moles				
		Toluene	Benzyl alcohol	Benzaldehyde	Benzoic acid	Benzyl benzoate
0.3M ($PhCH_2OH$ + PhCHO) in toluene	0	0.36430	0.00600	0.00600	0.00000	0.00000
	0.5	0.36550	0.00451	0.00580	0.00049	0.00000
	1	0.36520	0.00443	0.00585	0.00078	0.00002
	2	0.36510	0.00445	0.00598	0.00071	0.00004
	5	0.36500	0.00421	0.00605	0.00091	0.00007
	7	0.36500	0.00381	0.00611	0.00122	0.00009
0.3M ($PhCH_2OH$ + PhCOOH) in toluene	0	0.36430	0.006	0.00000	0.00600	0.00000
	0.5	0.36880	0.00461	0.00011	0.00262	0.00010
	1	0.36780	0.00448	0.00055	0.00331	0.00015
	2	0.36690	0.00441	0.00101	0.00372	0.00022
	5	0.36630	0.00425	0.00163	0.00386	0.00022
	7	0.36620	0.00383	0.00224	0.00375	0.00020
0.3M PhCHO in toluene	0	0.36430	0.00000	0.01200	0.00000	0.00000
	0.5	0.36468	0.00045	0.00851	0.00111	0.00155
	1	0.36400	0.00061	0.00885	0.00171	0.00114
	2	0.36362	0.00077	0.00829	0.00245	0.00117
	5	0.36322	0.00109	0.00724	0.00349	0.00125
	7	0.36276	0.00138	0.00683	0.00433	0.00100

Reaction conditions: Toluene = 40 ml, T = 160 °C, pO_2 = 10 bar, Stirring rate = 1500 rpm

Table 4.2. Liquid phase reaction of benzyl alcohol, benzaldehyde and benzoic acid in toluene at 160 °C without catalysts in the presence of He.

Reaction	Time (h)	Mol				
		Toluene	Benzyl alcohol	Benzaldehyde	Benzoic acid	Benzyl benzoate
0.3M (PhCH₂OH + PhCHO) in toluene	0	0.36430	0.00600	0.00600	0.00000	0
	0.5	0.36371	0.00622	0.00619	0.00018	0
	1	0.36440	0.00582	0.00591	0.00018	0
	2	0.36440	0.00580	0.00585	0.00025	0
	5	0.36414	0.00573	0.00619	0.00024	0
	7	0.36562	0.00517	0.00523	0.00028	0
0.3M (PhCH₂OH + PhCOOH) in toluene	0	0.36430	0.00600	0.00000	0.00600	0.00000
	0.5	0.36717	0.00600	0.00004	0.00310	0.00000
	1	0.36663	0.00587	0.00006	0.00374	0.00001
	2	0.36664	0.00583	0.00006	0.00375	0.00001
	5	0.36663	0.00582	0.00010	0.00405	0.00003
	7	0.36706	0.00547	0.00011	0.00361	0.00005
0.3M PhCHO in toluene	0	0.36430	0.00000	0.01200	0.00000	0
	0.5	0.36383	0.00003	0.01190	0.00054	0
	1	0.36351	0.00002	0.01215	0.00061	0
	2	0.36415	0.00003	0.01146	0.00066	0
	5	0.36481	0.00003	0.01086	0.00061	0
	7	0.36618	0.00003	0.00992	0.00016	0

Reaction conditions: Toluene = 40 ml, T = 160 °C, pHe = 10 bar, Stirring rate = 1500 rpm.

Table 4.3. Liquid phase reaction of benzyl alcohol, benzaldehyde and benzoic acid in toluene at 160 °C with catalysts in the presence of He.

Reaction	Time (h)	Mol				
		Toluene	Benzyl alcohol	Benzaldehyde	Benzoic acid	Benzyl benzoate
0.3M (PhCH₂OH + PhCHO) in toluene	0	0.3643	0.0060	0.0060	0	0
	0.5	0.3659	0.0045	0.0059	0	0
	1	0.3660	0.0044	0.0059	0	0
	2	0.3663	0.0042	0.0058	0	0
	5	0.3664	0.0040	0.0059	0	0
	7	0.3667	0.0037	0.0059	0	0
0.3M (PhCH₂OH + PhCOOH) in toluene	0	0.3643	0.0060	0.0000	0.0060	0
	0.5	0.3698	0.0037	0.0009	0.0018	0
	1	0.3691	0.0037	0.0010	0.0025	0
	2	0.3690	0.0036	0.0010	0.0027	0
	5	0.3689	0.0034	0.0010	0.0029	0
	7	0.3690	0.0033	0.0011	0.0029	0
0.3M PhCHO in toluene	0	0.3643	0.000000	0.012000	0	0
	0.5	0.3643	0.000000	0.011980	0	0
	1	0.3645	0.000000	0.011766	0	0
	2	0.3646	0.000000	0.011690	0	0
	5	0.3658	0.000000	0.010516	0	0
	7	0.3651	0.000000	0.011170	0	0

Reaction conditions: Toluene = 40 ml, T = 160 °C, pO_2 = 10 bar, Stirring rate = 1500 rpm, 0.4 g of catalyst, 1 wt% (Au-Pd)/C_{SIw}, SI- sol immobilisation, w – 1:1 wt Au:Pd

4. 3. Catalyst reusability studies:

In this study, stability of the catalysts has been investigated for the liquid phase oxidation of toluene. Because, it is crucial to confirm that high-activity catalysts can be reused. With the 1%Au-Pd/TiO$_2$ catalyst prepared by sol immobilisation the reaction was stopped after 7 hours, and the catalyst was recovered by decantation. Then, the recovered catalyst was loaded in the reactor containing fresh toluene and tested under the same reaction conditions. Identical conversion was obtained on reuse of the 1%Au-Pd/TiO$_2$ catalyst (Table 4.4).

Table 4.4: Liquid phase oxidation of toluene to evaluate the used catalyst.

| Catalyst[s] | Time h | Conv % | Selectivity (%) | | | | TON |
			Benzyl alcohol	Benzaldehyde	Benzoic acid	Benzyl benzoate	
[a]Au-Pd/TiO$_2$	7	2.1	2.9	6.6	1.0	89.5	135
[b]Au-Pd/TiO$_2$	7	2.2	2.2	6.5	2.3	89.0	141

Reaction conditions: T = 160 °C (433K), pO_2 = 10 bar (0.1 MPa), substrate - 20 ml toluene, catalyst − 0.4 g, substrate/metal molar ratio = 6500, stirring rate - 1500 rpm, TON (moles of products/moles of metal) at 7 h reaction. TON numbers were calculated on the basis of total loading of metals. [s] - 1wt % total metal loading (1:1 wt Au:Pd) prepared by sol immobilisation. [a] – fresh catalyst, [b] – used catalyst.

For the 1%Au-Pd/C catalyst prepared by sol immobilisation, the reaction was stopped after 7 hours and the catalyst was allowed to settle by centrifugation. The liquid phase was then carefully removed by decantation and fresh toluene was added to the catalyst to perform the reaction. The reaction was then allowed to proceed for a further 7 hours, and the whole process was repeated a further three times. The reaction profile obtained with the decantation experiments was identical to that obtained with the fresh

catalyst (figure 4.1). The decanted liquid was analysed for leached metals using atomic absorption spectroscopy and inductively coupled plasma spectroscopy and metal concentrations were below the detection limits.
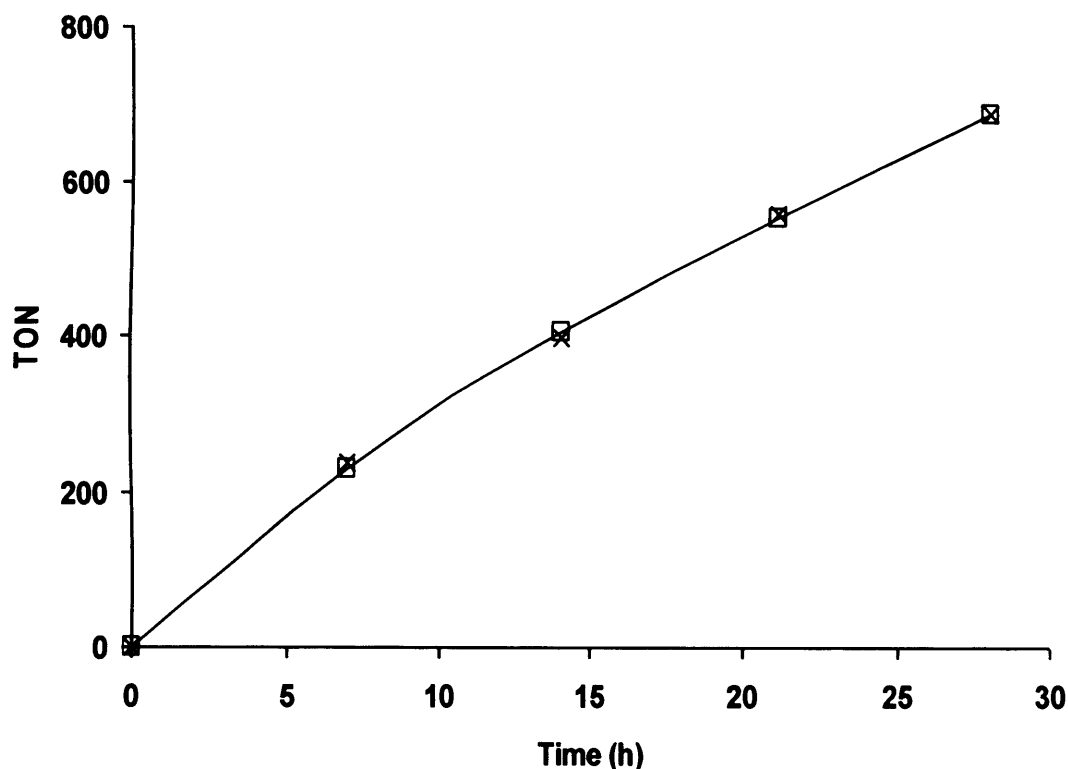
Figure 4.1. Standard reaction of AuPd/C compared with decantation of the reaction mixture at 7, 14, 21 and 28 h and fresh toluene added and the reaction continued. Reaction conditions: T = 160 °C (433K), pO_2 = 10 bar (0.1 MPa), substrate - 20 ml toluene, catalyst − 0.4 g 1%AuPd/C$_{SI}$ (1:1 wt) SI- Sol immobilisation, substrate/metal molar ratio = 6500, stirring rate - 1500 rpm, t = 28 h. TON (moles of products/moles of metal) numbers were calculated on the basis of total loading of metals. Key: □ indicates TON obtained with standard reaction, × indicates TON obtained with decantation procedure.

One of the key factors that must be considered for heterogeneous catalysts operating in three-phase systems is the possibility that active components can leach into the reaction mixture, thereby leading to catalyst deactivation or, in the worst case, to the formation of an active homogeneous catalyst. No metal was observed to have leached

into the liquid phase under the present reaction conditions. It is confirmed by an experiment, which involves the decantation of liquid phase after certain hours of reaction to remove the catalyst, and then subjecting the decanted part for the oxidation in the absence of catalyst. The decantation should be done at relatively hot condition (~50 °C), so that it is possible to find out whether the metals have got leached or not at higher temperature. The decanted liquid showed no further reaction in the absence of catalyst (figure 4.2 and table 4.5).
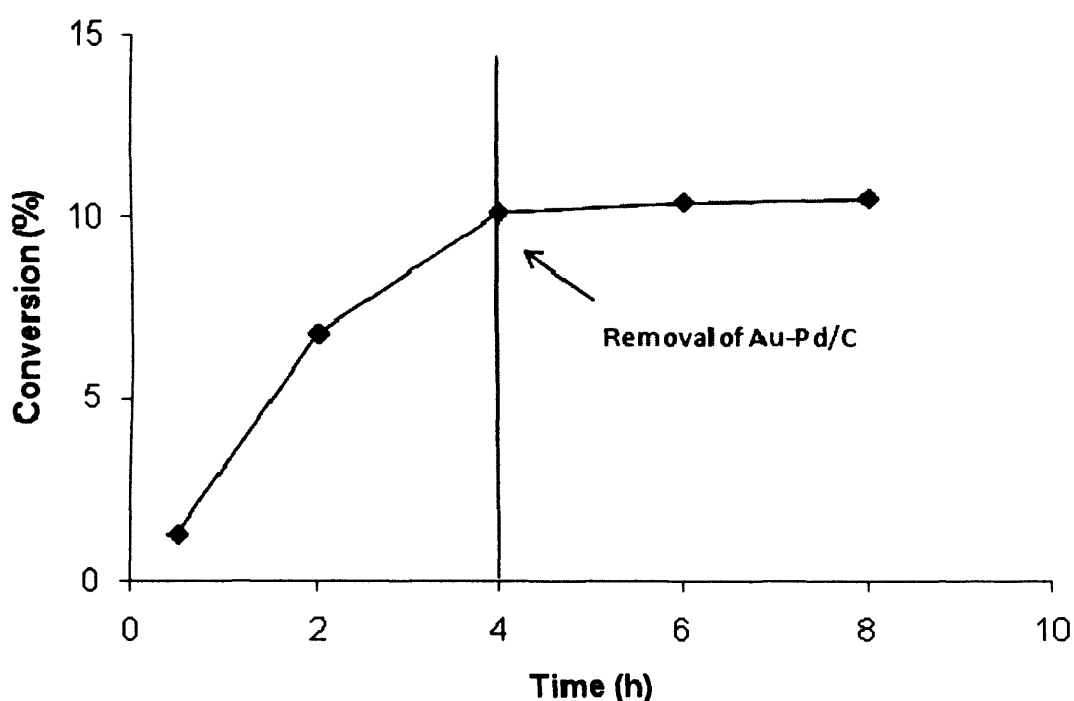
Figure 4.2: Effect of removing the catalyst by decantation at the reaction temperature.

Table 4.5: Investigation of leaching of metals from the catalyst during the liquid phase oxidation of toluene

Time	Conv	Selectivity (%)				TON
(h)	(%)	Benzyl alcohol	Benzaldehyde	Benzoic acid	Benzyl benzoate	
0.5	1.3	3.3	12.7	5.3	78.7	21.5
2	6.8	0.9	5.1	2.4	91.6	110.4
4[#]	10.1	0.4	5.7	6.4	87.4	164.6
6	10.4	1.2	6.7	11.1	81.1	169.6
8	10.5	0.6	7.2	11.3	80.9	171.3

Reaction conditions: T = 160 °C (433K), pO_2 = 10 bar (0.1 MPa), substrate - 20 ml toluene, catalyst − 0.8 g 1%AuPd/C_{SI} (1:1 wt) SI- Sol immobilisation, substrate/metal molar ratio = 3250, stirring rate - 1500 rpm, TON (moles of products/moles of metal) numbers were calculated on the basis of total loading of metals. [#]After 4h, the liquid was decanted at the reaction temperature to remove the catalyst and the decanted liquid was allowed to proceed for oxidation in the absence of catalyst. No reaction is observed. The decanted liquid was analysed for Au and Pd and levels were below detection levels.

Detailed STEM characterization shows that there is minimal particle growth or morphology change for the Au-Pd/C catalysts when studied over an extended reaction period (figure 3.5 − chapter 3), during which catalysts were recovered after 31 and 65 hours of reaction, followed by two reuse cycles of 7 hours (figures 4.3 and 4.4). Therefore, it is clear that any sintering or structural modification of these highly active catalysts is minimal, and it is considered that the catalysts are stable and reusable.
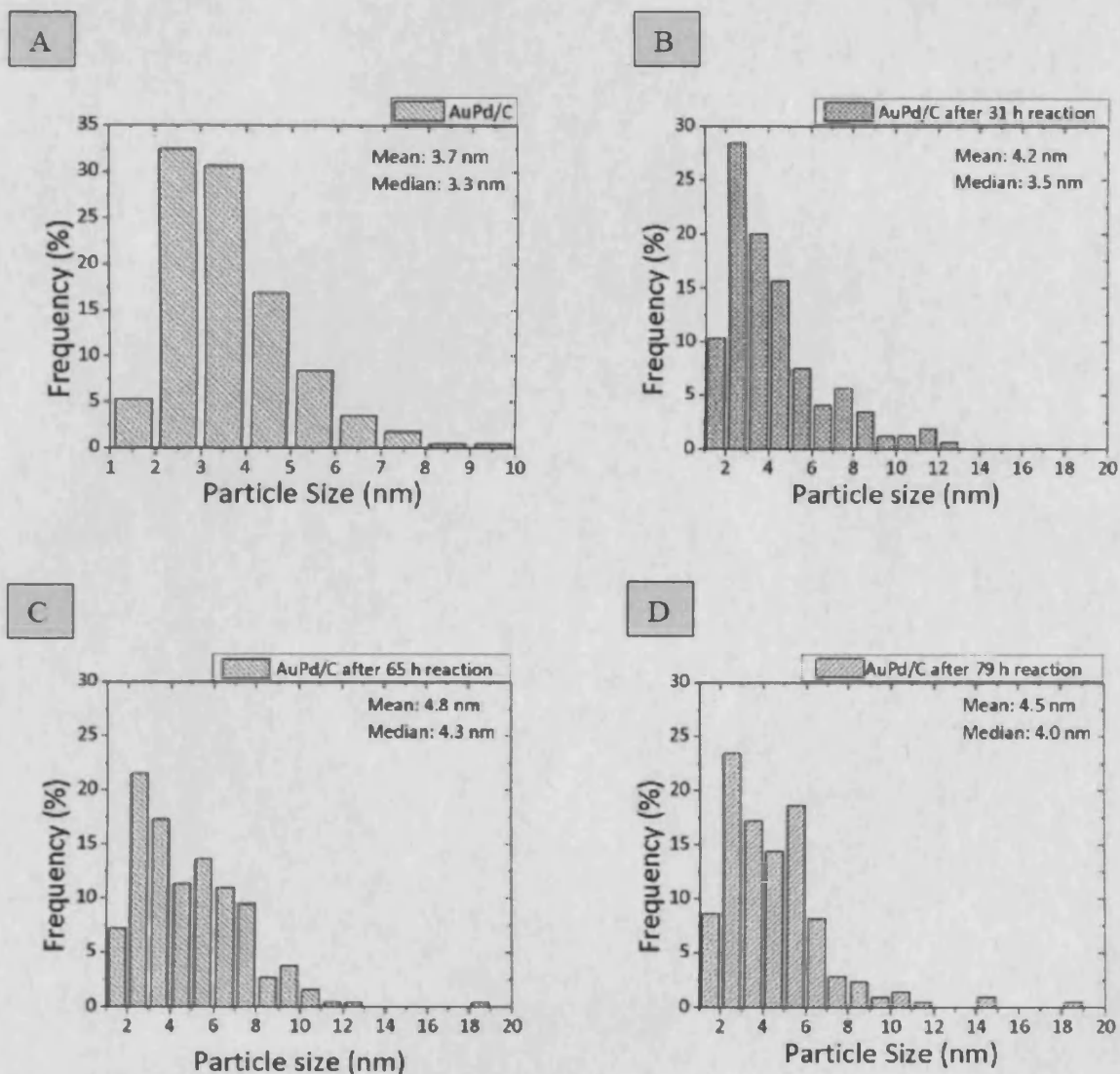
Figure 4.3. Particle size distributions for (A) unused sol immobilized AuPd/C catalyst, (B) sol immobilized AuPd/C after 31 h reaction, (C) sol immobilized AuPd/C after 65h reaction , (D) sol immobilized AuPd/C after 65 h reaction and two subsequent re-uses for 7 h giving a total time-on-line of 79h. It is clear that re-use and multiple use cycles cause only a very minor increase in median AuPd particle size. (The above data supplied by Ramachandra et al)
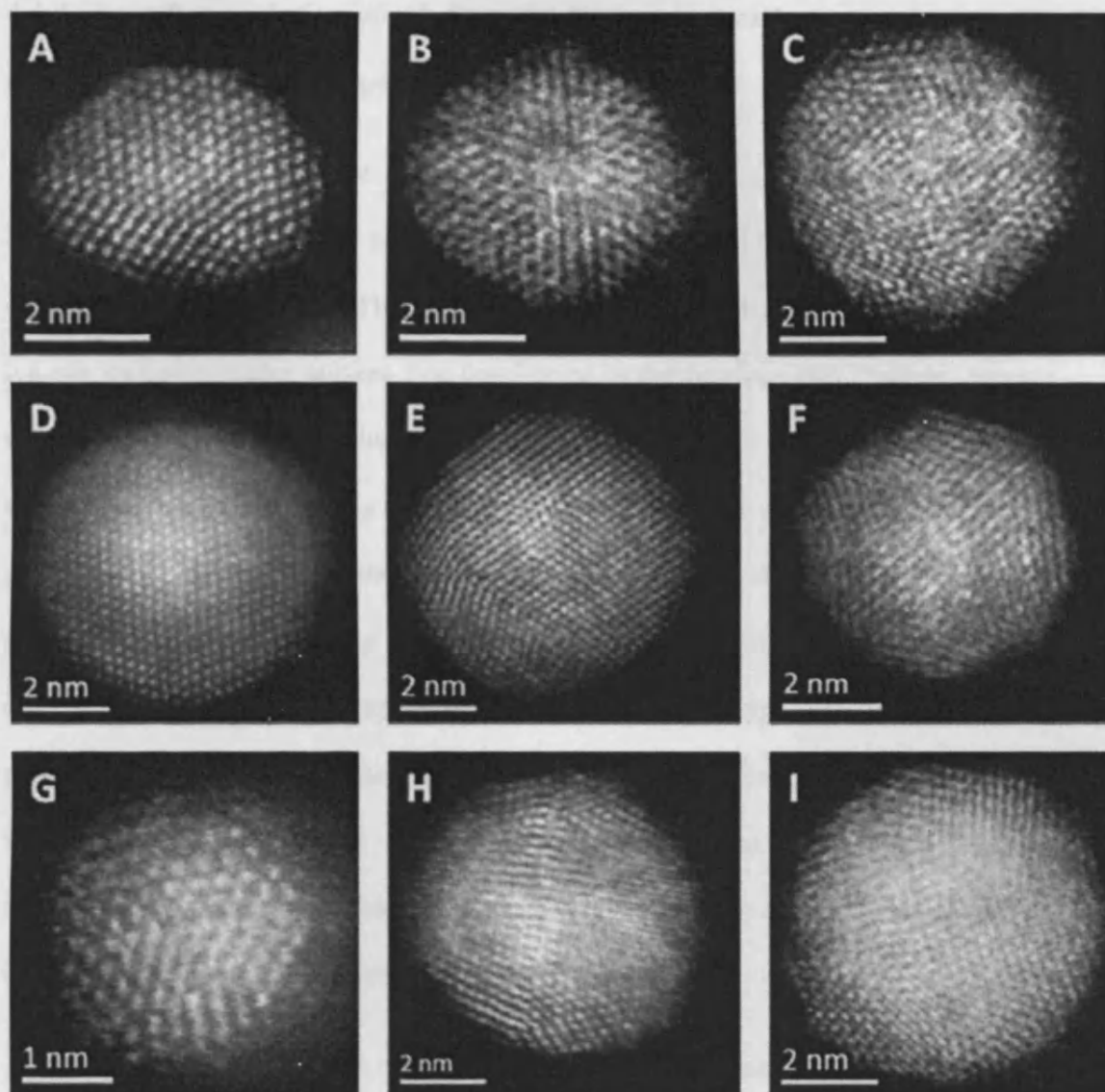
Figure 4.4: Typical STEM-HAADF images of AuPd nanoparticles of the re-used catalysts. (A, B, C) sol immobilized AuPd/C after 31 h reaction: (D, E, F) sol immobilized AuPd/C after 65 h reaction , and (G,H,I) sol immobilized AuPd/C after 65 h reaction and two subsequent re-uses for 7 h giving a total time-on-line of 79 h. (The above data supplied by Ramachandra et al)

4.4. Solvent free oxidation of substituted toluenes using carbon supported Au-Pd bimetallic nanoparticles prepared by sol immobilisation

This part deals with the general applicability of the carbon supported Au-Pd bimetallic alloy nanoparticles prepared by sol immobilisation in various heterogeneous oxidation catalysis systems. This material has been reported as an active catalyst for toluene oxidation under solvent free conditions in the previous two chapters. Having relevance with toluene, substituted toluenes such as methoxy toluenes, nitro toluenes, and xylenes are oxidized using this catalyst, again with no use of solvent. The oxidation of substituted toluenes is another interesting area to explore since these molecules are employed as feed stocks in the fine chemical industries. Often, these starting materials are oxidized by toxic and expensive organic reagents to get high turnover of the products. Hence, these processes are not environmentally benign and commercially viable as they produce much waste. It is reported here that Au-Pd bimetallic alloy nanoparticles prepared by sol immobilisation can be utilised to oxidise these feed stocks in the absence of any toxic oxidising reagents and solvents.
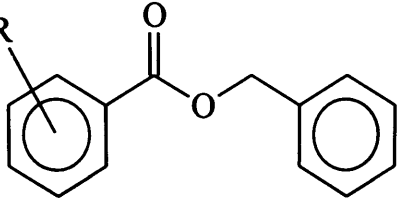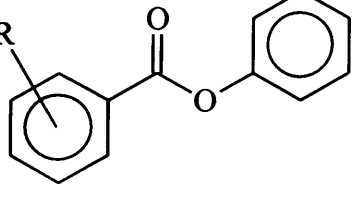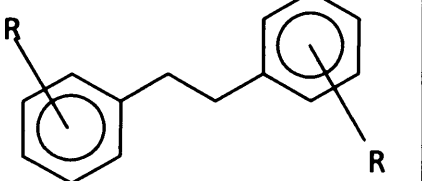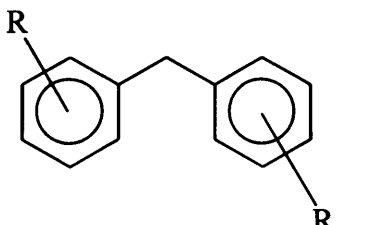
The liquid phase oxidation of 2-, 3-, and 4- methoxytoluenes (Table 4.6), and 2-, 3-, and 4-nitrotoluenes (Table 4.8), have been studied under the same conditions of toluene oxidation as it is reported in chapter 3.

Table 4.6. Comparison of the catalytic activity of substituted toluenes in the absence of solvent with O_2.

Substrate	Time (h)	Conv (%)	Selectivity (%)							TON
			Benzyl alcohol	Benzaldehyde	Benzoic acid	Benzyl benzoate				
Toluene	1	1.1	2.7	27.5	6.9	62.9				
	4	2.2	2.2	18.7	8.6	70.5				
	7	4.4	1.0	12.4	10.4	76.2				284
			n-Methoxy benzyl alcohol	*n*-Methoxy benzaldehyde	*n*-Methoxy benzoic acid	*n*-Methoxy benzyl *n*-methoxy benzoate	Toluene	Esters	C-C products	
4-Methoxy toluene	1	2.3	0.8	18.7	30.3	24.1	0.9	7.1	18.1	
	4	6.1	0.8	11.8	25.8	43.5	0.2	5.0	12.9	
	7	10.6	0.5	7.4	26.9	49.0	0.1	4.5	11.6	581
3-Methoxy toluene	1	1.7	1.4	16.4	46.5	8.1	7.4	1.2	19.0	
	4	2.0	1.1	33.3	30.6	2.2	19.5	0.8	12.5	
	7	3.7	0.9	12.6	43.3	17.0	6.8	1.2	19.0	204
2-Methoxy toluene	1	3.6	1.4	8.8	63.8	0.7	22.7	0.3	2.3	
	4	6.4	1.0	10.0	66.8	3.6	15.7	0.4	2.5	
	7	11.1	0.8	13.0	61.1	7.3	11.8	0.8	5.2	619

Reaction conditions: T = 160 °C (433K), pO_2 = 10 bar (0.1 MPa), substrate - 20 ml, catalyst – 0.4 g 1%Au-Pd/C (1:1.85 Au:Pd mol ratio) prepared by sol-immobilisation method. stirring rate - 1500 rpm, TON (moles of products/moles of metal) at 7 h reaction. TON numbers were calculated on the basis of total loading of metals. [s] - 1wt % total metal loading (1:1 wt Au:Pd) prepared by sol immobilisation.

Table 4.7. Additional oxidation products for methoxy toluene derivatives.

Methoxy toluene Derivatives	Additional Oxidation Product Structures	
R = 2- OMe, 3- OMe, 4- OMe		

In all the reactions, oxidised products containing the following functional groups; -OH, -CHO, -COOH, -COOR' and other by products have been identified. No CO_2 was observed in all the reactions, and the reactivity trend (4-methoxy- ~ 2-methoxy- >3-methoxy ~ toluene > 2-nitro- > 3-nitro ~ 4-nitro) is indicative of the involvement of

electron-deficient intermediate(s). The difference in activity could be attributed by the contribution of mesomeric effect coupled with hyper-conjugation, which is common in aromatic compounds having electron donating group ($-OCH_3$) and electron withdrawing group ($-NO_2$) as demonstrated by M. Szwarc (2).

Table 4.8. Liquid phase oxidation of 2-, 3-, 4- nitrotoluenes at 160 °C

Substrate	Time (h)	Conv (%)	Selectivity (%)						TON
			n-Nitro benzyl alcohol	*n*-Nitro benz-aldehyde	*n*-Nitro benzoic acid	Benzaldehyde	Toluene	Benzyl benzoate	
2- Nitro toluene	1	1.1	2.9	1.0	7.3	6.0	82.8	0.0	
	4	1.5	4.3	1.4	8.8	7.1	76.4	2.0	
	7	2.4	5.7	1.7	25.0	6.8	57.2	3.6	142
3-Nitro toluene	1	0.5	6.8	3.8	0.0	5.6	83.6	0.2	
	4	0.8	6.1	2.2	5.3	9.2	75.6	1.6	
	7	1.1	9.5	4.9	9.3	8.2	62.3	5.8	66
4-Nitro toluene	1	0.2	0.1	13.5	0.0	0.0	86.4	0.0	
	4	1.0	2.7	10.9	0.0	9.1	77.3	0.0	68

Reaction conditions: T = 160 °C (433K), pO_2 = 10 bar (0.1 MPa), substrate - 20 ml, catalyst – 0.4 g 1%Au-Pd/C (1:1.85 Au:Pd mol ratio) prepared by sol-immobilisation method. stirring rate - 1500 rpm, TON (moles of products/moles of metal) at 7 h reaction. TON numbers were calculated on the basis of total loading of metals.

These effects ultimately affect the bond energy of the methyl group in substituted toluenes which causes the difference in activity (2). There are some

additional products were formed during the oxidation of methoxy toluenes, which are identified as a family of esters and C-C coupling products (Table 4.7).

The liquid phase oxidation o-,m-,p- xylenes (Table 4.9) have been also investigated at 160 °C. The catalysts are equally effective for the oxidation of these substrates and formed the aldehyde, acid, and esters as products, with the relative amounts being dependent on the conversion (Table 4.9), confirming the wider applicability of the catalyst, 1%AuPd/C (1:1wt). Again the bond energy difference due to the association of mesomeric effect and hyper-conjugation makes these molecules to oxidize at different rates as demonstrated by M. Szwarc.

Table 4.9. Liquid phase oxidation of o-,m-,p- xylenes at 160 °C

Substrate	Time (h)	Conv. (%)	Selectivity (%)				TON[d]
			n-Toluyl alcohol	n-Tolualdehyde	n-Toluic Acid	C-C products/Esters	
o-xylene[a]	1	0.2	2.2	50.2	7.6	40.0	
	4	0.5	0.7	29.1	15.0	55.2	
	7	0.7	1.8	21.6	18.6	58.0	42[b]
m-xylene[a]	1	0.1	0.0	65.8	0.0	34.2	
	4	0.3	0.0	38.7	3.7	57.6	
	7	0.5	1.2	27.0	12.4	59.4	25[b]
p-xylene[a]	1	0.1	0.0	49.5	10.5	40.0	
	4	0.4	1.3	29.0	19.0	50.7	
	7	0.6	0.0	20.9	26.6	52.5	34[b]
p-xylene[b]	24	2.8	1.3	5.7	18.5	74.5	
	31	3.6	1.5	5.7	20.5	72.3	
	48	6.8	1.3	4.6	26.2	67.9	171[c]

Reaction conditions: T = 160 °C (433K), pO_2 = 10 bar (0.1 MPa), substrate - 20 ml, catalyst –1%Au-Pd/C (1:1.85 Au:Pd mol ratio) prepared by sol-immobilisation method, substrate/metal molar ratio =5600[a] (0.4 g catalyst) , substrate/metal molar ratio = 2800[b] (0.8 g catalyst) stirring rate - 1500 rpm, TON (moles of products/moles of metal) numbers were calculated on the basis of total loading of metals.

References:

1. J. Colby, D. I. Stirling, H. Dalton, Biochem. J. 165, 395 (1977).

2. W. Partenheimer, Catal. Today 23, 69 (1995).

3. A. Wittstock, V. Zielasek, J. Biener, C. M. Friend, M. Bäumer, Science, 327, 19 (2010).

4. M. Szwarc , J. Chem. Phys. 16, 128 (1948)

Chapter 5

Solvent-Free Oxidation of Benzyl Alcohol

5.1. Outline

This chapter deals with the results obtained from the liquid phase oxidation of benzyl alcohol using supported AuPd alloy nanoparticles as catalysts under solvent free conditions.

Supported metal nanoparticles are receiving significant attention as catalysts for a broad range of selective chemical transformations. In particular, Au nanoparticles have been shown to be particularly effective for a range of redox reactions (1-7). These include the low temperature oxidation of CO (7) especially when used as part of the processes for purifying a fuel cell feedstock (8) the synthesis of vinyl chloride by the hydrochlorination of ethyne (9) the selective oxidation of alkenes to epoxides (10, 11) and alcohols to aldehydes (12) as well as selective hydrogenation (13). Recently, it is reported that the alloying of Pd with Au can enhance the activity of the nanoparticles, and such materials have been found to be particularly effective for the direct synthesis of hydrogen peroxide from H_2 and O_2 (14, 15) and the oxidation of alcohols (16). As a matter of resemblance with toluene and experimental proof for oxidation catalysis, the supported Au-Pd bimetallic alloy nanoparticles prepared by sol immobilisation were also tested for benzyl alcohol under solvent free conditions at mild temperature.

5.2. Solvent free oxidation of benzyl alcohol using supported Au-Pd bimetallic nanoparticles prepared by sol immobilisation:

The synthesis of a systematic set of Au-Pd colloidal nanoparticles having a range of Au/Pd ratios has been examined for benzyl alcohol oxidation as it was demonstrated already for toluene oxidation (chapter 3 – Table 3.5). The catalysts have been structurally characterized using a combination of UV-visible spectroscopy, transmission electron microscopy, STEM HAADF/XEDS, and X-ray photoelectron spectroscopy. The Au-Pd nanoparticles are found in the majority of cases to be homogeneous alloys, although some variation is observed in the Au-Pd composition at high Pd/Au ratios. The optimum performance for the oxidation of benzyl alcohol is observed for a catalyst having a Au/Pd 1:2 molar ratio. These measured activity trends are discussed in terms of the structure and composition of the supported Au-Pd nanoparticles.

5.2.1. Results and discussion

The Au, Pd, and Au-Pd colloidal sols (Au/Pd=1:0, 7:1, 2:1, 1:1, 1:1.85, 1:2, 1:7, 0:1) were prepared and examined by UV-visible spectroscopy. For the pure Au sol, the appearance of the plasmon resonance was observed at 505 nm (figure 5.1). This resonance peak is characteristic for gold nanoparticles with particle sizes below 10 nm (17, 18). In the case of the Pd monometallic sol, there is no surface plasmon band (17). The spectra resulting from the $Au^x Pd^y$ bimetallic sols show the disappearance of the gold surface plasmon band on addition of Pd, as previously reported for this system (17, 19) which has been ascribed to changes in the band structure of the Au particles due to alloying with Pd. These results suggest the formation of bimetallic random-alloy nanoparticles, which is in agreement with previously reported data (20-22).
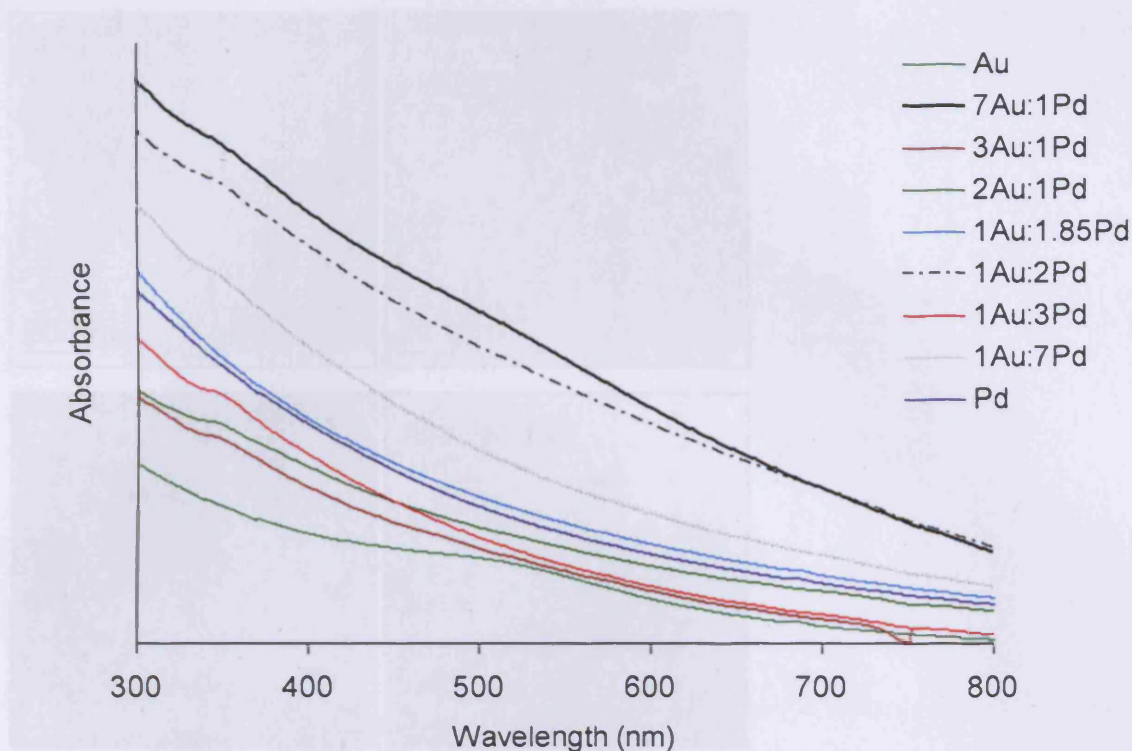
Figure 5.1. UV-Vis spectra obtained from the various Au_xPd_y colloidal solutions.

Representative bright field TEM micrographs (figure 5.2 & 5.3) were acquired in order to measure the particle size distributions of the colloidal metal nanoparticles after immobilization and drying on the activated carbon support. The particle size data for all the colloid compositions used in this study are summarized in Table 5.1. The median particles sizes for the monometallic Au and Pd colloids were found to be 3.5 and 5.4 nm, respectively. The median particle sizes for all the Au_xPd_y alloys were in the 2.9- 4.6 nm range, and did not show any discernible systematic size trend with colloid composition.
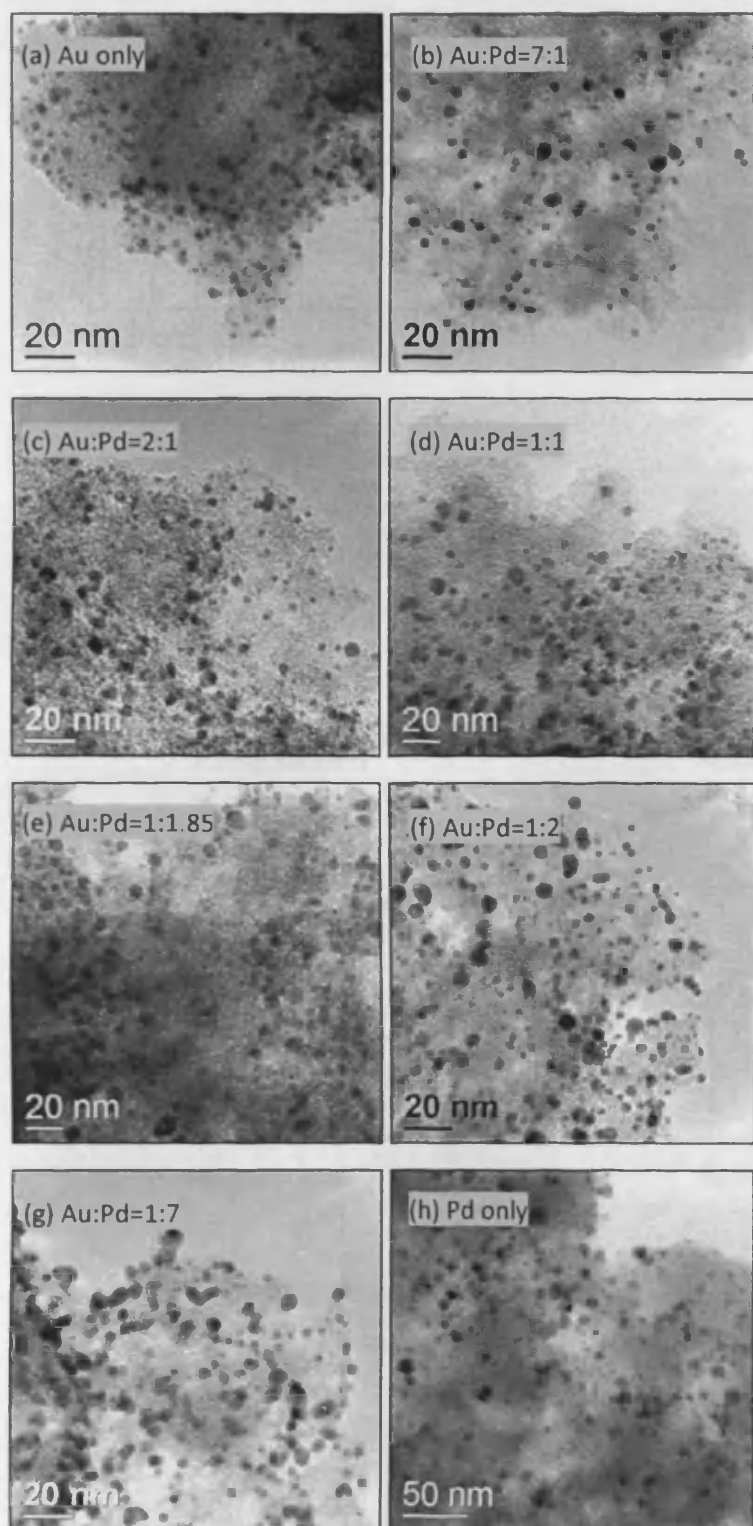
Figure 5.2: Representative bright field TEM micrographs showing AuPd particles immobilised on the activated carbon support: (a) Au only; (b) Au:Pd=7:1; (c) Au:Pd=2:1; (d) Au:Pd=1:1; (e) Au:Pd=1:1.85; (f) Au:Pd=1:2; (g) Au:Pd=1:7; (h) Pd only. (Images taken by Ram *et al*)
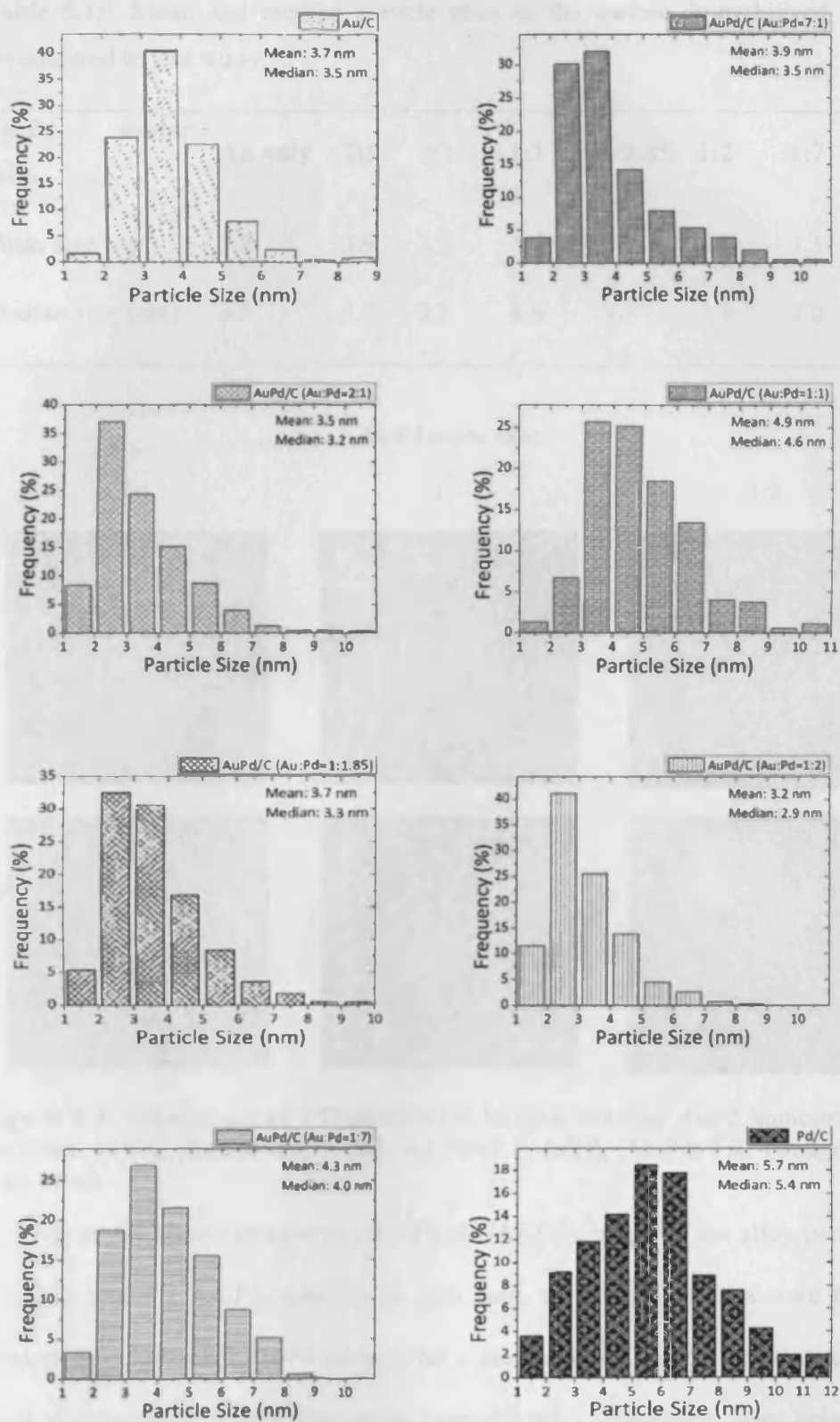
Figure 5.3 : Particle size distributions of the AuPd particles (various mol ratios) immobilised on the activated carbon support. (Data supplied by Ram *et al*)

Table 5.1: Mean and median particle sizes of the various immobilized Au-Pd sols investigated in this study.

Au:Pd molar ratio	Au only	7:1	2:1	1:1	1:1.85	1:2	1:7	Pd only
Mean size (nm)	3.7	3.9	3.5	4.9	3.7	3.2	4.3	5.7
Median size (nm)	3.5	3.5	3.2	4.6	3.3	2.9	4.0	5.4

Au:Pd molar ratio

    2:1   1:1   1:2
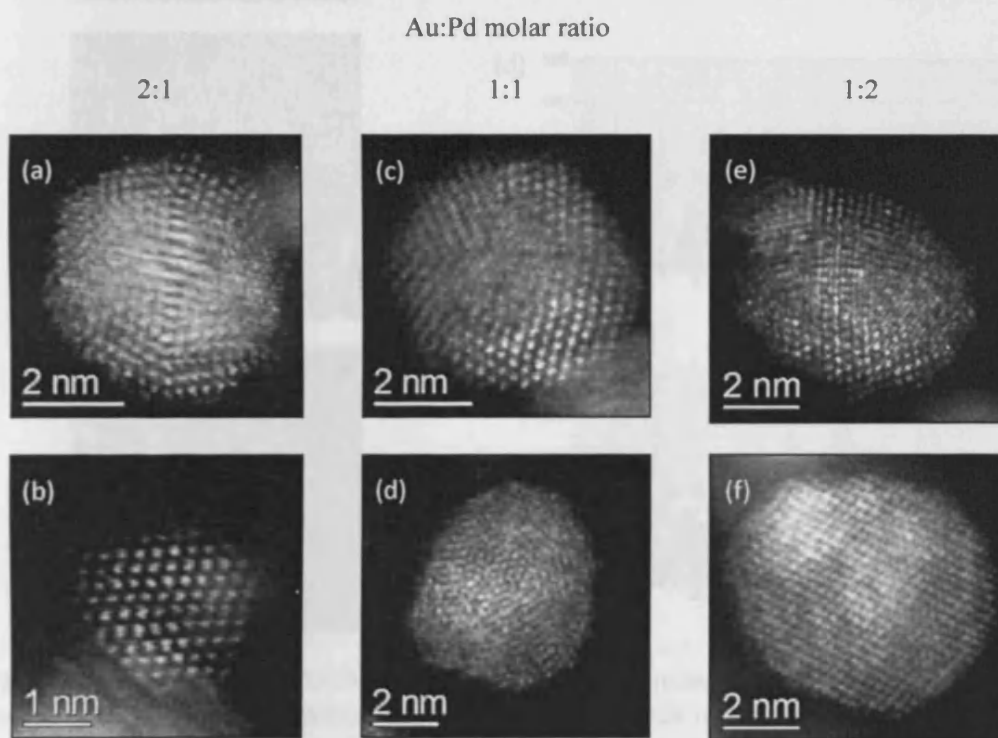
Figure 5.4: Representative STEM-HAADF images showing AuPd homogeneous alloy particles. (a)(b), Au:Pd=2:1; (c)(d), Au:Pd=1:1; (e)(f), Au:Pd=1:2. (Images taken by Ram *et al*)

Figure 5.4 shows representative STEM-HAADF images of the alloy particles in the 2:1, 1:1, and 1:2 Au-Pd samples. In each case, the metal particles were found to be random homogeneous Au-Pd alloys with a face-centered cubic (fcc) structure. If core-shell morphologies, or any other gross form of Au-Pd segregation, were present in these nanoparticles, these would have been apparent by atomic mass (z) contrast in these

HAADF images. It is interesting to note that the Au-Pd particles remained pseudospherical (i.e., did not strongly wet the activated C support material).
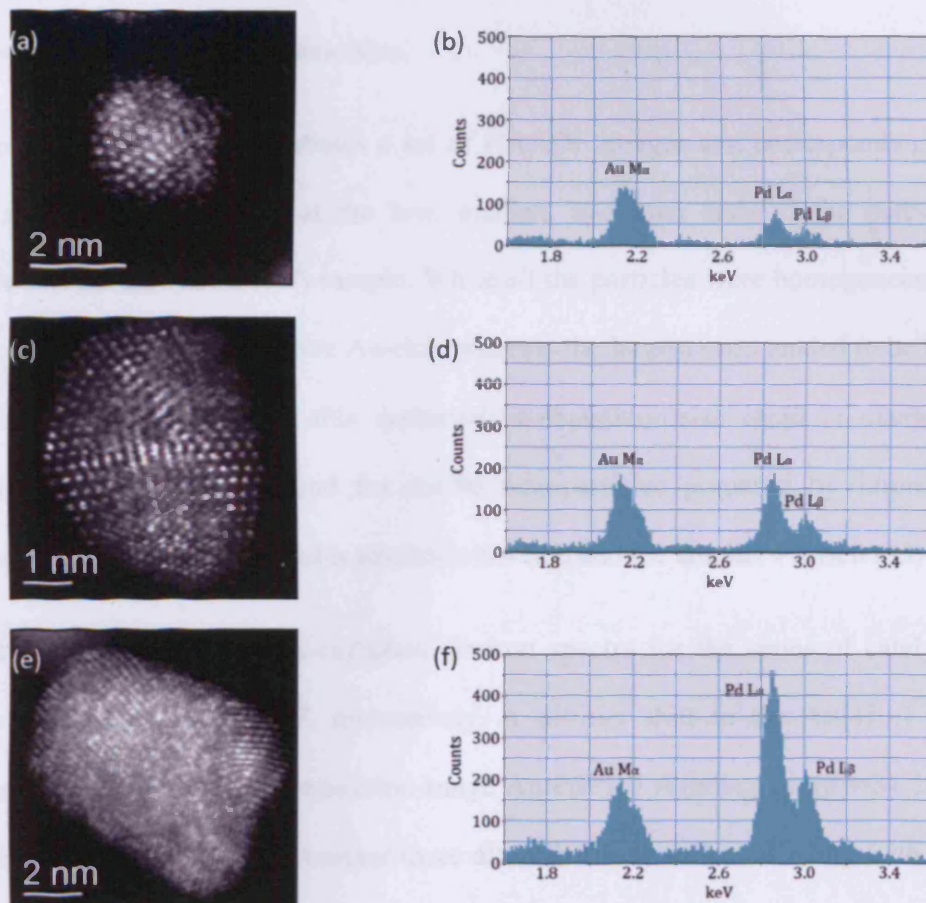
Figure 5.5: A set of HAADF images and corresponding XEDS point spectra from particles at the low (a,b), median (c,d) and high (e,f) ends of the particle size distribution for the Au:Pd (1:7) sample. They demonstrate a systematic particle size/composition variation, where the smaller particles progressively become more Au-rich and Pd-deficient. (Images taken by Ram *et al*)

Energy dispersive X-ray spectra were acquired from areas containing ~100 metal particles in order to qualitatively check alloy compositions. The relative Au to Pd peak areas from such "averaged" spectra agreed with the nominal x and y values for each of the Au_xPd_y alloy compositions. Furthermore, XEDS spectra obtained from individual particles showed characteristic Au M lines and Pd L lines confirming that intimately

mixed AuPd alloys had been formed rather than physical mixtures of pure Au and Pd particles. However, it was noticeable that, within specific Au_xPd_y samples, the XEDS spectra obtained from individual particles did show considerable systematic composition variations as a function of particle size.

For example, figure 5.5 shows a set of HAADF images and corresponding XEDS point spectra from particles at the low, median, and high ends of the particle size distribution for the Au/Pd (1:7) sample. While all the particles were homogeneous AuPd alloys, the smallest particles were Au-rich, whereas the largest ones tended to be Pd-rich. It is interesting to note that this systematic composition/size trend is diametrically opposite to the situation found for Au-Pd nanoparticles prepared by impregnation methods where the larger particles tended to Au-rich and the smaller Pd-rich (23)

The Pd(3d) and Au(4f) X-ray photoelectron spectra for the series of catalysts are shown in figures 5.6 and 5.7, respectively. A distinct shift in the $Au(4f_{7/2})$ binding energy is observed in the composition range Au/Pd=1:0 (binding energy=84.2 eV) to Au/Pd=1:1 (84.0 eV), being constant there after; this may reflect alloying with the Pd. Analysis of the Pd(3d) spectra is complicated by the severe overlap between the Pd(3d) doublet and the $Au(4d_{5/2})$ component. However, when we calculate the experimental surface Pd/Au molar ratios based on the $Pd(3d_{5/2})+Pd(3d_{3/2})+Au(4d_{5/2})$ combined integrated intensities and the Au(4f) intensity together with known relative sensitivity factors, we are able to correct the molar ratio by simply subtracting 0.5 from the raw experimental values.

The corrected experimental ratios are plotted against nominal ratios (based on the preparation recipes) in figure 5.8 and show a very clear linear correlation for Pd/Au

ratios up to Pd/Au=1:1, and the X-ray photoelectron spectroscopy (XPS)-derived Pd/Au

molar ratio matches the ratios used in the synthesis. However, as we increase the relative

ratio of Pd/Au in the synthesis above unity, XPS-derived surface ratios are consistently

approximately a factor of 2 lower than "expected". This could in principle arise from (i)

a systematic difference in alloy composition with particle size, (ii) the presence of

Pd(core)-Au(shell) nanoparticles, (iii) differential deposition of Au and Pd relative to the

intended composition, or (iv) preferential adsorption of smaller Pd-rich nanoparticles

deeper into the carbon structure.

The TEM characaterization we have described supports explanation (i) as the most

likely explanation. The STEMHAADF/XEDS analysis rules out explanation (ii), and

TEM-XEDS analysis and visual inspection during the immobilization procedure rule out

any significant contribution of (iii). An explanation based in (iv) would be in agreement

with similar suggestions in the literature (24) but still is purely speculative and lacks any

substantial evidence at this time.

Importantly, HAADF with XEDS point spectra analysis demonstrate that, for the

catalysts with a high Pd/Au ratio, a systematic particle size/composition variation

occurs. The larger particles progressively become more Pd-rich and Au-deficient, and

considering the high surface sensitivity of XPS, this effect alone could provide a

satisfactory explanation for the systematic deviation observed between Pd/Au ratios used

in the synthesis and calculated from XPS data. The Pd nanoparticles comprise

predominantly Pd^0 species ($Pd(3d_{5/2})$ binding energy ca. 335 eV) for Pd/Au ratios<1, but

the presence of Pd^{2+} species is indicated for higher Pd contents (figure 5.6), with the

highest concentration corresponding to the Pd-only catalyst.
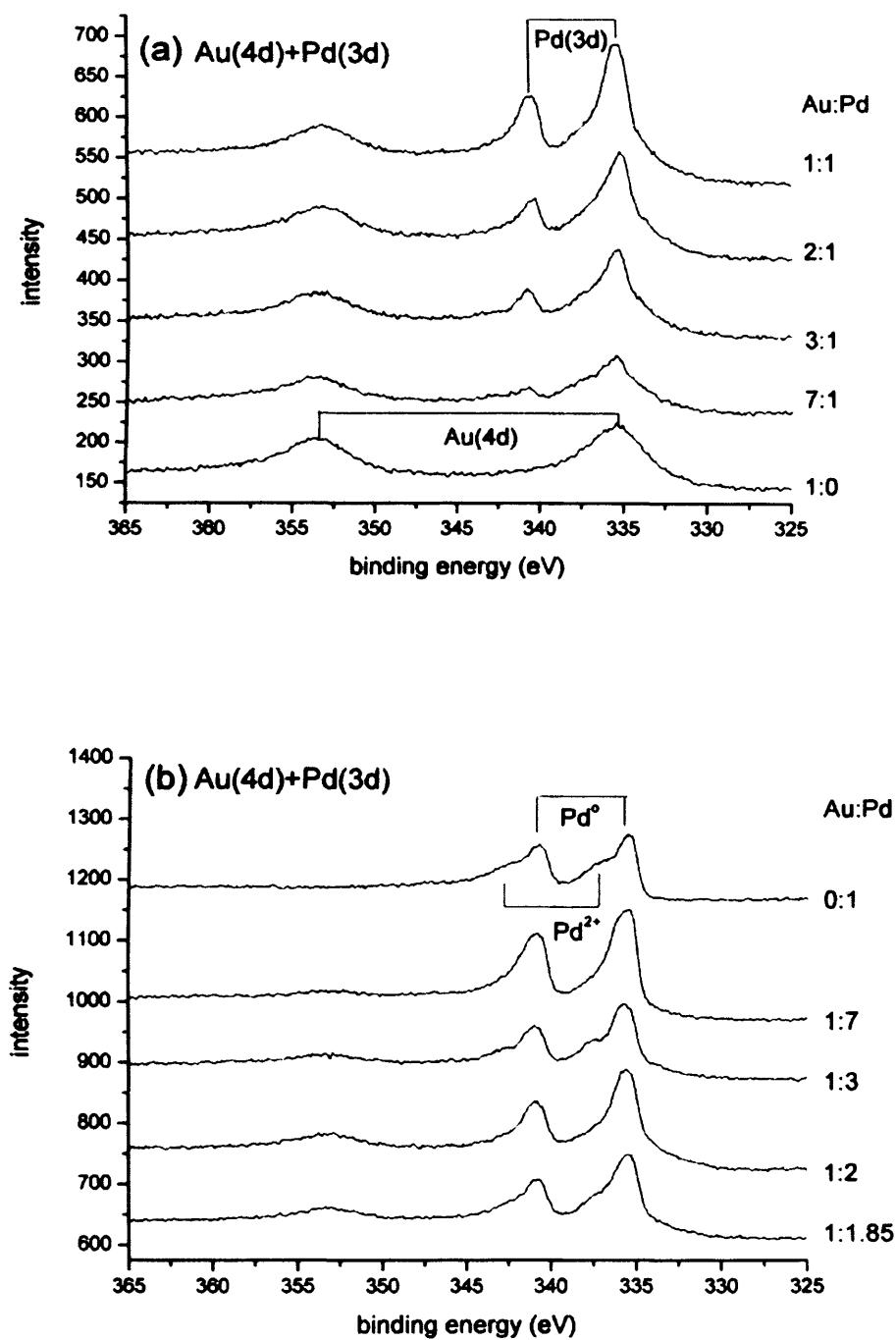
Figure 5.6: Pd (3d) spectra for the series of Au-Pd/carbon catalysts; nominal Au:Pd ratios are as indicated.
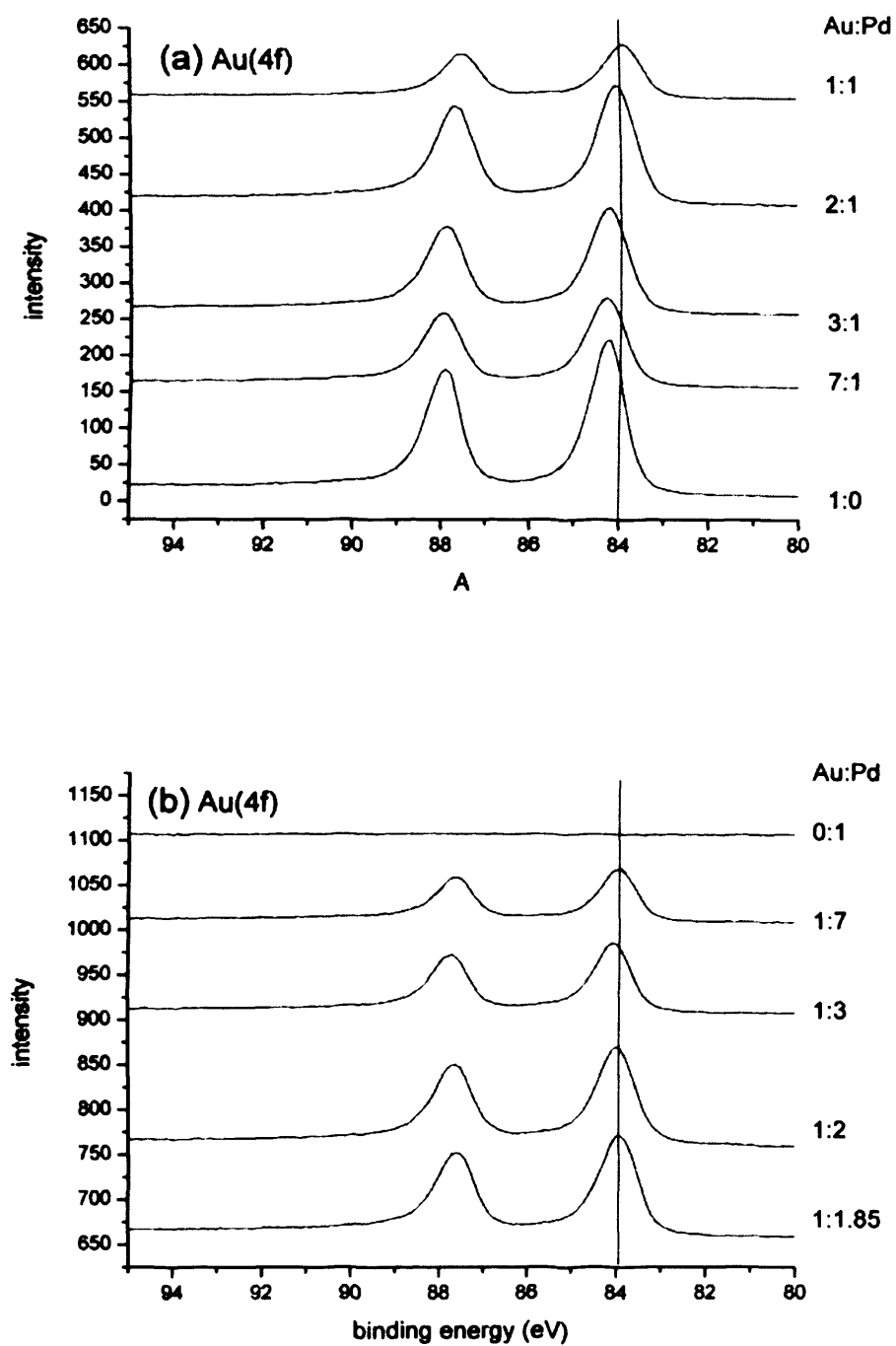
Figure 5.7: Au(4f) spectra for the series of Au-Pd/carbon catalysts; nominal Au:Pd ratios are as indicated.
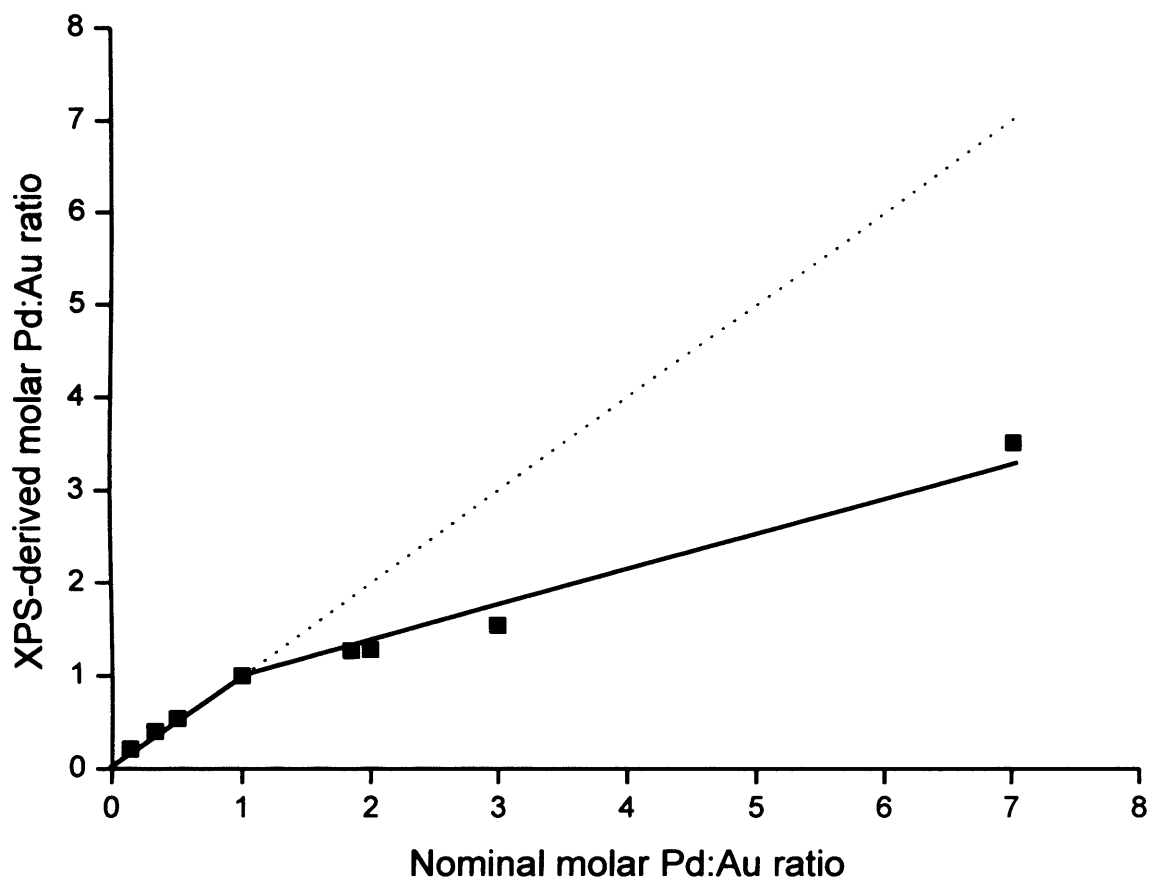
Figure 5.8: XPS-derived corrected Pd:Au molar ratios plotted as a function of nominal (expected) Au:Pd ratios. The dotted line shows the expected ratio.

The catalytic oxidation of benzyl alcohol under free solvent conditions has been chosen as an appropriate model reaction for exploring the catalytic performance of the bimetallic Au_x-Pd_y catalysts. The results of the catalytic tests at 120 °C are presented in Table 5.2.

Table 5.2: Effect of the molar Au:Pd ratio on benzyl alcohol oxidation results with 1 wt% $(Au_x\text{-}Pd_y)$/C catalysts prepared by sol immobilisation method

Catalyst	Conv. (%)	Selctivity (%)			
		Toluene	Benzaldehyde	Benzoic acid	Benzyl benzoate
1%Au/C_{SI}	6.6	23.9	63.9	3.1	9.0
1%(7Au-1Pd)/C_{SI}	11.6	1.9	66.3	7.2	24.5
1%(3Au-1Pd)/C_{SI}	23.3	6.0	72.5	8.6	12.9
1%(2Au-1Pd)/C_{SI}	52.0	10.9	77.5	3.5	8.1
1%(1Au-1Pd)/C_{SI}	71.1	4.0	69.8	19.9	6.3
1%(1Au-1.85Pd)$_{SI}$	80.7	3.4	67	23.1	6.4
1%(1Au-2Pd)/C_{SI}	90.8	4.5	67.4	22.9	5.1
1%(1Au-3Pd)/C_{SI}	94.7	4.2	67	23.5	5.3
1%(1Au-7Pd)/C_{SI}	88.7	1.7	68.4	24.1	5.8
1%Pd/C_{SI}	59.3	6.8	74.7	10.4	8.1

Reaction conditions: T = 120 °C (393K), pO_2 = 10 bar (0.1 MPa), stirring rate - 1500 rpm, substrate - 40 ml benzyl alcohol, catalyst – 0.05 g, t = 6 h.

The activity of the monometallic 1 wt%Au/C was very poor, but on increasing the Pd content we observed a progressive increase in catalytic activity. This increase of activity reached a broad maximum with a Au/Pd molar ratio between 1:1 and 1:3, as values above 95% conversion are achieved. A further increase in the Pd content resulted in a progressive decrease in catalytic activity. It is important to note that even in the presence of a minor amount of gold or palladium (i.e., in the case of 1:7 and 7:1 Au/Pd

molar ratios) a significant increase in the catalytic activity was observed; specifically, an increase in activity by a factor of 2.3-2.6 has been observed with respect to the monometallic Au and Pd catalysts.

In order to determine the effect of the Au/Pd molar ratio on selectivity, the catalytic data were compared at iso-conversion, and Table 5.3 shows the catalytic data at 50% conversion.

Table 5.3: Comparison of benzyl alcohol oxidation at iso-conversion of 50% with 1 wt% $(Au_x-Pd_y)/C$ catalysts prepared by colloidal method

Catalyst	Selctivity (%)			
	Toluene	Benzaldehyde	Benzoic acid	Benzyl benzoate
1%(2Au-1Pd)/C_{SI}	11.0	78.6	3.5	6.9
1%(1Au-1Pd)/C_{SI}	5.4	79.7	7.4	7.5
1%(1Au-1.85Pd)C_{SI}	4.3	81.9	6.6	7.2
1%(1Au-2Pd)/C_{SI}	7.5	83.6	3.5	5.4
1%(1Au-3Pd)/C_{SI}	6.6	85.4	2.4	5.5
1%(1Au-7Pd)/C_{SI}	1.9	85.8	5.5	6.8
1%Pd/C_{SI}	6.4	76.0	8.9	8.7

Reaction conditions: T = 120 °C (393K), pO_2 = 10 bar (0.1 MPa), stirring rate - 1500 rpm, substrate - 40 ml benzyl alcohol, catalyst − 0.05 g, t = 6 h. Catalysts containing higher amounts of Au could not be compared at iso-conversion as the conversion with these catalysts was typically <50% for reasonable reaction times.

These data show that the catalytic performance in terms of reaction specificity is not particularly significant and all catalysts give high selectivities to benzaldehyde which is
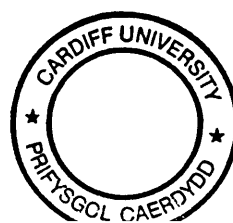
the primary product (Scheme 5.1). Hence, the main effect of alloying Au with Pd is an effect of enhancing activity. Although at high conversions with Pd-rich catalysts the selectivity to benzoic acid is enhanced. In particular, the formation of toluene, which is generated from benzyl alcohol by a hydrogen transfer reaction, does not increase at iso-conversion as the Pd content increases. It has been shown from the H_2O_2 hydrogenation studies that hydrogenation increases with Pd concentration in the Au-Pd alloy (25), hence it is expected to observe higher toluene selectivities as the Pd content is increased. To the contrary, selectivity values at iso-conversion indicate that the selectivity toward toluene is highest for the gold-rich catalysts (Pd/Au=0.5).
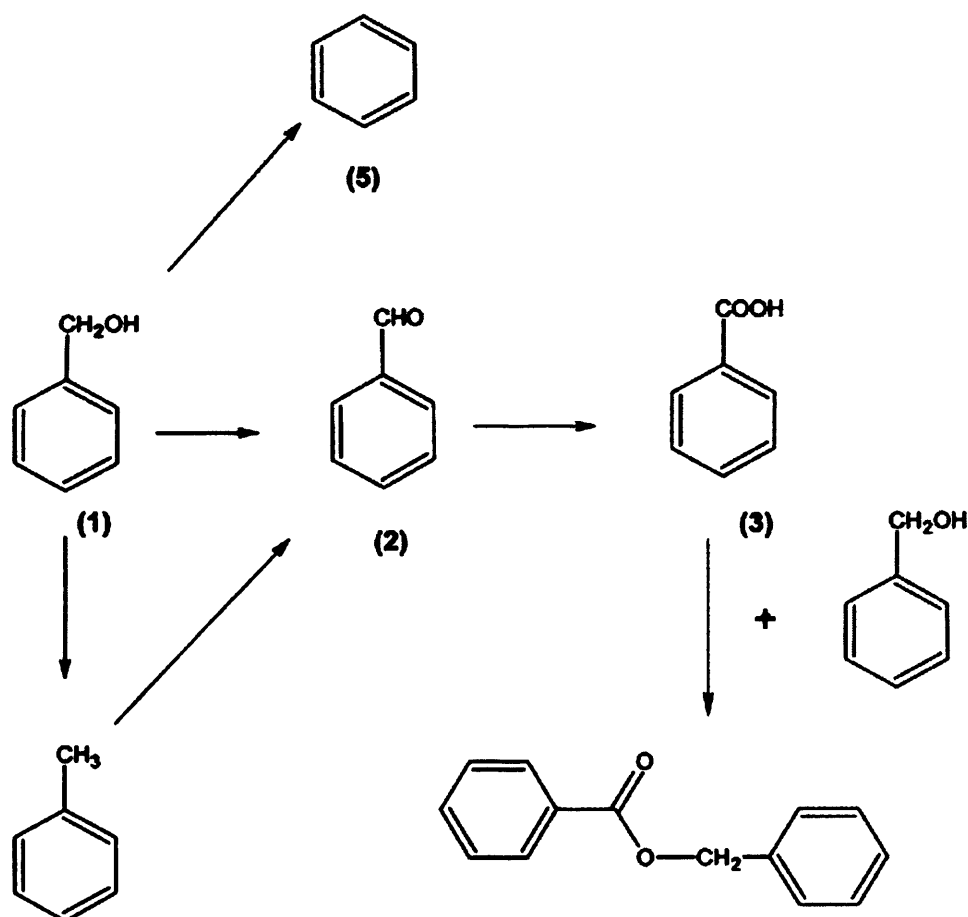
Scheme 5.1: General reaction pathway for benzyl alcohol oxidation.

Figure 5.9 shows a plot of turnover frequencies (TOF @ 0.5 h) obtained with the increase of Pd molar % in 1%AuPd/C catalyst prepared by sol immobilisation. The TOF value reaches maximum of >60 000 h^{-1} for the catalyst containing 65% Pd content out of 100% (Au+Pd), which is 1:1.85 Au/Pd catalyst, revealing it is the most active catalyst for benzyl alcohol oxidation under the described reaction conditions.
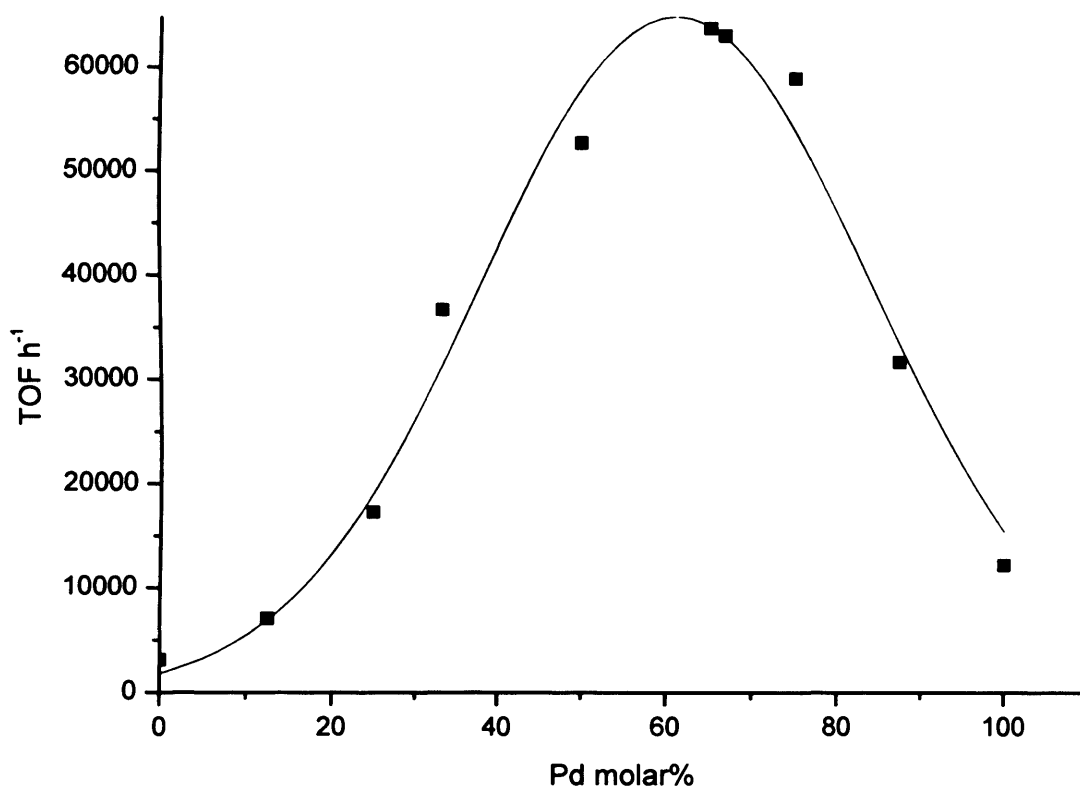
Figure 5.9: TOF (at 0.5 h) trend for the increasing molar % of Pd in 1%AuPd/C, tested for benzyl alcohol oxidation

Using the particle size distribution obtained via TEM, it has been possible to calculate the distribution of atoms on the catalyst surface for the composition of Pd/Au = 1.85 which coincides with the optimized activity catalyst. Taking these values into

account, the activities have been recalculated to use only those atoms exposed on the catalyst surface. For benzyl alcohol oxidation, a TOF of 1 96 000 mol benzyl alcohol reacted per surface atom of metal per hour is observed. This is further evidence of the very high activity that the Au-Pd alloy system can produce when the preparation method and composition are properly optimized.

References:

(1) Bond, G. C.; Thompson, D. T. Catal. Rev.-Sci. Eng. 1999, 41, 319–388.

(2) Bond, G. C.; Thompson, D. T. Gold Bull. 2000, 33, 41–51.

(3) Haruta, M. Gold Bull. 2004, 37, 27–36.

(4) Hashmi, A. S. K. Gold Bull. 2004, 37, 51–65.

(5) Meyer, R.; Lemaire, C.; Shaikutdinov, Sh. K.; Freund, H.-J. Gold Bull. 2004, 37, 72–124.

(6) Hashmi, A. S. K.; Hutchings, G. J. Angew. Chem., Int. Ed. 2006, 45, 7896– 7936.

(7) Haruta, M.; Kobayashi, T.; Sano, H.; Yamada, N. Chem. Lett. 1987, 16, 405–408.

(8) Landon, P.; Ferguson, J.; Solsona, B. E.; Garcia, T.; Carley, A. F.; Herzing, A. A.; Kiely, C. J.; Golunski, S. E.; Hutchings, G. J. Chem. Commun. 2005, 3385– 3387.

(9) Hutchings, G. J. J. Catal. 1985, 96, 292–295.

(10) Sinha, A. K.; Seelan, S.; Tsubota, S.; Haruta, M. Angew. Chem., Int. Ed. 2004, 43, 546–1548.

(11) Hughes, M. D.; Xu, Y.-J.; Jenkins, P.; McMorn, P.; Landon, P.; Enache, D. I.; Carley, A. F.; Attard, G. A.; Hutchings, G. J.; King, F.; Stitt, E. H.; Johnston, P.; Griffin, K.; Kiely, C. J. Nature 2005, 437, 1132–1135.

(12) Abad, A.; Conception, P.; Corma, A.; Garcia, H. Angew. Chem., Int. Ed. 2005, 44, 4066–4069.

(13) Corma, A.; Serna, P. Science 2006, 313, 332–334.

(14) Edwards, J. K.; Solsona, B.; Ntainjua, E.; Carley, A. F.; Herzing, A. A.; Kiely, C. J.; Hutchings, G. J. Science 2009, 323, 1037–1041.

(15) Edwards, J. K.; Hutchings, G. J. Angew. Chem., Int. Ed. 2008, 47, 9192–9198.

(16) Enache, D. I.; Edwards, J. K.; Landon, P.; Solsona-Espriu, B.; Carley, A. F.; Herzing, A. A.; Watanabe, M.; Kiely, C. J.; Knight, D. W.; Hutchings, G. J. Science 2006, 311, 362–365.

(17) Bianchi, C. L.; Canton, P.; Dimitratos, N.; Porta, F.; Prati, L. Catal. Today 2005, 102-103, 203–212.

(18) Link, S.; El-Sayed, M. A. J. Phys. Chem. B 1999, 103, 4212–4217.

(19) Lopez-Sanchez, J. A.; Dimitratos, N.; Miedziak, P.; Ntainjua, E.; Edwards, J. K.; Morgan, D.; Carley, A. F.; Tiruvalam, R.; Kiely, C. J.; Hutchings, G. J. Phys. Chem. Chem. Phys. 2008, 10, 1921–1930.

(20) Deki, S.; Akamatsu, K.; Hatakenaka, Y.; Mizuhata, M.; Kajinami, A. Nanostruct. Mater. 1999, 11, 59–65.

(21) Scott, R. W. J.; Wilson, O. M.; Oh, S.-K.; Kenik, E. A.; Crooks, R. M. J. Am. Chem. Soc. 2004, 126, 15583–15591.

(22) Dash, P.; Bond, T.; Fowler, C.; Hou, W.; Coombs, N.; Scott, R. W. J. J. Phys. Chem. C 2009, 113, 12719–12730.

(23) Herzing, A. A.; Watanabe, M.; Kiely, C. J.; Edwards, J.; Conte, M.; Tang, Z. R.; Hutchings, G. J. Faraday Discuss. 2008, 138, 337–351.

(24) Bianchi, C.; Porta, F.; Prati, L.; Rossi, M. Top. Catal. 2000, 13, 231–236.

(25) James Pritchard, Lokesh Kesavan, Marco Piccinini, Qian He, Ramchandra Tiruvalam, Nikolaos Dimitratos, Jose A. Lopez-Sanchez, Albert F. Carley, Jennifer K.

Edwards, Christopher J. Kiely, Graham J. Hutchings, Langmuir 2010, 26(21), 16568–16577

Chapter 6

Conclusions and Future Work

This chapter describes the conclusions derived from the experimental results, emerged out of this research project for the partial fulfilment of the completion of the PhD degree.

Selective oxidation of primary carbon-hydrogen bonds with oxygen is of crucial importance for the sustainable exploitation of available feedstocks. To date, heterogeneous catalysts have either shown low activity and/or selectivity or have required activated oxygen donors. It is reported here that supported gold-palladium (Au-Pd) nanoparticles on carbon or TiO_2 are active for the oxidation of the primary carbon-hydrogen bonds in toluene and related molecules, giving high selectivities to benzyl benzoate under mild solvent-free conditions. Differences between the catalytic activity of the Au-Pd nanoparticles on carbon and TiO_2 supports are rationalized in terms of the particle/support wetting behaviour and the availability of exposed corner/edge sites. Further these catalysts have been tested for substituted toluenes and benzyl alcohol, as these substrates have similarity in their structural configuration. The results are discussed with regard to structure activity relationship.

6.1. Conclusions:

➢ Blank toluene oxidation (without catalysts) has been done at 190 °C and 160 °C using oxygen as an oxidant and found that there is a contribution of homogeneous reaction between toluene and oxygen at 190 °C, which is not observed at 160 °C. Hence, it is concluded that reactions performed at 160 °C in the presence of catalysts are purely heterogeneous in nature. This important observation suggests that the earlier studies conducted at 190 °C (Table 6.1) may not in fact have been heterogeneously catalyzed. The previous studies concerning toluene oxidation using

heterogeneous catalysts using O_2 and tertiary butyl hydroperoxide (TBHP) is shown

in Table 6.1.

Table 6.1: Comparison of toluene oxidation activity of the Au-Pd supported catalysts with other reported catalytic systems.

Catalyst	T/P	Oxidant	Conv (%)	Selectivity (%)				TON
				Benzyl alcohol	Benzal- dehyde	Benzoic acid	Benzyl benzoate	
[1]Cu-Mn (1/1)	190 °C 1MPa	O_2	21.6	1.6	9.2	73.7	13.6	8
[2]Cu-Fe/γ- Al_2O_3	190 °C 1MPa	O_2	25.4	1.0	27.4	71.6	n.d.	74
[3]$MnCO_3$	190 °C 1MPa	O_2	25.0	5.3	9.7	80.8	n.d.	50
[4]CoSBA-15	80 °C 1 atm	TBHP	8.0	n.d.	64.0	n.d.	n.d.	103
[5]Cr/Silicalite	80 °C 1 atm	TBHP	18.4	5.2	23.3	25.7	n.d.	n.d.
[6]AuPd/C	160 C 0.1 MPa	O_2	50.8	0.1	1.1	4.5	94.3	3300

n.d – not determined

> Support materials like carbon, titania have been tested for toluene oxidation at 160 °C and shown that they have no activity over toluene activation under given reaction conditions. Therefore these supports have been chosen to immobilize metal nanoparticles on top of them.

➢ Titania supported Au-Pd nanoparticles prepared by the impregnation method has been tested for toluene oxidation and found to have no remarkable activity since the particle size was relatively large and particles had substantial compositional variations.

➢ Carbon and titania supported Au-Pd alloy nanoparticles prepared by a sol immobilization technique have been tested for toluene oxidation and observed to have considerable conversion of toluene. Carbon based catalyst has shown twice the activity of the titania representative and it was been chosen for further studies.

➢ A systematic set of carbon supported Au-Pd colloidal nanoparticles having a range of Au/Pd ratios (by keeping 1wt% total metal) prepared by sol immobilisation have been tested for toluene oxidation at 160 °C for 7 hrs and established that Au/Pd mol ratio of 1:2 is the optimum level of loading to get high activation in toluene. For the sake of convenience, Au/Pd mol ratio of 1:1.85 [(close to 2)] or 1:1 wt ratio has been chosen to explore the toluene oxidation.

➢ Also, a physical mixture of the separate Au/C and Pd/C catalysts showed no enhancement, highlighting the necessity of synergistic effect between Au and Pd.

➢ Attempts made to increase the conversion of toluene by i) increasing the mass of the catalyst, ii) prolonging the reaction time, gave positive results and revealed that there is no contribution of diffusion limitations.

➢ Toluene oxidation carried out using a lower substrate/metal ratio (~3250) for longer hours *ca.* 110h at 160 °C, promoted the conversion of toluene into 100%. Only, the bimetallic catalyst yielded full conversion, whereas monometallic ended up with maximum of 8%. Again, it is confirming the presence of

synergistic effect between Au and Pd, which is vital in activating toluene molecules. The selective product found at full conversion was benzyl benzoate (~85%).

➢ Toluene oxidation carried out using a very lower substrate/metal ratio (~1625) at 160 °C, reduced the reaction time drastically from 110 h to ~30 h, by retaining the complete conversion of toluene and the selectivity of benzyl benzoate

➢ Toluene oxidation performed at 140 °C to increase the selectivity of benzyl benzoate as the temperature could play a role of tuning the selectivity distribution of the products. The experiment resulted with ~95% yield of benzyl benzoate as per the expectation.

➢ Structure –activity relationship of Au-Pd bimetallic sol/toluene oxidation has been detailed with the help of STEM HAADF technique.

➢ The bimetallic colloids have a mean particle size of 2.9 nm and were found to be homogeneous Au-Pd alloys.

➢ After deposition of the colloids onto either activated amorphous carbon or TiO_2, the particle size went to a modest increase say 3.9 and 3.7 respectively. It is due to the low temperature drying process of these materials.

➢ The difference in activity of carbon and titania supported catalysts was detailed in terms of particle wetting behaviour, coordination number sites and the morphology of the particles.

➢ Low temperature and low pressure toluene oxidation have been carried out and they have shown poor activity.

➢ Finally it is concluded that carbon supported Au-Pd alloy nanoparticles prepared by a sol immobilization technique can give significantly improved activity for

the oxidation of toluene under mild solvent-free conditions. These catalysts have TONs that are a factor of ~30 greater than those of previous heterogeneous catalysts for this reaction and also display a remarkably high selectivity to benzyl benzoate.

➢ The rapid and high level formation of benzyl benzoate could result through four possible mechanistic pathways, which are

(i) coupling of the benzaldehyde and the benzyl alcohol to give the hemiacetal, followed by oxidation to the ester, benzyl benzoate.

(ii) direct thermal (catalyzed) dehydrative esterification between benzoic acid and benzyl alcohol.

(iii) Cannizzaro reaction between benzyl alcohol and benzaldehyde via alkoxide

(iv) Tishchenko coupling of two benzaldehydes via "dimer", directly to the ester.

➢ Experiments have been designed to test for the importance of each pathway and the results ruled out (ii), (iii), (iv), leaving (i) as a trusted route.

➢ Catalyst reusability studies have been done for toluene oxidation using carbon and titania supported AuPd alloy nanoparticles prepared by sol immobilisation and the results show that catalysts are reusable

➢ Investigation of leaching of metals from the catalyst has been studied and the results reveal that the catalyst is stable.

➢ To show the general applicability of the catalyst, substituted toluenes such as methoxy toluenes, nitro toluenes, and xylenes were tested under the same reaction conditions as that of toluene.

➢ As matter of relevancy with toluene, benzyl alcohol oxidation experiments have been studied under solvent free conditions at 120 °C. The products found were, toluene, benzaldehyde, benzoic acid and benzyl benzoate.

➢ A series of carbon supported Au-Pd colloidal nanoparticles having a range of Au/Pd ratios (by keeping 1wt% total metal) prepared by sol immobilisation been tested for benzyl alcohol oxidation at 120 °C for 6 hrs and established that Au/Pd mol ratio of 1:2 is the optimum level of loading to get high conversion of benzyl alcohol as it was observed in toluene oxidation. Further, the characterizations of the catalysts are well detailed.

6.2. Ongoing work:

There are few series of experiments have been planned as a follow up study of toluene and benzyl alcohol oxidation. Preliminary results have been obtained and characterizations of the catalysts have to be explored to understand the structure-activity relationship of the catalysts.

6.2.1. Effect of amount of solvent medium in sol preparation:

In this study, a series of 1%AuPd/C (1:1mol) catalysts have been prepared using a standard preparation protocol of sol immobilisation, except the volume of water (solvent medium) utilized. The standard amount of water for any sol immobilisation preparation is 800 ml. Now, we have tried to prepare the catalysts by changing the amount of water used, say 100 ml, 150 ml, 200 ml, 1500 ml, keeping all other preparation parameters constant. The idea behind these preparations is to have the particle size distributions in different windows, say 10-8 nm, 8-6 nm, 6-4 nm, 4- 2 nm, 2-0.5 nm and also different shapes if possible, since the concentration of the sol is different in each case.

These catalysts have been tested for benzyl alcohol oxidation and toluene oxidation. The results are compared at identical reaction conditions (Table 6.2 & 6.3).

Table 6.2: Toluene oxidation at 160 °C

| Variable | Time h | Conv % | Selectivity % | | | | TOF | TON |
			Benzyl alcohol	Benz aldehyde	Benzoic acid	Benzyl benzoate		
100 ml water	1.0	0.0	0.0	0.0	0.0	0.0	0.0	0.0
	4.0	1.5	0.2	7.9	1.1	90.8	24.0	95.9
	7.0	2.3	0.3	6.4	1.1	92.2	21.2	148.4

24.0	5.4	0.6	3.9	1.8	93.7	14.6	350.8
31.0	7.7	0.6	2.6	1.7	95.1	16.1	499.2
48.0	**9.0**	**0.6**	**2.1**	**1.4**	**95.8**	**12.2**	**584.6**

150 ml
water

1.0	0.4	4.2	23.4	4.7	67.8	27.2	27.2
4.0	1.4	1.5	9.2	1.6	87.6	22.8	91.1
7.0	2.1	1.1	5.7	1.2	92.0	19.5	136.4
24.0	6.9	0.5	2.7	1.8	95.0	18.6	446.2
31.0	8.7	0.4	2.1	1.6	95.9	18.3	567.4
48.0	**13.5**	**0.5**	**1.5**	**1.5**	**96.5**	**18.3**	**878.0**

200 ml
water

1.0	0.9	5.2	45.3	7.2	42.3	57.0	57.0
4.0	3.7	0.1	13.1	8.9	77.9	59.6	238.4
7.0	4.2	0.2	12.4	11.5	75.9	38.8	271.3
24.0	16.3	0.2	2.7	4.6	92.4	44.2	1059.8
31.0	18.5	0.3	2.5	2.9	94.3	38.8	1203.0
48.0	**30.3**	**0.2**	**1.1**	**2.4**	**96.3**	**41.1**	**1970.8**

800 ml
water

1.0	0.7	1.5	65.6	14.5	18.4	43.1	43.1
4.0	4.2	0.2	14.6	17.7	67.5	67.7	271.0
7.0	6.5	0.1	10.2	16.1	73.6	60.0	419.8
24.0	18.7	0.3	5.8	14.1	79.8	39.1	1213.2
31.0	21.4	0.2	3.5	10.5	85.8	58.1	1393.6
48.0	**32.8**	**0.3**	**2.4**	**11.8**	**85.6**	**44.4**	**2132.2**

1500 ml
water

0.5	0.1	91.1	8.9	0.0	0.0	6.5	3.2

7.0	3.7	0.3	7.3	3.7	88.8	34.8	243.6
24.0	8.7	0.1	2.2	0.5	97.3	23.6	565.7
31.0	10.9	0.0	1.6	0.7	97.6	22.9	710.5
48.0	**15.0**	**0.1**	**1.2**	**0.6**	**98.2**	**20.3**	**972.6**

Reaction conditions: Toluene – 20 ml, pO_2- 10 bar, T = 160 °C, t = 48 h, Catalyst – 0.4393 g of 1%AuPd/C prepared from XXX ml of water, substrate/metal mol ratio = 6500.

Table 6.3: Benzyl alcohol oxidation at 120 °C

Catalysts	Time h	Conv %	Selectivity % Toluene	Benz-aldehyde	Benzoic acid	Benzyl benzoate	TOF
100 ml water	0.5	13.5	14.3	84.7	0.1	0.9	31544.7
	1.0	21.1	12.9	81.2	1.0	4.9	24719.6
	2.0	32.3	11.5	83.1	1.7	3.6	18940.8
	4.0	56.1	9.8	82.7	3.5	4.0	16443.1
	6.0	78.5	8.1	80.3	7.9	3.8	15337.8
150 ml water	0.5	23.7	16.6	83.0	0.1	0.3	55563.2
	1.0	41.2	14.4	85.2	0.1	0.2	48349.4
	2.0	57.0	9.9	88.7	1.0	0.4	33432.2
	4.0	83.7	7.7	89.0	2.8	0.4	24520.0
	6.0	93.2	7.3	72.2	17.8	2.7	18217.6
200 ml water	0.5	17.9	15.6	81.2	0.4	2.8	41931.1
	1.0	32.6	13.4	80.5	1.0	5.1	38236.4
	2.0	54.5	11.1	82.1	2.1	4.7	31969.7
	4.0	75.7	9.3	79.6	6.6	4.5	22196.7
	6.0	90.6	8.0	65.7	22.1	4.3	17713.4
800 ml water	0.5	19.2	18.9	79.3	0.6	1.3	45016.1

	1.0	26.8	15.5	82.2	0.9	1.4	31423.9
	2.0	43.8	11.5	82.9	2.8	2.9	25690.0
	4.0	68.6	8.5	78.0	7.9	5.6	20099.1
	6.0	83.5	7.5	69.0	18.7	4.8	16315.6
1500 ml water	0.5	12.6	11.1	85.3	1.1	2.5	29639.2
	1.0	22.5	9.7	85.9	0.9	3.5	26354.2
	2.0	34.8	6.4	91.1	1.2	1.3	20376.9
	4.0	59.4	4.4	84.7	8.1	2.8	17422.2
	6.0	85.9	4.0	75.9	18.0	2.2	16786.1

Reaction conditions: Benzyl alcohol – 40 ml, pO_2- 10 bar, T = 120 °C, t = 6 h, Catalyst – 50 mg of 1%AuPd/C prepared from XXX ml of water

6.2.2. Effect of calcinations:

Treating the supported nanoparticles under various thermal conditions could result a change in particle size distribution as the heat energy helps to mobilise the metal particles on the surface of the support. To evaluate this, we have tested the catalysts, treated at different temperatures (under static air) say, 200 °C, 300 °C, and 400 °C for toluene and benzyl alcohol oxidation (Table 6.4 & 6.5). The results are compared at identical reaction conditions.

Table 6.4: Toluene oxidation at 160 °C

Catalysts	Time h	Conv %	Selectivity %				TOF	TON
			Benzyl alcohol	Benz aldehyde	Benzoic acid	Benzyl benzoate		
1%AuPd/C	7.0	6.5	0.1	10.2	16.1	73.6	60.0	419.8
1:1mol	24.0	18.7	0.3	5.8	14.1	79.8	39.1	1213.2
dried	31.0	21.4	0.2	3.5	10.5	85.8	58.1	1393.6

	48.0	32.8	0.3	2.4	11.8	85.6	44.4	2132.2
1%AuPd/C	7.0	2.6	0.5	3.7	4.3	91.5	24.0	168.0
1:1mol	24.0	7.6	0.4	1.5	1.0	97.1	20.7	496.8
200 °C calcin	31.0	9.1	0.5	1.6	1.0	97.0	19.1	591.9
	48.0	13.6	0.4	1.4	7.9	90.2	18.5	886.7
1%AuPd/C	7.0	1.8	0.9	12.3	1.8	85.0	16.5	115.3
1:1mol	24.0	4.3	0.7	3.1	0.8	95.5	11.8	283.3
300 °C calcin	31.0	5.4	0.5	2.5	0.6	96.4	11.3	351.2
	48.0	8.6	0.4	1.7	0.9	97.0	11.6	557.7
1%AuPd/C	7.0	0.5	6.0	18.9	3.7	71.4	5.0	35.3
1:1mol	24.0	3.0	5.9	9.3	2.9	81.9	8.0	192.8
400 °C calcin	31.0	3.5	4.1	5.1	2.3	88.5	7.3	227.2
	48.0	5.4	2.8	4.1	1.5	91.5	7.4	353.7
1%AuPd/TiO$_2$	7.0	1.9	1.3	3.3	4.9	90.4	16.3	114.4
1:1mol	24.0	5.5	0.8	2.3	4.0	92.9	13.7	328.1
dried	31.0	6.8	1.0	2.1	0.6	96.3	13.1	404.6
	48.0	10.5	0.3	2.2	2.2	95.4	12.9	618.9
1%AuPd/TiO$_2$	7.0	1.5	2.5	5.1	3.4	89.0	12.6	88.3
1:1mol	24.0	5.2	1.9	2.3	2.3	93.6	12.8	306.4
200 °C calcin	31.0	6.2	2.3	2.3	1.1	94.3	12.0	371.0
	48.0	11.0	1.4	1.5	0.9	96.2	13.5	647.9
1%AuPd/TiO$_2$	7.0	2.5	2.5	4.0	3.8	89.6	21.3	149.4
1:1mol	24.0	6.7	2.0	2.3	0.7	95.1	16.6	398.4
300 °C calcin	31.0	8.9	1.8	2.0	0.9	95.3	16.9	523.8
	48.0	12.6	0.7	1.8	1.3	96.3	15.6	747.6

1%AuPd/TiO$_2$	7.0	1.2	15.8	28.5	17.9	37.9	13.6	6.8
1:1mol	24.0	4.2	2.8	9.2	1.9	86.2	10.2	71.2
400 °C calcin	31.0	5.8	2.2	4.2	0.7	93.0	10.4	250.6
	48.0	9.6	1.9	3.4	1.1	93.6	11.9	569.6

Reaction conditions: Toluene – 20 ml, pO_2- 10 bar, T = 160 °C, t = 48 h, Catalyst – 0.4393 g, substrate/metal mol ratio = 6500.

The activity trend for the toluene oxidation is as follows.

Carbon: dried > 200 C > 300 C > 400 C

TiO$_2$: dried ~ 200 C < 300 C > 400 C < dried

Table 6.5: Benzyl alcohol oxidation at 120 °C

Catalysts	Time h	Conv %	Selectivity %			TOF
			Toluene	Benz-aldehyde	Benzoic acid	Benzyl benzoate	
1%AuPd/C	0.5	15.1	12.4	80.9	1.1	5.6	35431.0
1:1mol	1.0	32.0	10.5	83.5	1.9	4.1	37514.0
dried	2.0	51.9	8.4	83.0	3.8	4.8	30453.5
	4.0	76.0	6.6	77.4	11.8	4.2	22267.7
	6.0	88.1	4.7	66.4	24.7	4.2	17220.6
1%AuPd/C	0.5	20.9	7.7	85.0	2.2	5.2	49092.1
1:1mol	1.0	47.6	6.2	85.8	3.0	5.0	55868.4
200 °C calcin	2.0	75.1	4.9	85.2	5.1	4.7	44002.7
	4.0	87.5	4.9	72.5	17.6	4.9	25654.8
	6.0	92.4	4.7	56.2	34.0	5.2	18053.0
1%AuPd/C	0.5	2.4	0.8	91.1	0.9	7.2	5537.1
1:1mol	1.0	3.9	1.3	88.9	2.4	7.4	4570.9
300 °C calcin	2.0	7.2	1.7	85.9	3.3	9.2	4199.9

	4.0	22.9	5.9	82.8	4.3	6.9	6715.6
	6.0	64.3	6.7	80.6	6.1	6.6	12570.6
1%AuPd/C	0.5	1.0	2.7	82.4	7.0	7.8	2376.0
1:1mol	1.0	1.6	5.6	86.3	2.3	5.8	1863.1
400 °C calcin	2.0	3.1	3.1	88.8	2.6	5.5	1820.6
	4.0	8.3	3.8	87.0	2.9	6.3	2439.9
	6.0	25.1	7.3	86.6	2.8	3.3	4895.9
1%AuPd/TiO$_2$	0.5	11.5	10.5	88.8	0.6	0.0	26868.4
1:1mol	1.0	20.2	9.2	90.6	0.2	0.0	23640.5
dried	2.0	31.0	7.4	92.0	0.5	0.1	18171.7
	4.0	45.0	5.8	89.5	3.0	0.6	13185.0
	6.0	64.8	6.2	89.0	4.0	0.8	12663.5
1%AuPd/TiO$_2$	0.5	10.7	8.1	91.7	0.1	0.1	25059.1
1:1mol	1.0	19.4	7.5	92.2	0.2	0.1	22751.7
200 °C calcin	2.0	29.4	6.6	92.9	0.5	0.1	17223.7
	4.0	48.0	5.9	92.1	1.5	0.5	14059.7
	6.0	63.3	5.7	86.3	6.0	2.0	12361.1
1%AuPd/TiO$_2$	0.5	14.9	6.8	92.9	0.3	0.1	34984.5
1:1mol	1.0	20.7	5.5	93.8	0.4	0.3	24312.6
300 °C calcin	2.0	40.6	5.3	93.9	0.6	0.2	23829.6
	4.0	54.8	4.7	89.4	3.4	2.5	16071.4
	6.0	71.5	5.0	83.5	8.8	2.7	13981.5
1%AuPd/TiO$_2$	0.5	5.8	3.7	95.6	0.2	0.5	13493.5
1:1mol	1.0	8.4	3.2	95.4	0.5	0.8	9829.0
400 °C calcin	2.0	16.9	2.9	95.8	0.7	0.6	9923.4
	4.0	38.3	3.3	95.6	0.8	0.3	11216.0

6.0	58.3	3.2	87.1	4.8	4.9	11394.6

Reaction conditions: Benzyl alcohol – 40 ml, pO_2- 10 bar, T = 120 °C, t = 6 h, Catalyst – 50 mg

The activity trend for the benzyl alcohol oxidation is as follows.

Carbon: dried ~ 200 C > 300 C > 400 C

TiO_2: dried ~ 200 C < 300 C > 400 C

In TiO_2 supported catalysts, the agglomeration was very slow until 200 °C which leads to an almost similar conversion level of dried catalyst. At 300 °C, the capping PVA molecules were getting decomposed. Hence, we will have naked particles which correspond to high activity of the catalysts, calcined at 300 °C. Further at 400 °C, the particles start to agglomerate very fast since the stabiliser is absent. But this statement is not true with carbon based catalysts. In carbon supported catalysts, the agglomeration starts from 200 °C itself. The reason could be the better wetting surface behaviour of TiO_2, which stops the mobilisation of the metal particles until 300 °C, whereas there is no such wetting of particles with carbon surface. The characterizations of these catalysts have to be explored to confirm the above conclusions.

6.2.3. Effect of support:

In this study, we have tried to immobilise AuPd bimetallic alloy nanoparticles on various supports apart from conventional carbon and titania. These catalysts have been evaluated for benzyl alcohol and toluene oxidation (Table 6.6 & 6.7). Again the characterizations have to be done to understand the origin of activity difference between the catalsysts.

Table 6.6: Benzyl alcohol oxidation at 120 °C

Catalysts	Time h	Conv %	Selectivity %				TOF
			Toluene	Benz-aldehyde	Benzoic acid	Benzyl benzoate	
1%AuPd/MgO	0.5	7.1	1.6	97.5	0.0	0.9	15067.1
(1:1 wt)	1.0	11.1	1.9	97	0.0	1.1	11818.9
	2.0	15.2	2.8	95.9	0.1	1.2	8102.9
	4.0	22.0	3.6	95	0.1	1.3	5873
	6.0	30.5	3.9	94.9	0.4	0.9	5427.8
1%AuPd/acid	0.5	31.3	12.9	84	0.4	2.6	66862.2
carbon	1.0	52.6	10.8	88.2	0.6	0.5	56219.4
(1:1 wt)	2.0	73.7	7.7	85.9	2.3	4.0	39391.1
	4.0	90.6	6.7	84.6	4.5	4.2	24190.8
	6.0	95.1	6.4	63.7	25.3	4.6	16938.5
0.25%Au0.25%	0.5	3.2	2.7	93.8	0.5	3.1	13805.4
Pd/MCM41	1.0	4.7	3.3	93.4	0.5	2.7	10092.3
	2.0	8.2	4.6	91.5	1.0	2.9	8775.1
	4.0	14.1	6.0	89.2	1.9	2.8	7543.4
	6.0	21.2	6.2	87.7	2.9	3.2	7538.3
1%AuPd/	0.5	9.3	2.7	93.3	0.6	3.3	19841.8
hydroxyapatite	1.0	20.4	2.8	92.3	1.3	3.6	21806.9
(1:1 wt)	2.0	36.5	2.5	92.2	1.6	3.7	19469.7
	4.0	55.2	1.9	91.9	2.3	3.8	14733.7
	6.0	69.3	1.7	89.3	5.0	3.9	12338.5
1%AuPd/SiO$_2$	0.5	6.8	1.5	80.4	3.3	14.8	14488.4
(1:1 wt)	1.0	9.7	1.4	84.3	2.6	11.7	10382.6

	2.0	15.7	1.5	81.4	4.6	12.5	8362.8
	4.0	25.1	1.4	76.4	10.3	11.9	6716.7
	6.0	33.0	1.5	77.5	10.3	10.6	5871.4
1%AuPd/CeO$_2$	0.5	3.5	5.9	88.2	0.2	5.7	7464.5
(1:1 wt)	1.0	5.6	5.3	88.6	0.3	5.8	6016.7
	2.0	7.7	4.8	88.2	0.5	6.4	4135.6
	4.0	13.5	3.2	89.4	1.0	6.5	3608.8
	6.0	17.8	3.1	89.3	1.2	6.4	3160.4
1%AuPd/ZrO$_2$	0.5	8.0	4.9	90.2	0.4	4.6	17147.6
(1:1 wt)	1.0	12.5	4.1	90	0.9	5.0	13388.1
	2.0	17.0	3.6	89.7	1.6	5.1	9091.9
	4.0	26.2	3.0	89.3	2.2	5.6	7009.6
	6.0	33.9	2.7	88.6	3.2	5.4	6027.5
1%AuPd/	0.5	13.6	14.2	80.2	1.1	4.4	31871.8
Carbon	1.0	19.9	12.5	80	2	5.5	23293.9
nanotube	2.0	32.3	10.4	80.4	4	5.2	18952.4
(1:1 mol)	4.0	50.3	7.9	79.9	7.4	4.9	14745.4
	6.0	63.4	6.8	77.9	10.7	4.6	12389.0
1%AuPd/	0.5	13.9	0.6	90.1	3.9	5.5	29603.1
graphite	1.0	19.5	0.9	90.7	3.2	5.2	20843.0
(1:1 wt)	2.0	29.3	1.0	89.6	4.2	5.2	15626.2
	4.0	45.2	1.0	84.6	9.2	5.2	12081.4
	6.0	55.4	0.8	80.3	13.8	5.1	9857.2

Reaction conditions: Benzyl alcohol – 40 ml, pO_2– 10 bar, T = 120 °C, t = 6 h, Catalyst – 50 mg

Table 6.7: Toluene oxidation at 160 °C

Catalysts	Time h	Conv %	Selectivity %				TOF	TON
			Benzyl alcohol	Benz-aldehyde	Benzoic acid	Benzyl benzoate		
1%AuPd/acid	0.5	0.8	1.8	19.1	0.5	78.6	50.1	25
carbon	7.0	6.5	0.6	1.7	1.1	96.7	30.0	209.9
(1:1 wt)	24.0	16.3	0.3	0.9	0.4	98.5	22.1	529.8
	31.0	21.1	0.3	0.8	1.3	97.6	22.1	684.6
	48.0	30.5	0.2	0.6	1.1	98.0	20.6	989.7
	72.0	47.7	0.2	0.5	0.7	98.5	21.5	1550.3
0.25%Au0.25%	1.0	0.9	1.3	2.9	0.0	95.9	60	60
Pd/MCM41	4.0	1.7	1.2	3.7	0.0	95.1	28	112
	7.0	2.2	1.4	3.1	0.0	95.6	20.4	143.1
1%AuPd/	0.5	0.9	10.3	18.8	2.3	68.6	60.7	30.3
hydroxyapatite	7.0	4.4	2.7	3.4	0.7	93.2	20.4	142.6
(1:1 wt)	24.0	10.1	0.9	1.3	0.9	97.0	13.7	328.8
	31.0	14.6	1.0	1.7	1.8	95.5	15.3	474.9
	48.0	25.3	0.9	1.4	2.8	94.9	17.1	821.7

Reaction conditions: Toluene – 20 ml, pO_2- 10 bar, T = 160 °C, t = 48 h, Catalyst – 0.4393 g, substrate/metal mol ratio = 6500.

6.2.4. Oxidation of toluene using H_2O_2

There are few experiments designed to have alternate oxidants in place of molecular oxygen to oxidize toluene under high pressure. Obviously, the most desirable oxidant is H_2O_2 since it is environmentally benign. Preliminary results (Table 6.8) have been obtained and more attention is needed at this oxidation system as the product profile is entirely different from the other system which uses molecular oxygen as an oxidant.

Table 6.8: Toluene oxidation using H₂O₂

Catalysts	Conv %	Selectivity %					TON
		p-Cresol	Benz-aldehyde	Hydro quinone	Phenyl p-tolyl ether	Unknowns	
5%AuPd/TiO₂ (1:1wt)[a]	83.5	6.2	26.3	5.0	18.1	44.3	325.7

Catalysts	Conv %	Benzene	Benz-aldehyde	Hydro quinone	Unknowns	TON
1%AuPd/C (1:1wt)[b]	57.6	19.87	13.3	32.4	34.4	169.1

Reaction conditions: 10 ml of toluene solution (0.02 g of toluene in 50 ml water), Catalyst - [a]0.0276 g, [b]0.1381g, T = 50 °C, pHe = 0.3 Mpa, t = 0.5 h, Oxidant – 0.34 g H₂O₂, Stirring speed – 1500 rpm

References:

1. X. Li, J. Xu, L. Zhou, F. Wang, J. Gao, C. Chen, J. Ning, H. Ma, Catal. Lett. 110, 149 (2006)

2. F. Wang, J. Xu, X. Li, J. Gao, L. Zhou, R. Ohnishi, Adv. Synth. Catal. 347, 1987 (2005)

3. J. Gao, X. Tong, X. Li, H. Miao, J. Xu, J. Chem. Technol. Biotechnol. 82, 620 (2007)

4. R.L. Brutchey, I.J. Drake, A.T. Bell, T. Tilley, Chem. Commun. 3736 (2005)

5. A.P. Singh, T. Selvam, J. Mol. Catal. A: Chem. 113, 489 (1996)

LIST OF PUBLICATIONS

1. **Solvent-Free Oxidation of Primary Carbon-Hydrogen Bonds in Toluene Using Au-Pd Alloy Nanoparticles**

   Lokesh Kesavan, Ramchandra Tiruvalam, Mohd Hasbi Ab Rahim, Mohd Izham bin Saiman, Dan I. Enache, Robert L. Jenkins, Nikolaos Dimitratos, Jose A. Lopez-Sanchez, Stuart H. Taylor, David W. Knight, Christopher J. Kiely, Graham J. Hutchings.
   Science, 331, 2010, 195-199

2. **Facile removal of stabiliser-ligands from supported gold nanoparticles**
   Jose A. Lopez-Sanchez, Nikolaos Dimitratos, Ceri Hammond, Gemma L. Brett, Lokesh Kesavan, Saul White, Peter Miedziak, Ramchandra Tiruvalam, Robert L. Jenkins, Albert F. Carley, David Knight, Christopher J. Kiely and Graham J. Hutchings.
   Nature Chemistry, 3, 2011, 551–556

3. **Reactivity studies of Au–Pd supported nanoparticles for catalytic applications**

   Jose Antonio Lopez-Sanchez, Nikolaos Dimitratos, Neil Glanville, Lokesh Kesavan, Ceri Hammond, Jennifer K. Edwards, Albert F. Carley, Christopher J. Kiely and Graham J. Hutchings.
   Applied Catalysis A: General, 391, Issues 1-2, 2011, 400-406

4. **Direct Synthesis of Hydrogen Peroxide and Benzyl Alcohol Oxidation Using Au-Pd Catalysts Prepared by Sol Immobilization**

   James Pritchard, Lokesh Kesavan, Marco Piccinini, Qian He, Ramchandra Tiruvalam, Nikolaos Dimitratos, Jose A. Lopez-Sanchez, Albert F. Carley, Jennifer K. Edwards, Christopher J. Kiely, and Graham J. Hutchings.
   Langmuir, 26 (21), 2010, 16568-16577